

2012

## REMOVAL OF ARSENIC(III) FROM WATER WITH A NEW SOLID-SUPPORTED THIOL

Partha Jana

University of Kentucky, Partha.Jana@uky.edu

[Right click to open a feedback form in a new tab to let us know how this document benefits you.](#)

### Recommended Citation

Jana, Partha, "REMOVAL OF ARSENIC(III) FROM WATER WITH A NEW SOLID-SUPPORTED THIOL" (2012). *Theses and Dissertations--Chemistry*. 11.  
[https://uknowledge.uky.edu/chemistry\\_etds/11](https://uknowledge.uky.edu/chemistry_etds/11)

This Doctoral Dissertation is brought to you for free and open access by the Chemistry at UKnowledge. It has been accepted for inclusion in Theses and Dissertations--Chemistry by an authorized administrator of UKnowledge. For more information, please contact [UKnowledge@sv.uky.edu](mailto:UKnowledge@sv.uky.edu).

## **STUDENT AGREEMENT:**

I represent that my thesis or dissertation and abstract are my original work. Proper attribution has been given to all outside sources. I understand that I am solely responsible for obtaining any needed copyright permissions. I have obtained and attached hereto needed written permission statements(s) from the owner(s) of each third-party copyrighted matter to be included in my work, allowing electronic distribution (if such use is not permitted by the fair use doctrine).

I hereby grant to The University of Kentucky and its agents the non-exclusive license to archive and make accessible my work in whole or in part in all forms of media, now or hereafter known. I agree that the document mentioned above may be made available immediately for worldwide access unless a preapproved embargo applies.

I retain all other ownership rights to the copyright of my work. I also retain the right to use in future works (such as articles or books) all or part of my work. I understand that I am free to register the copyright to my work.

## **REVIEW, APPROVAL AND ACCEPTANCE**

The document mentioned above has been reviewed and accepted by the student's advisor, on behalf of the advisory committee, and by the Director of Graduate Studies (DGS), on behalf of the program; we verify that this is the final, approved version of the student's dissertation including all changes required by the advisory committee. The undersigned agree to abide by the statements above.

Partha Jana, Student

Dr. David A. Atwood, Major Professor

Dr. John Anthony, Director of Graduate Studies

REMOVAL OF ARSENIC(III) FROM WATER WITH A NEW SOLID-SUPPORTED  
THIOL

---

DISSERTATION

---

A dissertation submitted in partial fulfillment of the  
requirements for the degree of Doctor of Philosophy in the  
College of Arts and Sciences  
at the University of Kentucky

By  
Partha Jana

Lexington, Kentucky

Director: Dr. David A. Atwood, Professor of Chemistry

Lexington, Kentucky

2012

Copyright © Partha Jana 2012

## ABSTRACT OF DISSERTATION

### REMOVAL OF ARSENIC(III) FROM WATER WITH A NEW SOLID-SUPPORTED THIOL

Arsenic is a highly toxic, easily transportable and widespread contaminant in groundwater throughout the world. Arsenic causes acute toxicity by disrupting biological functions. In groundwater arsenic concentrations can reach up to a few milligrams per liter. Current regulations on arsenic content in drinking water are becoming more stringent and require the standard to be reduced to a few parts per billion. Arsenic exists as oxyanions in aqueous solution in either trivalent or pentavalent oxidation states depending on the oxidation-reduction potential and pH of the medium. Several treatment methods are available for removing arsenic from water. However, cost, operational complexity of the technology, skill required to operate the technology and disposal of arsenic bearing residual are factors that should be considered before the selection of any treatment method. Most of these techniques are also effective only in removing As(V) and not As(III). N,N'-bis(2-mercaptoethyl)isophthalamide, abbreviated BDTH<sub>2</sub>, is known to effectively precipitate soft heavy metals from water. A solid-supported reagent with the metal capture ability of BDTH<sub>2</sub> would be ideal to use as a filtration column packing material for removal of aqueous As(III). In order to attain this objective, a new dithiol compound, 2,2'-(isophthaloylbis(azanediyl))bis(3-mercaptopropanoic acid) (abbreviated ABDTH<sub>2</sub>) has been synthesized and immobilized on silica beads. Silica-supported reagent ABDTH<sub>2</sub> (SiABDTH<sub>2</sub>) thus prepared, completely removed As(III) from water by forming As-S bonds. In batch study, SiABDTH<sub>2</sub> reduced the concentration of As(III) in aqueous solutions from 200 ppb to below 5 ppb at pH 5, 7 and 9. XAFS study of ABDT-As(III) and SiABDT-As(III) indicated that arsenic was present in +3 oxidation state as well as As(III) was only bonded to sulfur atom of ABDT unit. When SiABDTH<sub>2</sub> was used as filtration column material, only 3% of ABDTH<sub>2</sub> was leached out from the column. However, 100% As(III) was removed from 20 L of 200 ppb As(III) aqueous solution at a flow rate of 20 mL/min.

KEYWORDS: Arsenic, ABDTH<sub>2</sub>, SiABDTH<sub>2</sub>, Filtration column, Remediation

---

Partha Jana

---

05/31/2012

---

REMOVAL OF ARSENIC(III) FROM WATER WITH A NEW SOLID-SUPPORTED  
THIOL

By

Partha Jana

Dr. David A. Atwood

---

Director of Dissertation

Dr. John Anthony

---

Director of Graduate Studies

May 31<sup>st</sup>, 2012

---

Date

*This work is dedicated to the memory of my father, late  
Bidhu Bhusan Jana and to my mother, Rekha Jana*

## ACKNOWLEDGEMENTS

My sense of fulfillment would not be complete without the mention of everyone who offered help and support, in one way or another, during the entire period of my PhD study. The briefness of this acknowledgement does not in any way downplay the support I have received from anyone mentioned, or not mentioned, herein.

First, I would like to sincerely thank my philosopher and guide, Dr. David A. Atwood for his guidance, encouragement, and most importantly, his friendship during my graduate studies at University of Kentucky. He has been a strong and supportive advisor to me throughout my graduate school career and has always given me great freedom to pursue independent work. Through his vast experience in this field of study, he has offered invaluable and constructive advice, and guidance to make this PhD possible. His mentorship was paramount in providing a well-rounded experience consistent with my long-term career goals. He encouraged me to not only grow as an experimentalist and a chemist but also as an independent thinker.

I would also like to extend my appreciation and thanks to Tricia Coakley and John May at the Environmental Research and Training Laboratory for always providing help with various analytical techniques. Without their endless support and friendship, this work would not have been possible. It was always a pleasure working with them.

I would like to acknowledge my collaborators Dr. Charles C. Chusuei and Frank E. Huggins for extending their help to carry out sample analyses. Their support with the experiments on solid state material helped to shape a significant part of my research and dissertation work.



My sincere thanks go to my doctoral committee members for their encouragement and support. I thank all of you for hanging in there with me with the guidance and valuable feedback I truly needed. The journey was so much more rewarding just knowing I had your support and advice when I needed it. I would specially like to thank Dr. John P. Selegue and Dr. Mark A. Lovell for agreeing to come so late on board and helping me when half of my initial committee left.

My thanks to all the past and present Dr. Atwood lab members for all the help they provided me at various stages of this work.

I would like to thank the Department of Chemistry at the University of Kentucky for the opportunity and support provided during my graduate study. The faculty of this department has provided me with a tremendous graduate education. They have provided me with scientific opportunities and economic support. I would also like to extend my thanks to Merloc, LLC., in Lexington, Kentucky and United States Geological Survey (USGS) Student Research Enhancement Program for the financial support they provided during this dissertation work.

Finally, I would like to thank my parents, Bidhu Bhusan Jana and Rekha Jana for always being there for me, for the love, the support I needed and the patience I often did not deserve. I truly could not have come this far without all of you. Special thanks to my brother, Prasun Jana, for his help and patience, for every period I was away. I would like to express my love and gratitude to my life-partner, Sony Soman for being my pillar of strength through so many difficult times. As a friend, fiancée and wife she is the best! They are the reason I did this; they are the reason I thrive to be better. Their pride for me is my main goal in life. *Thank you, thank you, and thank you.*

## TABLE OF CONTENT

ACKNOWLEDGEMENTS .....	iii
LIST OF TABLES .....	x
LIST OF SCHEMES .....	xi
LIST OF FIGURES .....	xii
LIST OF ABBREVIATIONS AND SYMBOLS .....	xiv
 CHAPTER 1 .....	 1
Introduction.....	1
1.1. Fundamental Chemistry .....	1
1.2. History.....	5
1.3. Aqueous Speciation .....	6
1.3.1 Eh-pH.....	8
1.3.2. Speciation.....	9
1.3.3. Mobility.....	11
1.4. Natural Sources .....	13
1.4.1. Mineralogy .....	13
1.4.2. Weathering .....	17
1.5. Anthropogenic Sources .....	18
1.6. Human Health .....	20
1.7. Remediation of Arsenic .....	24
1.7.1. Activated Alumina .....	26
1.7.2. Activated Carbon .....	28
1.7.3. Iron Removal Process .....	29
1.7.4. Membrane Filtration Process .....	30
1.7.5. Ion Exchange .....	32
1.7.6. Biosorbents .....	33
1.7.7. Solid Supported Reagents .....	34
1.8. BDTH <sub>2</sub> as Precipitation Agent.....	37
1.9. Interaction of BDTH <sub>2</sub> with Arsenic .....	40
1.10. Conclusion .....	43

CHAPTER 2 .....	46
ABDTH <sub>2</sub> : A Functional Reagent for As(III) .....	46
2.1. Introduction.....	46
2.2. Results and Discussion .....	49
2.2.1. Synthesis and Characterization .....	49
2.2.2. pK <sub>a</sub> Determination of ABDTH <sub>2</sub> .....	51
2.3. Experimental.....	53
2.3.1. Materials and Techniques .....	53
2.3.2. Synthesis .....	54
2.3.3. Titration.....	54
2.4. Conclusion .....	55
CHAPTER 3 .....	56
Synthesis of ABDT-As(III).....	56
3.1. Introduction.....	56
3.2. Results and Discussion .....	58
3.2.1. Synthesis and Characterization .....	58
3.2.2. XAFS Study .....	59
3.2.3. Leaching Study .....	68
3.3. Experimental.....	70
3.3.1. Materials and Techniques .....	70
3.3.2. Synthesis of ABDT-As(III).....	70
3.3.3. XAFS .....	71
3.3.4. Leaching Study .....	72
3.4. Conclusions.....	73
CHAPTER 4 .....	74
Preparation of Silica-Supported ABDTH <sub>2</sub> (SiABDTH <sub>2</sub> ).....	74
4.1. Introduction.....	74
4.2. Results and Discussion .....	77
4.3. Experimental .....	83

4.3.1. Materials and Techniques .....	83
4.3.2. Scale-up Procedure .....	84
4.3.2.1. 9 g SiABDTH <sub>2</sub> .....	84
4.3.2.2. 48 g SiABDTH <sub>2</sub> .....	86
4.3.2.3. 93 g SiABDTH <sub>2</sub> .....	88
4.3.2.4. 131 g SiABDTH <sub>2</sub> .....	89
4.3.3. Titrations of SiABDTH <sub>2</sub> .....	90
4.4. Conclusions.....	91
 CHAPTER 5 .....	 92
Arsenic and Mercury Removal Using SiABDTH <sub>2</sub> .....	92
5.1. Introduction.....	92
5.2. Results and Discussion .....	94
5.2.1. Arsenic Removal Batch Study .....	94
5.2.2. Arsenic Leaching Study of SiABDT-As(III) .....	100
5.2.3. XAFS Study of Arsenic Sorbents .....	102
5.2.4. Batch Study of Hg Removal by SiABDTH <sub>2</sub> .....	109
5.2.5. Leaching Study of SiABDT-Hg.....	110
5.2.6. XPS Study of SiABDT-Hg .....	112
5.3. Experimental .....	114
5.3.1. Materials and Techniques .....	114
5.3.2. As(III) Binding Study by SiABDTH <sub>2</sub> .....	115
5.3.2.1. Batch Study of As(III) Removal at pH 5, 7 and 9 .....	115
5.3.2.2. As(III) Removal by SiABDTH <sub>2</sub> as a Function of Time .....	116
5.3.2.3. Leaching Study of SiABDT-As(III) .....	118
5.3.2.4. XAFS Spectroscopy of Arsenic Sorbents .....	119
5.3.3. Mercury Binding Study by SiABDTH <sub>2</sub> .....	120
5.3.3.1. Batch Study of Hg Removal at pH 5, 7 and 9.....	120
5.3.3.2. XPS Study of SiABDT-Hg .....	121
5.3.3.3. Hg Leaching Study from SiABDT-Hg .....	121
5.4. Conclusions.....	123

CHAPTER 6 .....	124
Arsenic Filtration Column Study by SiABDTH <sub>2</sub> .....	124
6.1. Introduction.....	124
6.2. Results and Discussion .....	126
6.2.1. ABDTH <sub>2</sub> Leaching from Filtration Column .....	126
6.2.2. Column I: Low Flow Rate (20 mL/min).....	127
6.2.3. Column II: High Flow Rate (500 mL/min).....	129
6.3. Experimental .....	130
6.3.1. Materials and Techniques .....	130
6.3.2. Column Preparation .....	131
6.3.3. ABDTH <sub>2</sub> Leaching from Filtration Column .....	131
6.3.4. Column I: Low Flow Rate (20 mL/min).....	132
6.3.5. Column II: High Flow Rate (500 mL/min).....	134
6.4. Conclusion .....	135
CHAPTER 7 .....	137
Continued Research: HBDTH <sub>2</sub> and HABDTH <sub>2</sub> .....	137
7.1. Introduction.....	137
7.2. Results and Discussion .....	140
7.2.1. HBDTH <sub>2</sub> Synthesis and Characterization.....	140
7.2.2. HABDTH <sub>2</sub> Synthesis and Characterization .....	142
7.3. Experimental .....	146
7.3.1. Materials and Techniques .....	146
7.3.2. Synthesis of HBDTH <sub>2</sub> .....	146
7.3.3. Synthesis of HABDTH <sub>2</sub> .....	148
7.4. Conclusion .....	150
CHAPTER 8 .....	151
Conclusions and Future Direction .....	151
8.1. Conclusions.....	151

8.2. Future Direction .....	154
REFERENCES .....	156
VITA.....	179

## LIST OF TABLES

Table 1.1: Selected fundamental properties of arsenic .....	2
Table 1.2: Bond energies of selected arsenic bonds .....	3
Table 1.3: The $K_{sp}$ of arsenic containing minerals at ambient temperature (23-25°C).....	15
Table 3.1: Least-squares fitting parameters derived for $As_2S_3$ .....	63
Table 3.2: Least-squares fitting parameters derived for BDT-As(III) .....	64
Table 3.3: Least-squares fitting parameters derived for ABDT-As(III) .....	64
Table 3.4: As leaching from 10 mg of ABDT-As(III) after 24 h, 1, 2 and 3 weeks.....	69
Table 4.1: Sulfur concentration and ABDTH <sub>2</sub> loading per g of SiABDTH <sub>2</sub> in different batches.....	81
Table 5.1: Determination of As removal by SiABDTH <sub>2</sub> at pH 5, 7 and 9 .....	95
Table 5.2: Time dependent As removal by SiABDTH <sub>2</sub> at pH 5 .....	98
Table 5.3: Time dependent As removal by SiABDTH <sub>2</sub> at pH 7 .....	98
Table 5.4: Time dependent As removal by SiABDTH <sub>2</sub> at pH 9 .....	99
Table 5.5: As leaching from 0.2 g of SiABDT-As(III) after 24 h, 1, 2, 3 and 4 weeks .....	101
Table 5.6: Least-squares fitting parameters derived for $As_2S_3$ (Values in parentheses were held fixed during fitting) .....	106
Table 5.7: Least-squares fitting parameters of EXAFS data derived for SiABDT-As(III) .....	107
Table 5.8: Least-squares fitting parameters of EXAFS data derived SiABDT-As(III) <sub>LCH</sub> .....	107
Table 5.9: Hg concentration in supernatant solution after treatment with SiABDTH <sub>2</sub> ...	110
Table 5.10: Hg leaching study of SiABDT-Hg .....	111
Table 6.1: ABDTH <sub>2</sub> leaching from SiABDTH <sub>2</sub> filtration column .....	127
Table 6.2: Arsenic leached from SiABDT-As(III) column material .....	129
Table 6.3: Arsenic captured at a flow rate of 500 mL/min .....	130

## LIST OF SCHEMES

Scheme 1.1: Eh-pH diagram of inorganic As(III) and As(V) species .....	9
Scheme 1.2: $pK_a$ values of arsenic acid .....	10
Scheme 1.3: $pK_a$ values of arsenious acid .....	11
Scheme 2.1: Synthesis of ABDTH <sub>2</sub> .....	50
Scheme 7.1: Two-Step Synthesis of HBDTH <sub>2</sub> .....	142
Scheme 7.2: Synthetic pathway of HABDTH <sub>2</sub> : Step 1 - NS5HIPE; Step 2 - S-trityl-HABDT; Step 3 - HABDTH <sub>2</sub> .....	145



## LIST OF FIGURES

Figure 1.1: Structures of orpiment and realgar clusters .....	3
Figure 1.2: Structure of common arsenic compounds .....	4
Figure 1.3: Structure of (a) BDTH <sub>2</sub> and its (b) Hg, (c) Cd and (d) Pb compounds .....	39
Figure 1.4: Coating of BDTH <sub>2</sub> on pyrite through formation of Fe-S covalent bond.....	40
Figure 1.5: Tricoordinated arsenic compounds .....	42
Figure 2.1: The molecular structures of (a) BDTH <sub>2</sub> and (b) ABDTH <sub>2</sub> .....	47
Figure 2.2: Cd(II)-Cysteine complexes in solution at pH 7.5 (a) and pH 11 (b) .....	48
Figure 2.3: Titration of ABDTH <sub>2</sub> with 0.025 M sodium hydroxide (NaOH) (pK <sub>a1</sub> 3.20 and pK <sub>a2</sub> 4.60) .....	52
Figure 2.4: Structure of (a) terephthalic acid and (b) <i>m</i> -phthalic acid.....	53
Figure 3.1: S-(Dimethylarsino)-DL-cysteine.....	57
Figure 3.2: Structure of (a) As(SC) <sub>3</sub> and (b) [As(SC)(OH) <sub>2</sub> ] <sup>-</sup> .....	58
Figure 3.3: Arsenic <i>K</i> -edge spectra for As <sub>2</sub> S <sub>3</sub> (orpiment), BDT-As(III) and ABDT- As(III) .....	60
Figure 3.4: Arsenic EXAFS (k <sup>3</sup> chi) spectra for As <sub>2</sub> S <sub>3</sub> (orpiment), BDT-As(III) and ABDT-As(III).....	61
Figure 3.5: Arsenic RSF spectra for As <sub>2</sub> S <sub>3</sub> (orpiment), BDT-As(III) and ABDT- As(III) .....	62
Figure 3.6: Comparison of FEFF model function and least-squares fitting for As <sub>2</sub> S <sub>3</sub> . Left: q-mode fits; right: R-mode fits over the range 1.2 – 2.4 Å .....	64
Figure 3.7: Comparison of FEFF model function and least-squares fitting for ABDT- As(III). Left: q-mode fits; right: R-mode fits over the range 1.2 – 2.4 Å .....	65
Figure 3.8: Structure of (a) tris(phenylthiol)arsine and (b) As <sub>2</sub> S <sub>3</sub> .....	66
Figure 3.9: Proposed structure of ABDT-As(III) .....	67
Figure 4.1: Cysteine functionalized silica.....	75
Figure 4.2: Poly-L-Cysteine functionalized silica .....	75

Figure 4.3: Ethylene sulfide immobilized silica .....	75
Figure 4.4: Particle size distribution of Si60 .....	78
Figure 4.5: Thermogravimetric analysis for (a) Si60, (b) SiNH <sub>2</sub> and (c) SiABDTH <sub>2</sub> .....	80
Figure 4.6: Titration of SiABDTH <sub>2</sub> with NaOH.....	82
Figure 5.1: Removal of As(III) from water by 0.2 g of SiABDTH <sub>2</sub> as a function of pH .....	99
Figure 5.2: Removal of As(III) from water by 0.6 g of SiABDTH <sub>2</sub> as a function of pH .....	100
Figure 5.3: Arsenic <i>K</i> -edge spectra for As <sub>2</sub> S <sub>3</sub> , SiABDT-As(III) <sub>LCH</sub> and SiABDT-As(III) .....	103
Figure 5.4: Arsenic EXAFS ( <i>k</i> <sup>3</sup> chi) spectra for As <sub>2</sub> S <sub>3</sub> and arsenic sorbents SiABDT- As(III) <sub>LCH</sub> and SiABDT-As(III) .....	103
Figure 5.5: Arsenic RSF spectra for As <sub>2</sub> S <sub>3</sub> , SiABDT-As(III) <sub>LCH</sub> and SiABDT-As(III) .....	105
Figure 5.6: Comparison of FEFF model function and least-squares fitting for SiABDT- As(III). Left: q-mode fits; right: R-mode fits over the range 1.2 -2.4 Å .....	108
Figure 5.7: XPS of Hg 4f and Si 2p in SiABDT-Hg .....	113
Figure 5.8: XPS of S 2p in SiABDT-Hg .....	114
Figure 7.1: Molecular structures of (a) 5-hydroxy- <i>N,N'</i> -bis(2- mercaptoethyl)isophthalamide and (b) 2,2'-((5- hydroxyisophthaloyl)bis(azanediyl))bis(3-mercaptopropanoic acid) .....	139

## LIST OF ABBREVIATIONS AND SYMBOLS

### General:

Å	angstrom, $10^{-10}$ meters
AA	activated alumina
ABDTH <sub>2</sub>	2,2'-(isophthaloylbis(azanediyl))bis(3-mercaptopropanoic acid)
AC	activated carbon
AMD	acid mine drainage
BDTH <sub>2</sub>	1,3-benzenediamidoethanethiol
CCA	chromated copper arsenate
cm	centimeter
CV	curve verifier
dec	decomposed
DI	18 MΩ (mega-ohm) deionized water
DMA	dimethylarsinic or cacodylic acid
DMSA	2,3-dimercaptosuccinic acid
EA	elemental analysis
EPA	environmental protection agency
ESI	electrospray ionization
EtOH	ethanol
EXAFS	extended X-ray absorption fine structure
g	grams
GAC	granular activated carbon
GFAA	graphite furnace atomic absorption spectroscopy
GSH	glutathione
h	hours
Hz	Hertz, $s^{-1}$
ICP OES	inductively coupled plasma optical emission spectroscopy
IR	infrared spectroscopy
kJ	kilojoules
kg	kilogram
LCS	laboratory control sample
µg	microgram
MCL	maximum contaminant level
MF	microfiltration
MMA	monomethylarsonic acid
min	minute
mg	milligram
mmol	millimole
mL	milliliter
mp	melting point
MS	mass spectrometry
NF	nanofiltration
NMR	nuclear magnetic resonance

ppb	parts per billion
ppm	parts per million
RO	reverse osmosis
s	seconds
SiABDTH <sub>2</sub>	ABDTH <sub>2</sub> immobilized modified silica
SiNH <sub>2</sub>	amine functionalized silica
t	time
T	temperature
THF	tetrahydrofuran, C <sub>4</sub> H <sub>8</sub> O
TGA	thermogravimetric analysis
UF	ultrafiltration
XAFS	X-ray absorption fine structure
XANES	X-ray absorption near edge structure
XPS	X-ray photoelectron spectroscopy
ZVI	zero-valent iron

For infrared (IR) spectra:

br	broad
cm <sup>-1</sup>	wavenumbers
IR	Infrared Spectra
s	strong
vs	very strong
w	weak

For nuclear magnetic resonance (NMR) spectra:

δ	chemical shift, in parts per million
d	doublet
m	multiplet
q	quartet
s	singlet
t	triplet

## CHAPTER 1

### Introduction

#### 1.1. Fundamental Chemistry

Arsenic, a group 15 metalloid element, is the 20<sup>th</sup> most abundant element in the Earth's crust. It is most commonly found as sulfide ores. Arsenic is present in various allotropes. It is found in elemental form as metallic grey and yellow arsenic with specific gravities of 5.73 and 1.97 g/cm<sup>3</sup>, respectively.<sup>1,2</sup> The element is very brittle, crystalline and a semimetallic solid. When heated in the presence of oxygen it forms arsenic oxide (As<sub>2</sub>O<sub>3</sub>). The 1<sup>st</sup>, 2<sup>nd</sup> and 3<sup>rd</sup> ionization energy of arsenic are 947 kJ/mol, 1798 kJ/mol and 2735 kJ/mol, and ionization energy increases with the increase in positive charges (Table 1.1). The higher ionization energy is attributed to the relatively high effective nuclear charge ( $Z_{\text{eff}}$ ) of As. The electrons in arsenic 3*d* orbital provide less screening of nuclear charge due to their directionality and diffuse nature. This rationalizes the relatively high fourth and fifth ionization energy of arsenic. The electron affinity of arsenic is 78 kJ/mol. This suggests that arsenic can be present in an anionic oxidation state in various compounds. Arsenic is a 4<sup>th</sup> row element in the periodic table. According to the hard soft acid base (HSAB) principle, hard acids prefer to bind with hard bases, while soft bases form covalent bonds to soft acids. Both thiol and arsenic are soft species.<sup>3,4</sup> As a result arsenic forms strong covalent bonds with sulfur. The atomic and covalent radii of arsenic are 125 and 121 pm, respectively, which are very similar to the corresponding radii of sulfur.<sup>5,6</sup>

**Table 1.1.** Selected fundamental properties of arsenic<sup>5</sup>

Parameter	Arsenic
<i>Atomic Number</i>	33
<i>Atomic Mass (g/mol)</i>	74.92
<i>Ionization Energies (kJ/mol)</i>	
As	947
As <sup>+</sup>	1798
As <sup>2+</sup>	2735
As <sup>3+</sup>	4837
As <sup>4+</sup>	6043
<i>Electron Affinity (kJ/mol)</i>	78
<i>Radius</i>	
Atomic (pm)	125
Covalent (pm)	121
As(III) (pm)	58
As(V) (pm)	46
Van der Waals (pm)	200
<i>Common Oxidation States</i>	As(III), As(V)

The chemistry of arsenic-containing compounds is closely related to the structure and the nature of bonding within the molecules. Arsenic adopts wide varieties of coordination numbers and geometries depending on the substituents. The common mineral forms of arsenic (realgar and orpiment) show molecular cage structures, shown in Figure 1.1, whereas arsenic trioxide adopts cubic structures.<sup>7,8</sup>

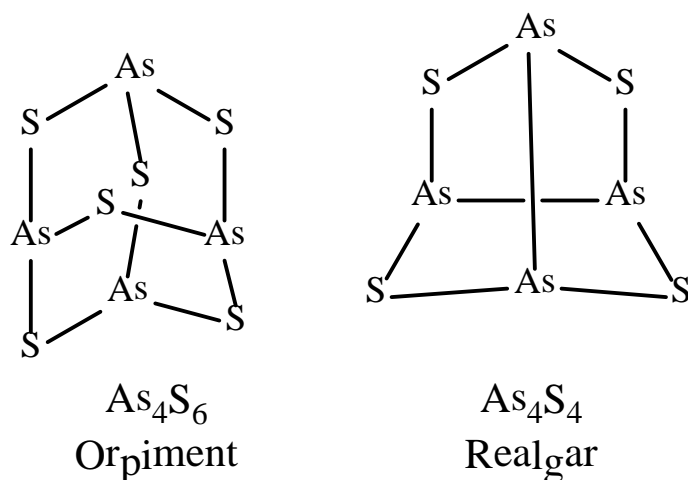


**Figure 1.1.** Structures of orpiment and realgar clusters

Arsenic forms stable covalent bonds with most elements, which leads to the high bond dissociation energy of these bonds. Table 1.2 shows experimentally determined bond energies of common arsenic-containing bonds.<sup>9</sup> Due to the strong bond energy of As-S, arsenic is commonly deposited with the sulfide-bearing ores. Arsenic occurs naturally in the environment with 4 valence states of -3, 0, +3, and +5 and when dissolved in water, it usually binds with oxygen to form arsenite and arsenate species.<sup>10</sup> The common arsenic compounds are shown in Figure 1.2.<sup>11</sup>

**Table 1.2.** Bond energies of selected arsenic bonds

Bonds	Energy (kJ/mol)
As-H	$274.0 \pm 2.9$
As-O	$484 \pm 8$
As-N	$489 \pm 2.1$
As-S	$379.5 \pm 6.3$
As-Cl	448

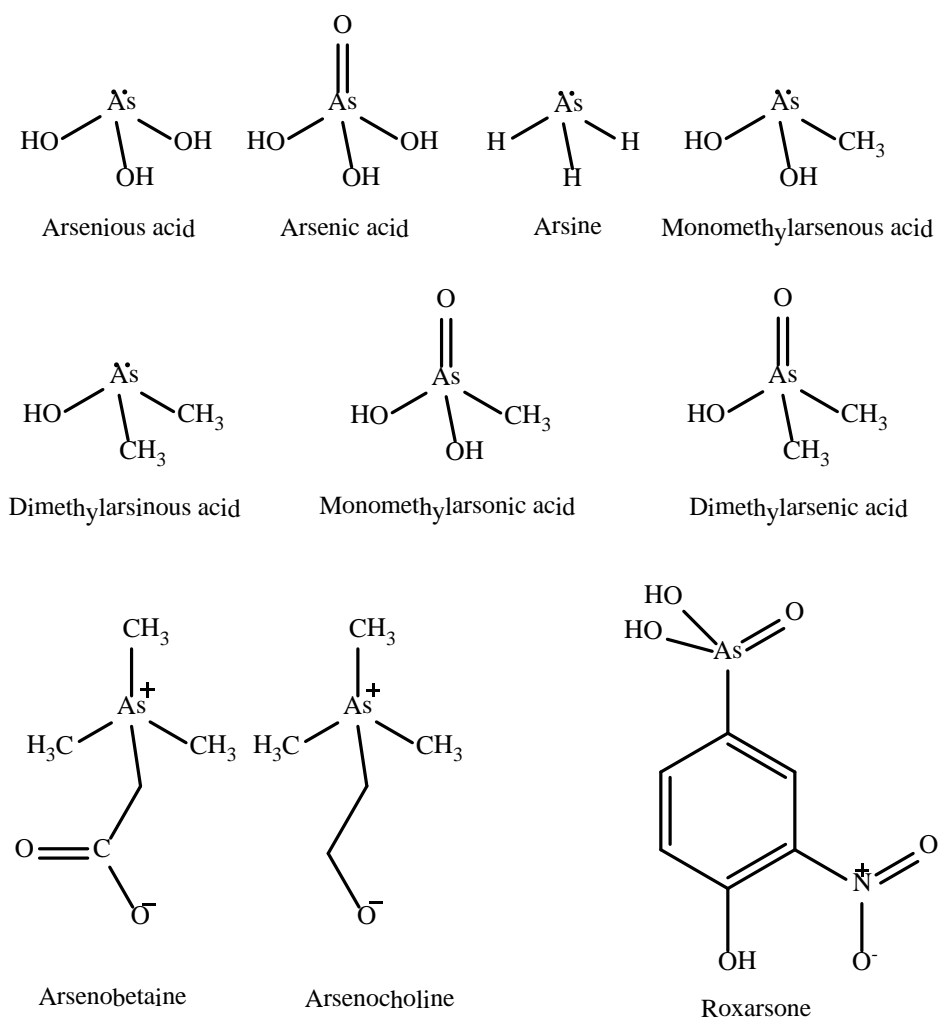


**Figure 1.2.** Structure of common arsenic compounds

Arsenic is widely distributed throughout nature with varying concentrations with as low as 0.1 ppb in Lake Superior to as high as 2,76,000 ppb in the Waioatapu Valley Rivers of New Zealand.<sup>12</sup> The concentration of arsenic in fresh water is highly dependent on the geothermal activity and the geological composition of the drainage area. The active volcanic activity including mud volcanoes, geysers, hot springs in the Taupo Volcanic Zone (TVZ) is the source of high concentrations of arsenic in Waioatapu Valley Rivers.<sup>13</sup>



Arsenic is a well known carcinogen that raises much concern from both environmental and human health standpoints mentioned in the Environmental Protection Agency (EPA) and the World Health Organization (WHO) list. Prolonged exposure of arsenic through drinking water causes diseases like skin pigmentation, keratoes and skin cancers. It enters into groundwater systems from both natural sources and/or agricultural and industrial practices. The presence of arsenic in groundwater is due to the geological composition of soils and rocks. It is introduced to groundwater through the dissolution of minerals. Arsenic in drinking water is a global problem affecting many countries distributed over the entire world. Arsenic is present in the environment in various forms such as arsenious acids ( $\text{H}_3\text{AsO}_3$ ,  $[\text{H}_2\text{AsO}_3]^-$ , and  $[\text{HAsO}_3]^{2-}$ ), arsenic acids ( $\text{H}_3\text{AsO}_4$ ,  $[\text{H}_2\text{AsO}_4]^-$ , and  $[\text{HAsO}_4]^{2-}$ ), arsenites, arsenates, methylarsenic acid, dimethylarsenic acid, arsine with +3 and +5 being the prominent oxidation states.<sup>11</sup>

Various techniques are available for arsenic removal from drinking water. Among these techniques, enhanced coagulation, lime softening, reverse osmosis, nano filtration, in-situ sub-surface arsenic removal, adsorption by activated alumina, ion exchange, and adsorption by iron oxide coated sand and granular ferric hydroxide have been widely used to obtain arsenic free water. The choice of an appropriate arsenic removal technique depends on the removal effectiveness, efficiency, cost, suitability for central and point of use, and simplicity of techniques.<sup>11,14</sup>

## 1.2. History

The name arsenic is derived from the Persian word *az-zarnikh*, meaning yellow orpiment pigment, which was borrowed from the Syriac word *zamiqa*. The ancient

Greeks referred to it as *arrenikos* or *arsenikos* which means ‘potent’. This was further evolved to *arsenicum* in Latin and ultimately to *arsenic* in French. In ancient times arsenic sulfides (orpiment and realgar) and oxides had been used in Persia and many other places. During the Bronze Age, arsenic was often mixed with the bronze to make the alloy harder. It is believed that Albertus Magnus was the first person to isolate arsenic in 1250 AD by heating soap with arsenic trisulfide. For centuries, arsenic compounds have been utilized as pigments, medicines, alloys, pesticides, herbicides, glassware etc. Due to its toxic properties, arsenic was frequently used by ruling class people to commit murder. It has also been used as chemical warfare agents during war.<sup>15,16</sup>

### 1.3. Aqueous Speciation

Knowledge of arsenic sources and processes that are controlling arsenic mobility is required to understand the factors controlling the distribution of arsenic in ground water. Speciation and mobility of arsenic are controlled by pH, oxidation-reduction potential, adsorption/ desorption, precipitation/dissolution, the concentration of competing ions and biological transformation. Arsenic concentration in groundwater is reaching an alarming rate in many parts of the world, mainly in Argentina, Bangladesh, Cambodia, Chile, Ghana, Hungary, India (West Bengal, Ganges Delta Basin), Mexico, Philippines, Taiwan and parts of the United States. The average arsenic concentration ranges between 0.1 – 80 ppb, though it can reach as high as 2500 ppb in places like Taiwanese wells due to close contact of groundwater with arsenic-bearing rocks. Arsenic is generally found in very shallow aquifers between 30–70 meters. Over the last two

decades in West Bengal, India and Bangladesh, tube well water has been used as an alternative source of safe, microbiologically free drinking water to reduce the water-borne pathogens related to infant mortality rates.<sup>10</sup> As a result 4 million tube wells were installed throughout Bangladesh over the period of several decades. However this vast region contains arsenopyrite minerals in the sediments. Uncontrolled pumping of groundwater from aquifers for drinking water and irrigation caused the lowering of water table to arsenic containing sulfide rock. This results in rapid diffusion of oxygen within the pore spaces of the sediments and increased levels of dissolved oxygen in the upper part of groundwater. Arsenopyrite is not soluble in water, but it decomposes to ferrous sulfate and ferric sulfate when exposed to oxygen or aerated groundwater. This leads to the dissolution of arsenopyrite, thus arsenic is released in groundwater causing the largest mass poisoning in history by nature.<sup>10</sup>

Along with inorganic arsenic, organic arsenic is also present in groundwater. Methylarsonous acid and dimethylarsinous acid have been found in lake and shallow water along with other organic arsenic species such as methylarsonate, dimethylarsinate and tetramethylarsonium ion in trace amounts. Other arsenic species that are found in fungi are arsenobetaine and arsenocholine.<sup>12</sup> In nature, fungi can methylate arsenic through a series of reaction that involves reductions, methylation and adenosylation.<sup>17,18</sup>

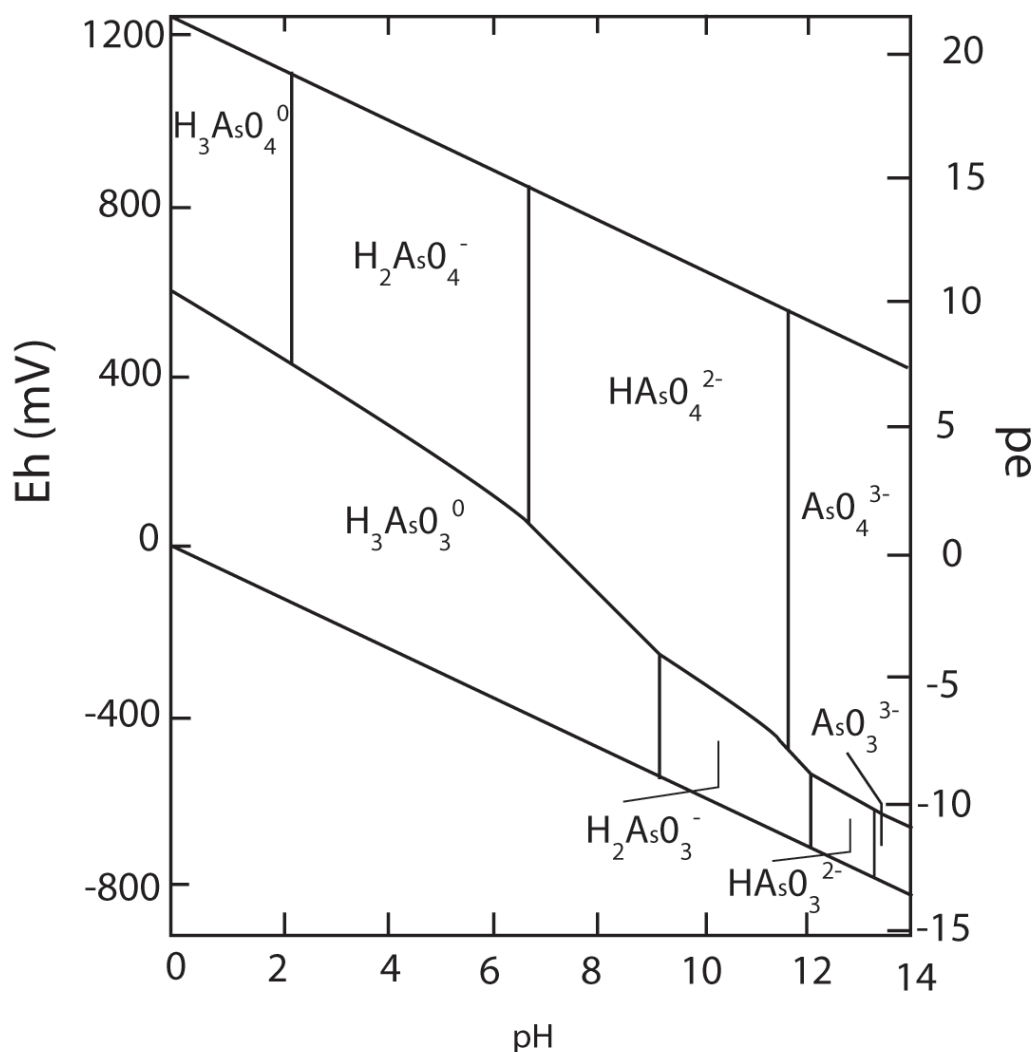
In sediment and soil, the common arsenic species are arsenite [As(III)], arsenate [As(V)], methyl arsonate and dimethylarsinate. The average arsenic content of soil is 5-6 ppm but ranges from 0.2 - 40 ppm.<sup>10</sup> Under aerobic conditions arsenate [As(V)] is the predominate form over the arsenite [As(III)] which is predominate oxidation state in anaerobic condition.<sup>12,19-21</sup> Adsorption affinity and mobility of arsenic in the environment

is strongly dependent on the formation of complexes with metal oxide, pH and redox potential of sediment and soil.<sup>21-25</sup>

### **1.3.1 Eh-pH**

Both the redox potentials and pH have an effect on the speciation and solubility of arsenic in groundwater. When the redox potential of soil reaches into the range of 200 - 500 mV, As(V) is the major dissolved species, contributing more than 95% of total arsenic. Whereas at a lower redox potential of 0 and -200 mV, As(III) is the predominant species.<sup>18</sup>

The redox potentials (Eh) and pH (Scheme 1.1)<sup>26</sup> have a strong influence on arsenic speciation, change in oxidation state of arsenic, and its solubility in water. In groundwater, different types of redox reactions can happen such as aerobic degradation, denitrification, ferric iron reduction and sulfate reduction.

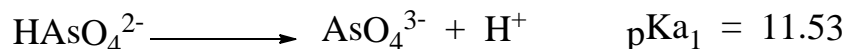
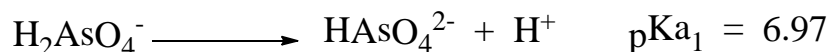


**Scheme 1.1.** Eh-pH diagram of inorganic As(III) and As(V) species<sup>26</sup>

### 1.3.2. Speciation

Arsenic is soluble in water under highly acidic conditions ( $\text{pH} < 2.0$ ), but it can also be soluble in other pH ranges (2–11) under suitable chemical and physical conditions.<sup>27</sup> As a predominant species in aerobic conditions, arsenate can exist as arsenic acid in groundwater. Depending on the pH of water and soil it can exist in various charged forms such as  $[\text{H}_2\text{AsO}_4]^-$ ,  $[\text{HAsO}_4]^{2-}$  and  $\text{AsO}_4^{3-}$ . Though,  $[\text{H}_2\text{AsO}_4]^-$  and  $[\text{HAsO}_4]^{2-}$  are the dominant forms in the pH range of 2.2 - 6.5. The  $\text{pK}_a$  values of arsenic

acid are 2.20, 6.97 and 11.53 according to the following equilibrium relationship (Scheme 1.2), which is very similar to the  $pK_a$  of phosphoric acid leading to the competition between arsenate and phosphate for the sorption site in soil such as aluminum, manganese, iron (oxy)hydroxide and clay.<sup>20,21,28-34</sup>  $[H_2AsO_4]^-$  is the dominant species at pH less than 6.9 under oxidizing conditions, whereas  $[HAsO_4]^{2-}$  is the dominant species at higher pH under similar conditions. In extremely acidic and basic conditions,  $H_3AsO_4$  and  $AsO_4^{3-}$  are present in aqueous media due to protonation and deprotonation of oxyanion which is evident from the low and high  $pK_a$  values of  $H_3AsO_4$  and  $[HAsO_4]^{2-}$ . The redox potential ( $E_0$ ) for converting As(III) to As(V) is +0.56V according to the equation 1.<sup>35</sup> The oxidation of As(III) to As(V) is very slow. It takes days for the process. In presence of air, oxidation happens in four to nine days. While in presence of pure oxygen, oxidation occurs in two to five days.

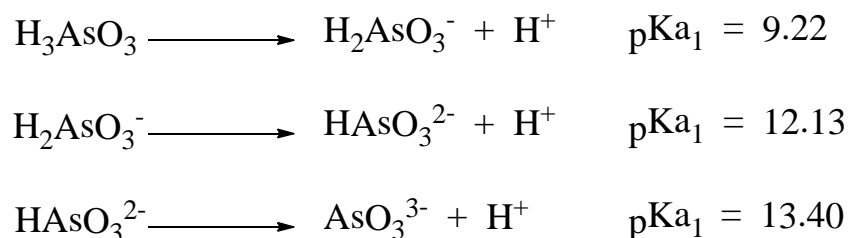


**Scheme 1.2.**  $pK_a$  values of arsenic acid

The other predominant oxidation state of arsenic is +3, which is referred to as arsenite and is favorable in anaerobic conditions. Arsenite is present in groundwater as

arsenous acid ( $\text{H}_3\text{AsO}_3$ ) with  $\text{pK}_a$  values of 9.22, 12.13 and 13.40 (Scheme 1.3).<sup>12,17,20</sup>

Arsenious acid ( $\text{H}_3\text{AsO}_3$ ) is the predominant species present at low pH (<9.2) under mildly reducing conditions, whereas  $[\text{HAsO}_3]^{2-}$  is present at a high alkaline pH (>12).



**Scheme 1.3.**  $\text{pK}_a$  values of arsenious acid

### 1.3.3. Mobility

The charge differences between arsenite and arsenate, pH of soil, sediment and groundwater and surface charges on soil components are responsible for mobility and biological uptake of arsenite and arsenate species. The strength of adsorption and desorption reactions between different arsenic species and surfaces of soil and sediments is largely dependent on the charge of the arsenic species, as it controls the electrostatic interactions between charged species and surfaces. Arsenate and arsenite are adsorbed to surfaces of aluminum oxides, iron oxides and clay materials. However, adsorption on iron oxides surfaces is important as iron oxides are widely distributed in the hydrogeologic environment. The binding and uptake of As(V) by amorphous, highly hydrated iron oxides is greater than As(III).<sup>30,36</sup> As(III) is preferably adsorbed on negatively charged surfaces at pH 7, whereas As(V) is likely to be adsorbed on positively charged surfaces at pH 4 to near-neutral pH.<sup>30,37</sup> However, arsenate is desorbed from iron oxide surfaces when pH is increased to alkaline conditions. The pH dependent adsorption

and desorption of arsenate to iron oxide surfaces is closely related to the net surface charge on iron oxide surfaces. As pH increases above the zero-point-of-charge of about 7.7 for crystalline iron oxide and 8.0 for amorphous iron oxide, the net surface charge changes from positive to negative. This results in repulsion between negative net surface charge on iron oxide surfaces and negatively charged ionic species of arsenate which leads to the desorption of arsenate species at higher pH. The adsorption of arsenate and arsenite to iron oxide surfaces decreases with increase in pH, mainly in the range of pH 6 to pH 9. This pH dependence can affect the adsorption and desorption behavior of arsenate and arsenite with change in pH of groundwater. Also solid-phase diagenesis (water-rock interaction) tends to consume  $H^+$  from groundwater with residence time resulting in increase in pH of groundwater and along the groundwater flow paths. This leads to increased mobility of arsenic in groundwater as arsenic mobility is directly affected by the change in pH of soil and sediment. In aerated environments, a decrease in pH has a direct effect in mineral dissolution and affinity of protons towards binding site, whereas an increase in surface potential leads to increased arsenic mobility. Similarly increased pH destabilizes the metal oxide complexes promoting arsenic mobility. Reductive dissolution of arsenic containing minerals can also increase arsenic contamination in environments.<sup>25,30,37</sup>

The adsorption of arsenate on iron oxide in soil and sediments is highly affected by the presence of phosphate anion. Arsenate and phosphate anions are chemically analogous. They have similar geochemical behavior leading to a competition between arsenate and phosphate for sorption sites. In comparison to arsenate, phosphate anion has smaller size compared to arsenate, which results in strong bonding between mineral



surfaces and phosphate anion. As a result, desorption of arsenate is elevated due to increased phosphate in soil and sediments.<sup>38,39</sup>

Precipitation and dissolution also play a major role in arsenic contamination of groundwater. Due to the strong affinity of arsenic towards iron oxide and hydrous ferric oxide (HFO), the fate of iron oxide and HFO in precipitation and dissolution processes in sediments controls the mobility of arsenic in groundwater. Ferrous iron contents are commonly present in anoxic groundwater. When iron is oxidized, it is precipitated as iron oxide and HFO along with arsenic as arsenate and arsenite, which are co-precipitated or adsorbed onto the iron oxide and HFO surfaces. In alkaline and reducing condition, iron oxide and HFO release arsenate and arsenite in groundwater.<sup>38,40,41</sup>

## **1.4. Natural Sources**

### **1.4.1. Mineralogy**

Arsenic is found in approximately 300 minerals.<sup>27,42,43</sup> It is mainly associated with the ores of Au, Ag, Cu, and Fe. The major arsenic ores present in the environment are realgar ( $\text{As}_4\text{S}_4$ ), orpiment ( $\text{As}_2\text{S}_3$ ), arsenopyrite ( $\text{FeAsS}$ ), tennantite ( $\text{Cu}_{12}\text{As}_4\text{S}_{13}$ ) and loellingite ( $\text{FeAs}_2$ ) contributing to arsenic contamination through erosion of the earth's crust.<sup>42,44</sup> The other minerals, which contain arsenic to some extent, are arsenolite,  $\text{As}_2\text{O}_3$ ; olivenite,  $\text{Cu}_2\text{OHAsO}_4$ ; dimorphite,  $\text{As}_4\text{S}_3$ ; cobaltite,  $\text{CoAsS}$ ; enargite,  $\text{Cu}_3\text{AsS}_4$ ; and proustite,  $\text{Ag}_3\text{AsS}_3$ .<sup>44</sup> Arsenic is mainly found in sulfide ores. Arsenic forms strong covalent bonds with sulfur in sulfide minerals. The bond energy of the covalent bond between arsenic and sulfur is  $379.5 \pm 6.3$  kJ/mol. The arrangements of bonds in sulfide minerals are found to contain As-S and As-As dimeric units that creates a common

structural basis. In many arsenide and arseno-sulfide minerals arsenic has a valence state of -1 or 0 similar to sulfur in sulfide minerals. Due to its strong association with various ores such as  $\text{Ag}_3\text{AsS}_3$ ,  $\text{Cu}_3\text{AsS}_4$  and  $\text{FeAsS}$ , arsenic was often used as a pathfinder element in the past in order to find out the presence of significant deposits of Ag, Cu and Fe ores.<sup>10</sup>

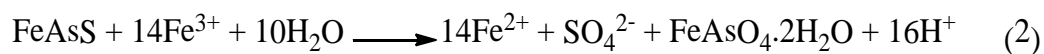
Arsenic present in most of the arsenic bearing ores is immobile in the environment. The mobility of arsenic in the environment depends on the solubility of arsenic containing minerals in groundwater. Solubility of minerals is defined by the solubility product constant ( $K_{\text{sp}}$ ).  $K_{\text{sp}}$  describes the dissociation of a solid in water. Most of the arsenic bearing minerals have very low solubility product constant in room temperature suggesting the insolubility of those minerals at ambient temperature. The  $K_{\text{sp}}$  of amorphous  $\text{As}_2\text{S}_3$  is  $1.25 \times 10^{-8}$ , whereas the  $K_{\text{sp}}$  of crystalline  $\text{As}_2\text{S}_3$  varies in the range of  $5.01 \times 10^{-26}$  to  $5.01 \times 10^{-47}$ .<sup>45</sup> The  $K_{\text{sp}}$  of other arsenic bearing minerals are shown in Table 1.3.

**Table 1.3.** The  $K_{sp}$  of arsenic containing minerals at ambient temperature (23-25°C)

Arsenic Compounds	$K_{sp}$
$Ag_3AsO_4$	$1.00 \times 10^{-22}$ to $3.98 \times 10^{-24}$
$Ba_3(AsO_4)_2$	$2.69 \times 10^{-22}$ to $2.95 \times 10^{-24}$
$Ca_3(AsO_4)_2 \cdot 3H_2O$	$7.24 \times 10^{-22}$
$Ca_5H_2(AsO_4)_4 \cdot 9H_2O$	$3.22 \times 10^{-33}$
$Cd_3(AsO_4)_2$	$1.99 \times 10^{-33}$ to $5.01 \times 10^{-34}$
$FeAsO_4 \cdot 2H_2O$	$3.89 \times 10^{-25}$ to $1.47 \times 10^{-26}$
$Cu_3(AsO_4)_2$	$2.51 \times 10^{-36}$

The widespread presence of scorodite in arsenic –bearing ore deposits suggests that the solubility of scorodite could control the concentration of arsenic in groundwater.

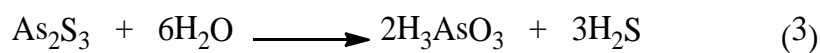
Scorodite ( $FeAsO_4 \cdot 2H_2O$ ) is deposited as a weathering mineral of FeAsS according to the equation 2.



The insolubility of scorodite is related to its very small  $K_{sp}$  value at 23°C (Table 1.3). It is stable under oxidizing conditions below pH 3.<sup>46</sup> Blasting and tunneling of rocks during mining exposes the rock to an oxidizing environment through cracking and fracturing leading to an oxidative conversion of minerals that produces water soluble arsenic species. Metal-reducing bacteria also releases arsenic into the groundwater.<sup>10,47</sup> It is

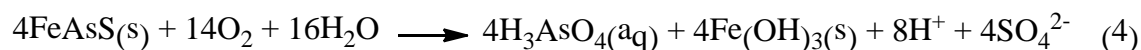
estimated that an average of 6 mg As/kg is present on the earth's crust.<sup>42,48</sup> Coal is another source of arsenic in the environment which contains as much as 1.5 g As/kg with an average arsenic concentration of 13 mg As/kg.<sup>42</sup> Volcanic eruption emits 17,150 t of arsenic in the atmosphere, whereas burning of wood in forest fire provides 125 to 3,345 t of arsenic in the environment.<sup>42,49,50</sup>

Arsenic is often deposited in the form of secondary arsenic minerals. Secondary arsenic minerals are those which arise by hydrothermal alteration or weathering of primary minerals. Secondary arsenic minerals are found as deposits near hot springs in the form of orpiment ( $\text{As}_2\text{S}_3$ ) and realgar ( $\text{As}_4\text{S}_4$ ). In hot spring water, arsenic concentration ranges from 0.1 to 0.3 mg  $\text{Kg}^{-1}$  which is deposited in reducing condition. In most of the hydrothermal fluids,  $\text{H}_3\text{AsO}_3$  is the dominant species in reducing conditions and in the pH range of 0 to 8. However, concentration and composition of arsenic species in any hydrothermal fluid depend on redox conditions, the pH of solutions and temperature. Under anoxic conditions,  $\text{As}_2\text{S}_3$  is mainly involved in dissolution and precipitation/coprecipitation reactions according to the reaction shown below (Equation 3). Realgar, arsenopyrite ( $\text{FeAsS}$ ) and arsenianpyrite ( $\text{FeS}_2$ ) are also involved in the hydrothermal reactions conditions.  $\text{As}_2\text{S}_3$  is dissolved in water under reducing conditions and low  $\text{H}_2\text{S}$  concentration at temperatures up to 300°C. However the reverse reaction and precipitation of  $\text{As}_2\text{S}_3$  occurs when the concentration of sulfide increases in hydrothermal water.<sup>51-53</sup>



### 1.4.2. Weathering

The weathering of arsenic containing minerals has significant role in the arsenic contamination of groundwater, soil and sediments. The major source of arsenic contamination of aquifer matrix is via deposition of eroded arsenic containing minerals followed by the oxidation of arsenic containing pyrites that releases dissolved arsenic into groundwater.<sup>54</sup> Arsenic is present in high concentration in areas containing organic matter-rich sediments.<sup>55</sup> Iron hydroxide, arsenic and organic matters often coexist due to the high affinity of iron hydroxide towards both arsenic and organic matter.<sup>56</sup> In sediment, arsenic species in the form of arsenate (As(III)) and arsenite (As(V)) are strongly adsorbed on iron oxide and hydroxide in oxic conditions in nature and released to the groundwater system in an anoxic environment.<sup>57-61</sup> The adsorption of arsenic species on iron hydroxide happens through a anion adsorption process. In oxic conditions, the adsorption happens either by proton uptake or release of hydroxide anions.<sup>62</sup> The mobilization of arsenic occurs through bacteria-mediated reductive dissolution of iron hydroxide in anoxic environment of sediment.<sup>63,64</sup> Oxidation of arsenic rich pyrite also contributes to the arsenic contamination of groundwater.<sup>56</sup> Due to a strong affinity of arsenic towards sulfur, arsenic is deposited and incorporated with iron and sulfur in minerals of pyrite ( $\text{FeS}_2$ ) and arsenopyrite ( $\text{FeAsS}$ ). Oxidative weathering of pyrite and arsenopyrite releases arsenic into sediment and groundwater which increases the concentration of arsenic according to the following reaction (Equation 4).<sup>10,65</sup>



Arsenic preferably exists as inorganic oxide in two predominant oxidation states of arsenite ( $\text{NaAsO}_2$ , As(III)) and arsenate ( $\text{Na}_2\text{HAsO}_4$ , As(V)). However in water, arsenic is present as arsenic ( $\text{H}_3\text{AsO}_4$ ) and arsenous ( $\text{H}_3\text{AsO}_3$ ) acid, respectively depending on the pH and oxic nature.  $[\text{H}_2\text{AsO}_4]^-$  is also the preferable arsenic species in the pH range of 2.24-6.96.<sup>43,65</sup>

### 1.5. Anthropogenic Sources

The use of arsenic has varied widely. Arsenic containing compounds are highly consumed in agricultural as herbicides and pesticides. Arsenic is also used to some lesser extent as wood preservatives, and in glass, alloys and electronics. The common oxidation states of arsenic are +III as in  $\text{As}_2\text{O}_3$  and +V as in  $\text{As}_2\text{O}_5$ . The trioxide has moderate solubility in water but it dissolves easily in alkali to produce a solution of arsenite. In the past, arsenic trioxide has been used to treat leukemia and other forms of cancer. It was also used as an ingredient in hide tanning and as a pigment in paints and dyes. As a result, arsenic became one of the first recognized occupational hazards chemical. Arsenic has also been used in chemical warfare. Arsenic in the form of cacodylic acid (dimethyl arsenic acid) was used as a herbicide in the Vietnam War. Diphenylchloroarsine, diphenylcyanoarsine and phenyldichloroarsine were used in World War I as chemical warfare agents. These uses introduced a large cumulative quantity of anthropogenic derived arsenic causing a potentially hazardous environment.<sup>42,66</sup>

Arsenic compounds have been used as pesticides, herbicides and wood preservatives. These compounds are the major sources of anthropogenic arsenic contamination in soil, sediments and groundwater. Chromated copper arsenate (CCA) is a very well known arsenic contaminant which has been used as wood preservative. CCA is a mixture of chromium and copper(II) arsenate which protects wood from humidity, mold, bacteria and insects. The most common formulation of CCA, type C, is comprised of 47.5%  $\text{CrO}_3$ , 18.5%  $\text{CuO}$  and 34%  $\text{As}_2\text{O}_5$ .<sup>67</sup> Copper acetoarsenite pigment, commonly known as Paris green  $(\text{CH}_3\text{COO})_2\text{Cu} \cdot 3\text{Cu}(\text{AsO}_2)$ , is an arsenic compound, which has long been used in agriculture as a pesticide. Lead arsenate ( $\text{PbHAsO}_4$ ) is another extensively used arsenic-based insecticide. It was first used as an insecticide in 1892 for use against gypsy moths invading hardwood forests in Massachusetts. Lead arsenate was prepared by combining soluble lead salts with sodium arsenate.<sup>68</sup> Scheele's green ( $\text{CuHAsO}_3$ ), which was used as a coloring agent, was also a source of arsenic in the environment. Other common arsenic containing compounds that have been used as horticultural pesticides are calcium arsenate ( $\text{Ca}_3(\text{AsO}_4)_2$ ), magnesium arsenate ( $\text{Mg}_3(\text{AsO}_4)_2$ ) and zinc arsenate ( $\text{Zn}_3(\text{AsO}_4)_2$ ).<sup>69</sup> The continuous use of arsenic containing pesticides, herbicides and wood preservatives leads to residual arsenic in soils and sediments at a level up to 2 g As/kg.<sup>70</sup> Arsenic trioxide is the most commonly used as herbicide and is obtained as a by-product of the smelting process of copper and lead ores. Arsenic is released to the environment as fine dust when sulfide ores of copper and lead are heated in the smelter leading to its deposition on soil surface and consequent arsenic contamination.<sup>71</sup> Due to the strong affinity of arsenic towards ferric oxyhydroxide and to some extent towards magnesium hydroxide and aluminum

hydroxide in soil, arsenic remains in a significant amount in the soil surface even decades after its application.<sup>71</sup>

Roxarsone (3-nitro-4-hydroxyphenylarsonic acid) is commonly used as a feed additive for poultry as a growth promoter. Most of the roxarsone is excreted from the poultry body unchanged in poultry litter, which is disposed as a fertilizer to the farm lands. Under an open environment, roxarsone is decomposed to produce a mixture of arsenic compounds including both inorganic and organic arsenicals, which is finally mixed with and transported by groundwater and runoff water resulting in an arsenic content in the range of 10.7-130 mg As/kg.<sup>72</sup>

The smelting processes of Cu, Ni, Pb and Zn ores are also a source of arsenic in soils and sediments. It is estimated to be approximately 62000 t of arsenic that is emitted from the smelting process. Arsenic is found in high concentrations near the smelters of these metals. The amounts of arsenic near lead smelter, copper smelter and gold smelter are measured to be 2 g As/kg, 0.55 g As/kg and 0.5 to 9.3 g As/kg, respectively.<sup>73</sup>

Mining activities also cause arsenic contamination of soils and sediments in the range of 5 µg/L to 72 mg/L of arsenic in mine drainage.<sup>26,74</sup>

## **1.6. Human Health**

Throughout history, water quality has been an indicator and determining factor of human life and welfare. The presence of arsenic in groundwater and drinking water has affected more than 100 million people throughout the world causing arsenic related disease. Chronic exposure to arsenic leads to arsenical poisoning.<sup>43</sup> Chronic toxicity is a property of a substance that has toxic effects on a living organism, when organism is



exposed to the substance repeatedly. Prolonged exposure to a substance and prolonged internal exposure due to the substance remains in the body for a long time causes chronic toxicity. Arsenic toxicity arising from drinking arsenic containing water can cause bladder, lung, kidney, liver, colon, prostate and skin cancers, as well as hyper- and hypopigmentation, keratosis, hypertension, cardiovascular diseases and diabetes.<sup>75-86</sup> Acute arsenic toxicity damages the cardiovascular, pulmonary, immunological, neurological, endocrine and reproductive systems. Arsenic also affects the central and peripheral nervous systems, as well as heart and blood vessels. Arsenic is genetically harmful because it inhibits the repair of DNA damage by bonding with sulfur in cysteine unit. Whereas inorganic mercury is toxic when inhaled and it is absorbed into the blood. It can pass through the blood-brain barrier and accumulate in the brain and damage the central nervous system. Methylmercury forms complex with cysteine. This complex is similar to methionine and can more easily gain entry into cells. Arsenic related diseases are of major concern in Bangladesh as well as in West Bengal, India, due to arsenic contamination of groundwater in the Ganges Delta basin. Chronic exposure to arsenic is possible by drinking water having arsenic concentration >10 ppb. This causes severe acute arsenic toxicity in humans resulting in gastrointestinal discomfort, vomiting, diarrhea, bloody urine, convulsions, coma and death.<sup>76,77,87-95</sup>

Most of the arsenic species are toxic for humans. But toxicological properties of organic arsenic compounds are different from inorganic arsenic compounds.

Arsenosugars and arsenobetaine, the common forms of organic arsenic compounds, are less toxic than inorganic arsenic species. Arsenosugars are arsenic-containing riboses which are commonly found in seafood like mussels, oysters and clams as well as in

marine algae.<sup>36,96</sup> Arsenic poisoning is more common compared to any other toxin known to human.<sup>42,97</sup> Inorganic arsenic compounds are highly toxic compared to their organic counterparts, which is evident from the fatal dose limit. The two forms of inorganic arsenic, trivalent As (reduced) and pentavalent As (oxidized), can be absorbed and accumulated in tissues and body fluids. Among various species of arsenic, arsine gas ( $\text{AsH}_3$ ) is the most toxic with a fatal dose of  $250 \text{ mg As/m}^3$  at an exposure time of 30 minutes. Whereas, the fatal dose for arsenic trioxide is  $34.5 \text{ mg As/kg}$ . The fatal dose for sodium arsenite, sodium arsenate, monomethylarsonic acid, dimethylarsinic acid and trimethylarsine is  $4.5 \text{ mg As/kg}$ ,  $14 \text{ to } 18 \text{ mg As/kg}$ ,  $1800 \text{ mg As/kg}$ ,  $1200 \text{ mg As/kg}$  and  $8000 \text{ mg As/kg}$ .<sup>42</sup> Human beings are exposed to arsenic through medicine, food drinking water and groundwater, and environmental surroundings such as ingestion of arsenic-containing particulates through breathing.

The extent of arsenic toxicity depends primarily on the metabolic capability for arsenic in the human body. The extent of methylation of inorganic arsenic and subsequent excretion depends on the form of arsenic ingested. Inorganic arsenic is metabolized mainly in the liver through a sequential process which involves a two-electron reduction of pentavalent arsenic to trivalent arsenic, followed by oxidative methylation to pentavalent organic arsenic.<sup>36,98</sup> Inorganic arsenic is metabolized in kidney and liver to the methylated forms of monomethylarsenous acid ( $\text{MMA(III)}$ ), monomethylarsonic acid ( $\text{MMA(V)}$ ), dimethylarsinous acid ( $\text{DMA(V)}$ ) and dimethylarsinic acid ( $\text{DMA(V)}$ ) (Figure 1.2) and primarily excreted in urine.<sup>98,99</sup>  $\text{DMA(V)}$  is the predominant inorganic arsenic metabolite which is rapidly excreted in urine by most mammals. However,

MMA(III) and DMA(III) are more cytotoxic, genotoxic, and potent inhibitors of the activities of some enzymes than the parent inorganic arsenic.<sup>12,100,101</sup>

The reduction of arsenate occurs nonenzymatically in the presence of glutathione (GSH). In the human liver on the other hand, conversion of arsenate to MMA is dependent on enzymes such as MMA reductase which appears to be a glutathione-S-transferase (omega). The methylation process also requires Sadenosylmethionine (SAM) and a methyltransferase.<sup>98,102-106</sup> Arsenic is also eliminated through the face, sweat and incorporation into hair and nails.<sup>107,108</sup> Arsenic is not an essential element for mammals. It mainly binds with protein sulfhydryl groups and disrupts enzymatic activity causing arsenic toxicity. As a result, it causes disruption in cellular glucose uptake, gluconeogenesis, fatty acid oxidation and glutathione production. Arsenate also inhibits oxidative phosphorylation of the cellular level causing disruption in cell energy production and substitutes phosphate compounds leading to arsenocholine.<sup>12,109-113</sup> Due to similarity in structure and properties, arsenate replaces phosphate *in vitro* forming glucose-6-arsenate and 6-arsenogluconate which is similar to glucose-6-phosphate and 6-phosphogluconate, respectively. As a result, hexokinase is inhibited by glucose-6-phosphate. Arsenate also hinders sodium pump and the anion exchange transport system of the human red blood cell by replacing phosphate. Arsenite readily binds *in vitro* with thiol-containing molecules such as glutathione (GSH) and cysteine inhibiting important biochemical events which could lead to toxicity. GSH is the most abundant thiol containing molecule in cells. The average concentration of GSH is about 7 mM in hepatocytes.<sup>114</sup> Arsenite prefers to bind with dithiol compounds than monothiol compounds, which is evident by the favorable transfer of arsenite from a (GSH)<sub>3</sub>-arsenic

complex to the arsenite complex of dithiol compound 2,3-dimercaptosuccinic acid (DMSA).<sup>98</sup> <sup>13</sup>C NMR studies have shown that the addition of DMSA to a solution of (GS)<sub>3</sub>As(III) induced the immediate release of GSH. DMSA is also oxidized to form cyclic and acyclic dimers and trimers when it reduces As(V) to As(III). Human urine contains DMSA that constitutes 90% of mixed disulfides DMSA(cysteine)<sub>2</sub> and 10% cyclic disulfides. This binds with arsenite in human body by replacing GSH and is excreted from the body with urine. DMSA is thought to form (DMSA)<sub>3</sub>[As(III)]<sub>2</sub> complex similar to the previously reported structure for a complex of antimony(III) with DMSA, (DMSA)<sub>3</sub>[Sb(III)]<sub>2</sub>.<sup>114,115</sup>

### 1.7. Remediation of Arsenic

Arsenic contamination commonly occurs in groundwater, surface water and drinking water as well as in soil and sediments through industrial wastewaters and mine drainage. There is a limit of maximum contaminant level (MCL) for arsenic in drinking water in various countries. The lowering of MCL for arsenic in drinking water from 50 to 10 ppb in many countries has necessitated the improvement and development of existing and new technologies. The U.S. EPA's MCL for arsenic in drinking water is 10 ppb, whereas Australia's MCL for arsenic is 7 ppb.<sup>116</sup> The concentration of arsenic in water will have an effect on the ability of water suppliers to comply with the drinking water standard. Throughout the world, 3.6% of water suppliers supply drinking water that contains more than 10 ppb of arsenic, and 5% supply water containing more than 20 ppb arsenic.<sup>117,118</sup> Various physical and chemical treatment processes are available to remove arsenic from aqueous solutions. These processes including sorption, chemical

precipitation/coprecipitation, ion exchange, filtration, reverse osmosis and electrodialysis have been used over the last few decades.<sup>119</sup> Reverse osmosis, nanofiltration and membrane distillation are also capable of removing more than 95% of arsenic from contaminated groundwater. The effectiveness of any of these technologies depends on various factors such as concentrations of arsenic in aqueous solutions, pH of solutions and the presence of competing ions such as phosphates.<sup>120</sup>

The chemical properties of the water (pH, iron content, competing ions etc) and the costs related to the removal of arsenic will attribute to the large number of various arsenic removal technologies. Although many technologies have been developed for household and community/municipal use, co-precipitation/adsorption and sorptive filtrations are the most commonly used technologies in developing countries like Bangladesh, Vietnam and Thailand.<sup>121</sup> These technologies are intended to remove As(V) from water. As a result, peroxidation of As(III) to As(V) is required by oxidants like ferric chloride, potassium permanganate and chlorine for most of these technologies. Co-precipitation/adsorption processes depend mainly on the coagulant. Coagulants like ferric sulfate or aluminum sulfate perform well to remove arsenic at nearly neutral pH values, but sludge disposal remains a problem. In presence of water, coagulants hydrolyse to form hydroxide which agglomerates during arsenate adsorption and settles down at the bottom. The sludge generated at the bottom contains up to 32% water and creates a disposal problem. Lime softening of water using  $\text{CaCO}_3$ ,  $\text{Mg(OH)}_2$  and  $\text{Fe(OH)}_3$  is also effective for removing arsenic especially at  $\text{pH} > 10.5$ . At extremely low arsenic concentrations, this method does not work well.<sup>121-123</sup>

Sorptive filtration technique uses solid supported active media to remove arsenates by sorption. Activated alumina, granular activated carbon, granular ferric hydroxide and iron oxide coated sand are commonly used as sorption material for arsenates. When the sorption sites are completely spent during arsenate removal, sorption materials are either discarded or regenerated. At a high total dissolved solid (TDS) concentration, activated alumina works well but competing ions decrease the efficiency of activated alumina. The regeneration of activated alumina also remains an issue to date. Spent activated alumina is regenerated by washing with dilute alkali solution followed by neutralization with either HCl or H<sub>2</sub>SO<sub>4</sub>. Drawbacks of using ion exchange resin include ion competition and iron precipitate clogging. Reverse osmosis and nanofiltration can remove 95% and > 90% of arsenic; however a high operating cost is associated with these methods.<sup>117,118</sup>

### **1.7.1. Activated Alumina**

Activated alumina (AA) falls in the category of a physical/chemical process, as it is used as a fixed bed adsorbent for removing arsenic from drinking water. Arsenic is removed from water through adsorption on the available binding site on the oxide surface of AA. AA is a dehydration product of Al(OH)<sub>3</sub> at high temperature which contains amorphous alumina oxide.<sup>124</sup> AA has been used as sorbent to remove arsenic in point of use systems as well as in full-scale water treatment facilities.<sup>125</sup> However AA has a slow rate of adsorption and removes As(V) more effectively than As(III), thus requiring the pre-oxidation of As(III) to As(V).<sup>126</sup> This process thus increases the complexity of the system as well as the viability of its utility in small scale house-hold

treatment units. A batch test at pH 6.5 and 8.5 has shown that approximately 87% and 65% of As(V), respectively could be removed from 10 mg/L of arsenic solution using 0.1 g of AA.<sup>125</sup> The removal of arsenic by AA was investigated by Jiang et al. AA has removed only 43% to 51% of arsenic from water that contains 21 to 1100 ppb arsenic at a pH range of 5.5 to 6.<sup>127</sup> The presence of competing ions such as sulfates, phosphates, fluorides and chlorides reduce the adsorption capacity to 50%. The studies of removing As(V) from an initial concentration range of 34 to 87 ppb have shown to achieve 87% to 98% of As(V). But the capacity of AA is only 0.25 g/kg of adsorbent. AA is effective only in the range of pH 5.5 to 6 to capture As(V). At low pH, the surfaces of alumina can attract As(V) by gaining positive charges due to protonation. But at pHs above 8, the charges on the alumina surfaces approach to zero point of charge (approximately 8.4-9.1). As a result, less number of positive charges are present on the surface to attract oxyanions which makes it less effective for arsenic removal at higher pH.<sup>128,129</sup>

The energetics of arsenate sorption on amorphous aluminum hydroxide (AHO) has been studied using flow adsorption calorimetry. The molar heats of adsorption are exothermic in the range of -3.0 to -66 kJ/mol at pH 5.7. Based on the sorption study, the mole ratio of arsenate sorption on alumina surface is obtained in the ratio of 1:8 (As:Al). This suggests that arsenate sorption capacity is mainly dependent on the presence of anion exchange capacity sites on the alumina surfaces. For each mole of arsenate adsorbed, an average of 1.61 moles of anion exchange capacity sites are lost during arsenate sorption.<sup>130</sup>

### 1.7.2. Activated Carbon

Adsorption of arsenic by activated carbon is another form of arsenic removal technology that has been used for decades. Adsorption is the adhesion of atoms, ions or molecules from a gas, liquid or dissolved solid to the surface of solid. Activated carbon is amorphous in nature and is highly porous with a high surface area. This provides a large number of sorption sites that are useful for removing arsenic from water. Coconut shells, wood char, lignin, petroleum coke, bone-char, peat, sawdust, carbon black, rice hulls, sugar, peach pits and various other waste materials are the major sources of preparing activated carbon. These materials are charred followed by heating and chemical treatments to obtain activated carbon. The adsorption capacity of activated carbon depends on many factors such as temperature, pH of solutions, ionic strength and presence of competing ions in solution. Although activated carbon captures As(V) in water, it is ineffective for removing As(III). The study of adsorption of As(III) and As(V) on activated carbon versus pH and temperature has shown that adsorption of As(III) is constant in the pH range of 0.16 to 3.5, but maximum adsorption of As(V) is observed at pH 2.35. The heat of adsorption for As(V) and As(III) varies from 4 to 0.75 kcal/mol and 4 to 2 kcal/mol, respectively, which suggests that arsenic is physisorbed on activated carbon through weak Van der Waals interaction. As a result, leaching of arsenic to groundwater, soil and sediments is possible after the disposal of arsenic containing activated carbon.<sup>11</sup> The efficiency of activated carbon produced from oat hulls in adsorbing As(V) also depends on the initial pH value. The adsorption capacity decreased from 3.09 to 1.57 mg of As per gram of activated carbon as pH of solution is increased from 5 to 8.<sup>131</sup>



### 1.7.3. Iron Removal Process

Iron-based materials show strong affinity towards arsenic. Various iron containing sorbents including zero-valent iron (ZVI), granular ferric hydroxide and ferric oxide have been explored for arsenic remediation from contaminated water.<sup>132-135</sup> However, removal of arsenite species is difficult compared to arsenate species.<sup>136</sup> Nano-sized ZVI has shown arsenic removal capacity from drinking water. However due to its tiny particle size, it has limited application in public water systems and small scale water treatment facilities. Activated carbon supported nanoscale ZVI has shown arsenite and arsenate adsorption capacity of 18.2 and 12.0 mg/g, respectively at pH 6.5. However, the presence of phosphates and silicates decreases the removal capacity of both arsenite and arsenate.<sup>137,138</sup> The effects of dissolved oxygen and pH of solutions on arsenic removal by ZVI have been investigated in both batch and column set up. Under oxic conditions, about 99.8% and 82.6% of the As(V) and As(III), respectively, is removed at pH 6. After the removal of dissolved oxygen by purging nitrogen, less than 10% of the As(III) and As(V) is removed by ZVI suggesting the oxidation of As(III) to As(V) as well as the oxic corrosion of Fe(0) to iron hydroxides.<sup>139</sup> A column study of As(III) capture by ZVI was conducted by Lien et al. The study shows that 7.5 mg As(III) was captured by one gram of iron.<sup>140</sup> However, other column and batch studies have shown arsenic removal capacity only in the range of 0.77 to 1.77 mg As/g Fe.<sup>141-143</sup>

The time dependent As(V) adsorption at different temperatures and at pH 6.5 indicates a rapid initial uptake of arsenic followed by a slower removal. About 80–95% of As(V) removal can be achieved within the first 30 min of contact with granular iron hydroxide. After this time period only 3–15% of additional As(V) is removed in the

following 24 h. A similar pattern is also observed at pH 7.5. The decrease in the concentration difference between the bulk solution and the surface is the driving force for slower removal rate. Ferrihydrite shows a similar trend of adsorption of As(V). As(III) adsorption at both pH conditions follows an identical pattern. About 90% of the total As(III) was adsorbed at equilibrium.<sup>41,144,145</sup>

In laboratory scale study, iron rich arsenic removal columns have been tested by pH leaching test. The sludges that have been tested for leaching studies contain 1270 mg/kg, 705 mg/kg and 313 mg As/kg. About 50–60% of the total As in the sludges is strongly bound with amorphous iron hydroxides. The concentration of dissolved arsenic in leachate solution is 35-45 times higher at high alkaline conditions (pH 11) compared to pH 3 indicating that strongly bounded As would be released in the environment at high alkaline and low redox conditions. This suggests that maintaining non-alkaline and high redox conditions are required for minimum As solubility and mobilization from the sludges.<sup>146</sup> Iron oxide shows an adsorption capacity of 2.2 mg As/g at pH 6.5.

Comparison of arsenic adsorption by iron oxide at pH 3 and 6.5 shows that the adsorption capacity of iron oxide decreases with increase in pH. Increase in pH causes the decrease of surface positive charge ( $\text{FeOH}_2^+$ ), which results in decreased attraction between iron oxide surfaces and arsenite and arsenate species.<sup>147</sup>

#### **1.7.4. Membrane Filtration Process**

Different types of filtration process such as microfiltration (MF), ultrafiltration (UF), nanofiltration (NF) and reverse osmosis (RO) can also be used to remove arsenic from water. These processes are useful to remove particulate arsenic from arsenic

contaminated water. In ground water when pH and arsenic concentration is low and suspended sediment loading is high, arsenic is present in suspended particulate form rather than dissolved form.<sup>148</sup>

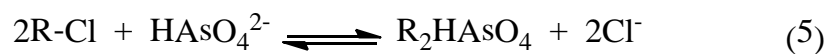
RO has been applied to remove low level naturally occurring groundwater arsenic in the presence and absence of chlorine. A 58% of arsenic can be removed by RO from unchlorinated water (from 79 ppb down to 33 ppb), whereas it can remove 91% arsenic from water (109 ppb to 10 ppb) in presence of chlorine suggesting the preoxidation of As(III) to As(V) in presence of chlorine.<sup>149</sup> RO removes 95% to 97% of As(V) in the pH range of 3 to 10 as compared to only 80% of As(III) in the pH range of 3 to 7 due to the neutral charge of As(III) species ( $\text{H}_3\text{AsO}_3$ ) exists at lower pH. Higher percentage of As(III) removal can be achieved by RO at pH 10 and above. Although RO is a reliable technique, it requires high capital operational costs. Another disadvantage of RO is formation of scales and deposits on the membrane as it also removes other inorganic contaminants (Fe, Ca etc.) from groundwater and drinking water.

NF is another membrane filtration technique which behaves like RO. The arsenic removal efficiency is primarily dependent on the pH and varying species of arsenic present in groundwater and drinking water. This technique removes 95% As(V) at an applied pressure of less than 1.1 MPa but it only removes 75% of As(III) which is very low compared to pentavalent arsenic.<sup>150</sup> Active poly-amide layers containing nanofiltration (NF) membrane are effective in removing 90 and 100% As(V), while As(III) removing efficiency which is less than 10% is very poor. Furthermore, percent As(III) removing capacity decreases with increasing As(III) concentration in aqueous solution.<sup>151</sup> Polyacrylonitrile (PAN) containing electro-ultrafiltration (EUF) membrane

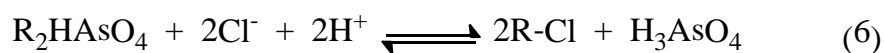
shows wide difference in removing As(III) and As(V) from water. About 90% of As(V) can be removed by EUF at voltages as low as 25 V, whereas only 10% of As(III) can be removed at same voltage without any pH adjustment. As(III) removing capacity increases to 76% at pH 10. This is due to the fact that As(III) is present as neutral species at lower pH values.<sup>152,153</sup>

#### 1.7.5. Ion Exchange

The ion-exchange process has similar principles to that of activated alumina, but it contains synthetic resins of enhanced ion-exchange capacity. The synthetic resin is primarily made of cross-linked polymer matrix. The charged functional groups can be acidic or basic, and are attached to the matrix surfaces through covalent bonding. The resins can be pretreated with anions such as  $\text{Cl}^-$  that can be used for the removal of negatively charged species arsenate. The capacity of ion exchange to remove arsenic is dependent on the presence of competing ions in water. Sulfates, nitrates and phosphates are the common competing ions present in water. These ions have a higher affinity for ion exchange resin than arsenate species and will decrease the efficiency of arsenic capture from water. Typical theoretical exchange capacities for strong base anion exchange resins range from 1.0 to 1.4 mEq/mL. Arsenate is adsorbed on the resin surfaces according to the equation 5 shown below.



The resin can be regenerated by using both HCl and NaCl. In presence of HCl, the arsenate is converted to arsenic acid (H<sub>3</sub>AsO<sub>4</sub>) as per the following reaction (Equation 6).<sup>154,155</sup>



#### 1.7.6. Biosorbents

Biosorption of arsenic has been examined as an alternative method to conventional techniques. Positively charged groups such as amine, hydroxyl and thiol groups at low pH, act as the potential adsorptive sites for negatively charged ions such as arsenate and arsenite species. Although a number of biosorbents are capable of removing arsenic from water, the poor selectivity of biomass associated with unspecific ion exchange reactions in the presence of competing ions is one of the main limitations towards its applications.

Keratin, a fibrous protein containing cysteine amino acid residues, based biomass has been explored for As(III) sorption. Biomass prepared from treated white chicken feathers shows 29.9 % As(III) and 5.1% As(V) removal capacity at pH 5.<sup>156</sup> X-ray absorption near edge structure (XANES) and extended X-ray absorption fine structure (EXAFS) determines that one arsenic atom is bonded to three sulfur atoms. The coordination number of arsenic and the interatomic distance obtained from structural parameters analysis are  $2.52 \pm 0.4$  and  $2.26 \pm 0.01$  Å, respectively.<sup>156,157</sup> Tea fungus, a waste produced during black tea fermentation, has also been examined to capture As(V) and As(III) from ground water samples. Autoclaved tea fungal mats as well as

autoclaved tea fungal mats pretreated with  $\text{FeCl}_3$  are exploited to remove As(V) and As(III). Autoclaved fungal mats and  $\text{FeCl}_3$  pretreated mats have been shown to remove 100% As(III) after 30 min and 77% As(V) after 90 min, and the capture capacity increases with increasing contact times and adsorbent loading with an optimum adsorbent dosage of 1.0 g/50 mL of water sample.<sup>158</sup>

#### **1.7.7. Solid Supported Reagents**

Many technologies including coagulation/filtration, ion-exchange, membrane technologies, chemical precipitation and adsorption can remove As(V) from drinking water. A large fraction of rural population in developing countries is exposed to high concentration of arsenic in drinking water. This requires the development of specifically designed technologies for water treatment in domestic use. However most of the existing methods are unsuitable for domestic and small-scale applications as required by disperse populations situated in rural areas. Coagulation/filtration process is not suitable for domestic application as it requires the handling of sludge disposal as well as the difficulty in achieving complete separation of arsenic from water. Membrane filtration processes have a relatively high operational cost. It also needs electric power and technically skilled operators for the application purpose which represents a disadvantage for isolated users. Application of Ion-exchange resins is also disadvantageous in rural areas due to its high costs of application.<sup>147</sup>

Numerous solid supported adsorbents have been developed for the effective removal of arsenic, by impregnating or modifying porous media surfaces with iron oxide, thiols and other metal oxides. Thiol based solid supported media including

polymer resins and silica gels have been specifically developed for heavy metal and metalloid capture from water. Soft heavy metals like cadmium, mercury, lead and arsenic show high selectivity and binding affinity towards thiols.<sup>159-161</sup> Solid supported thiols have also been widely investigated for the removal and preconcentration of metals like As(III), Cu(II), Cd(II), Ni(II), Hg(II), Pb(II) and Zn(II).<sup>162,163</sup> Solid supported reagents have been used due to their relative easiness of application and separation of solid media from aqueous solution. It also provides high surface areas which increases better interaction between reagents on the surface and metal contaminants in aqueous media.<sup>156,164,165</sup> Extensive research has been carried out to develop metal oxide based adsorbents to remove As(V) from aqueous solutions but these are less effective for removing As(III) from aqueous solution. Hybrid adsorbents prepared from organic and inorganic materials containing thiol groups have been effective for removal of As(III).

#### *Activated Carbon*

Iron impregnated granular activated carbon (GAC) has been studied by Gu et al. for arsenic removal from drinking water. Ferric ions are impregnated on GAC surfaces using aqueous ferrous chloride followed by oxidation using NaClO. Iron impregnated GAC is able to capture arsenic in wide pH range (4.4-11) but the efficiency decreases at higher pH values. Arsenic removal capacity is greater at an iron loading of about 6%. The maximum adsorption capacity of iron impregnated GAC is 2.96 mg As/g.<sup>11</sup> L-Cysteine methyl ester immobilized glassy carbon (CysOMe-GC) removes Cu(II), Cd(II) and As(III). Removal of As(III) requires a greater amount of CysOMe-GC as compared to removal of Cu(II) and Cd(II).<sup>166</sup>

## *Alumina*

Arsenic removal by adsorption on AA has been studied extensively. However, the pore structures of the conventional commercially available AA are ill-defined, and shows low adsorption capacities and exhibits slow kinetics.<sup>167</sup> Alum-impregnated activated alumina (AIAA) is used as an adsorbent for the removal of As(V) from water by batch mode. The efficiency of arsenic removal by AIAA from drinking water is much higher than that of activated alumina. AIAA predominantly adsorbs  $[\text{H}_2\text{AsO}_4]^-$  and  $[\text{HAsO}_4]^{2-}$  species in the pH range of 2.8 to 11.5 through physical adsorption as well as through intraparticle diffusion. It can remove As(V) to below 40 ppb from water containing an initial concentration of 10 mg As(V)/l.<sup>168</sup>

Activated alumina (AA) modified with mercaptopropyl-functionalized silica has enhanced As(III) uptake compared to non-modified activated alumina.<sup>167,169</sup> Thiol functionalized AA (AA-SH) is prepared by treating AA with pre-synthesized (3-mercaptopropyl)triethoxysilane (MPTS) with a capacity parameter of 5.6 mg As/g of adsorbent. The surface area of AA-SH is 2.02 m<sup>2</sup>/g and the pore diameter is 47.8 Å. AA-SH shows 80% binding with arsenic at pH 4. The binding falls to 40% at pH 11 and maximum binding is observed at pH 7 when 5 mg/L of As(III) is treated with 1.0 g/L of adsorbent. At a higher pH,  $[\text{H}_2\text{AsO}_3]^-$  is the predominant species. The electrostatic repulsion between  $[\text{H}_2\text{AsO}_3]^-$  and negatively charged surfaces at higher pH leads to the decrease in arsenic (III) adsorption.<sup>167</sup>



## *Silica*

Silica is most often used as a solid support due to its natural abundance and high mechanical and thermal stability of the support due to Si-O-Si network formation.<sup>161</sup> SiO<sub>2</sub> is formed by strong, directional covalent bonds, and has a well-defined local structure that contains four oxygen atoms at the corners of a tetrahedron around a central silicon atom. Iron oxide coated sand (IOCS) has been shown to remove As(III) from solution. The efficiency of As(III) removal increases with increasing pH after pH 4.5. A maximum of 88% As(III) removal is observed at pH 7.5 and remained constant with increasing pH. The percentage of As(III) removal increases with increasing contact time between the solution and IOCS. Removal efficiency of 90% is achieved within 125 min and remains constant after that.<sup>170</sup> In another experiment, iron oxide coated sand showed about 75% As(III) capture within 2 h at pH 7.5-7.8 when 10 ppm As(III) solution was treated with 10 g/L of sorbent dose. It showed 80% of As(V) binding ability within 3 h at same sorbent loading.<sup>171</sup>

### **1.8. BDTH<sub>2</sub> as Precipitation Agent**

1,3-benzenediamidoethanethiol (BDTH<sub>2</sub>) (Figure 1.3.a) is a dithiol chelating agent which has emerged as the best precipitating agent for various soft heavy metals. Although BDTH<sub>2</sub> contains two thiol groups in the molecular framework, it does not form disulfide bonds (-S-S-) through oxidation which is the most common problem of many thiol containing reagents.<sup>172,173</sup> The oxidation potential of BDTH<sub>2</sub> determined by cyclic voltammetry is 1.6 V. Due to its high affinity for soft heavy metals, BDTH<sub>2</sub> binds with soft heavy metals under a wide range of conditions and can remove these metals

from various sources such as gold ore processing effluent, lead battery recycling effluent, acid mine drainage and contaminated soil.<sup>174,175</sup> It acts as a precipitating agent for metals such as copper, cadmium, mercury, lead, arsenic and selenium by forming insoluble metal-ligand complexes which are stable under a wide pH range and oxidizing conditions.<sup>172,175,176</sup> The insolubility of the BDT–M compounds is due to the formation of strong, non-polar, covalent M–S bonds. BDTH<sub>2</sub> has been explored for low level mercury removal from groundwater with different concentration of 65.6 ppb and 188.0 ppb Hg. It shows complete removal of mercury from aqueous solution to well below 0.05 ppb, which satisfies the drinking water limit of 2 ppb.<sup>177,178</sup> It will remove 99.8% lead and 96% mercury within an hour from 50 ppm metal concentration on BDTH<sub>2</sub> application in a 1:1 molar ratio to metal.<sup>176</sup>

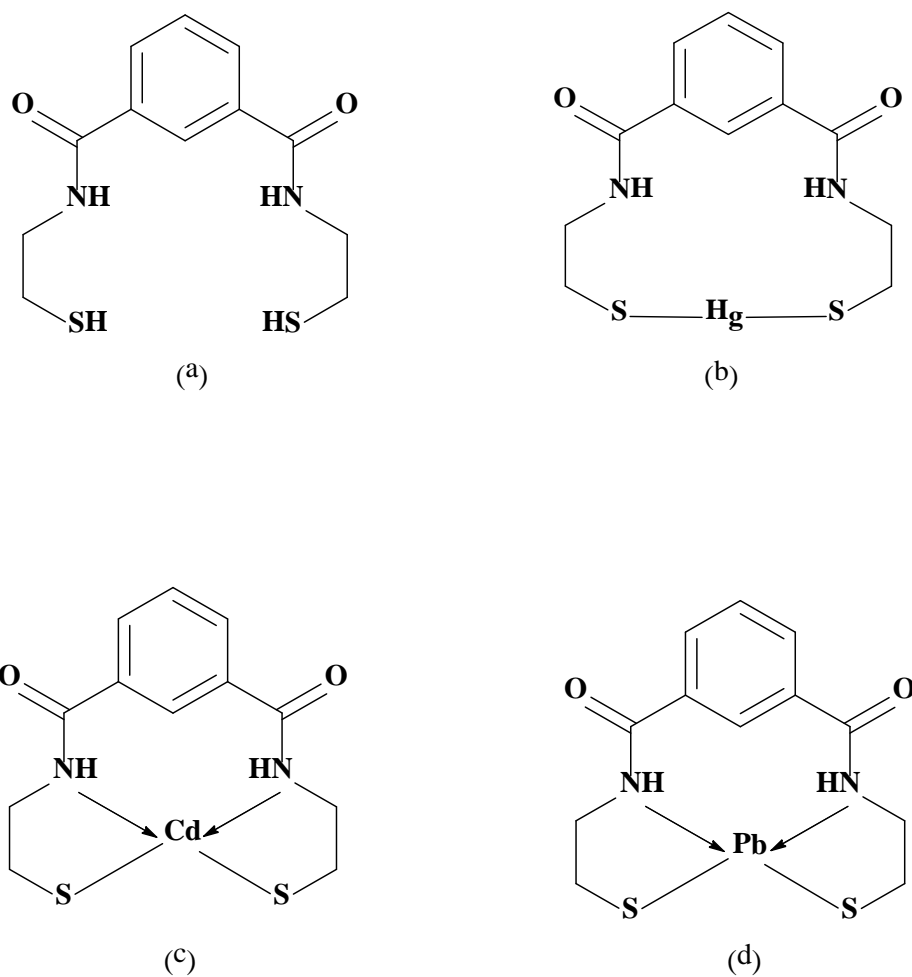


**Figure 1.3.** Structure of (a) BDTH<sub>2</sub> and its (b) Hg, (c) Cd and (d) Pb compounds<sup>179</sup>

Wastewater from lead battery recycling plant contains considerable amount of lead and other metals including Sb, As, Cd, Cu, Fe, Se and Sn in low concentration. Treatment of this wastewater with BDTH<sub>2</sub> is found to remove more than 99.4% of lead from an average initial concentration of 3.61 ppm.<sup>180</sup> Mercury contamination from Gold-Cyanide Process (GCP) is a serious environmental issue due to the improper treatment of the residual gold leachate solution. BDTH<sub>2</sub> effectively removes more than 99% of mercury from 34.5 ppm solution with increased dose of precipitating agent.<sup>174</sup> It also irreversibly binds and removes mercury from contaminated soil with percent

immobilization increasing from 82.6 % to 99.6% with increased BDTH<sub>2</sub> dosage.<sup>181</sup>

BDTH<sub>2</sub> will precipitate heavy metals from acid mine drainage (AMD) solutions.<sup>182</sup> Acid mine drainage is the result of oxidation of pyrite (FeS<sub>2</sub>) and various other metal sulfides leading to leaching of heavy metals into acid run-off water and is most commonly observed in coal refuse areas. Microencapsulation is often used to prevent AMD from coal refuse piles. BDTH<sub>2</sub> is an effective coating material on pyrite via formation of covalent Fe-S bonds (Figure 1.4). Iron leaching is reduced by 99.3%, 97.5% and 66.4% at pH 6.5, pH 3.0 and acidic oxidative condition, respectively due to the formation of BDTH<sub>2</sub> coating on coal. Other metals such as Mn, Cu, Ni, Zn and Co also show reduced leaching.<sup>183</sup>

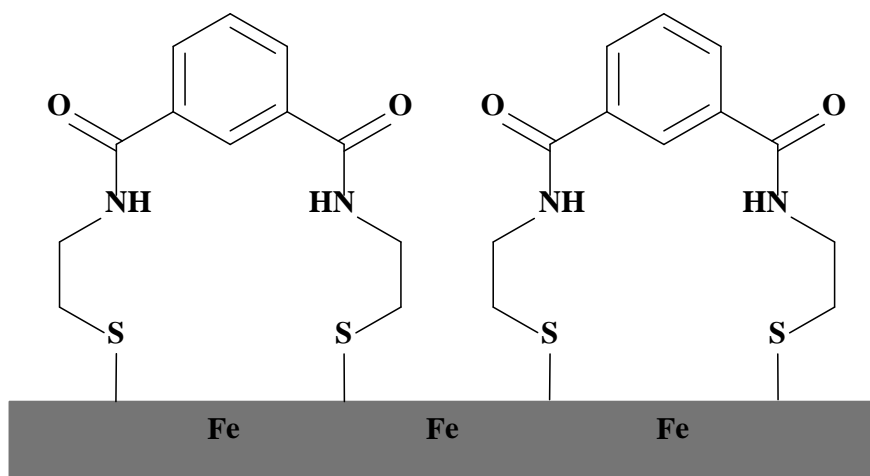


**Figure 1.4.** Coating of BDTH<sub>2</sub> on pyrite through formation of Fe-S covalent bond<sup>184</sup>

### 1.9. Interaction of BDTH<sub>2</sub> with Arsenic

BDTH<sub>2</sub> has been explored in arsenic removal by batch test and field test filtration columns. The batch test As(III) removal by using direct addition of BDTH<sub>2</sub> showed

100% arsenic capture at pH 5 and 7, both under nitrogen and air. Similarly 97% and ~100% As(III) capture was observed at pH 9 under nitrogen and air, respectively. On the other hand, poor As(III) removal (34.5% under air and 22.9% under nitrogen) was noticed at pH 3 due to the presence of solely uncharged species  $\text{H}_3\text{AsO}_3$  in the pH range of 0 to 5. Above pH 5,  $[\text{H}_2\text{AsO}_3]^-$  species starts to form at a very low concentration ( $10^{-10}$  M). With increasing pH the concentration of  $[\text{H}_2\text{AsO}_3]^-$  species increases which makes it easier to remove arsenite species effectively between pH 5 and pH 9. Negatively charged  $[\text{H}_2\text{AsO}_3]^-$  species formed are electrostatically attracted to thiol groups resulting in better interactions between thiol groups and  $[\text{H}_2\text{AsO}_3]^-$  species in solution. Also the  $\text{pK}_a$  of thiol varies in the range of 7.45 to 10.70.  $\text{pK}_a$  is the logarithmic measure of the acid dissociation constant. The  $\text{pK}_a$ 's of the most common thiol containing molecules are relatively non-acidic such as cysteamine (8.35), cysteine (8.58-10.36), N-acetyl cysteine (9.52), glutathione (8.63) and dihydrolipoic acid (10.70).<sup>185-187</sup> As a result, at higher pH both the thiol and arsenite species will be negatively charged. This will result in poor binding interactions between thiol and arsenite species. At very low pH, neutral arsenite species and protonated thiol groups of BDTH<sub>2</sub> are present in solution, which makes it difficult to form a bond between As(III) and sulfur. The batch test study showed poor removal of As(V) by BDTH<sub>2</sub>. The soft sulfhydryl groups of BDTH<sub>2</sub> will not bond with arsenate which is hard Lewis acid. This is in agreement to the fact that arsenate does not react with sulfhydryl groups.<sup>188,189</sup> As(III) forms a strong bond with sulfhydryl groups of cysteine in proteins, which causes enzyme inactivation resulting in arsenic toxicity. The toxicity of arsenite is about 60 times more than arsenate due to the difference in reactivity of arsenite and arsenate with sulfhydryl groups.<sup>188</sup> BDT-As(III) was

synthesized in small and large batch by reacting  $\text{NaAsO}_2$  with  $\text{BDTH}_2$  and then characterized by melting point, infrared spectroscopy and mass spectroscopy. It is proposed that the structure of BDT-As(III) compound is  $\text{BDT}_3\text{As}_2$ , where one As(III) is coordinated with three sulfur atoms. This proposed BDT-As(III) is similar to the structure of mono and dithiol containing thioarsenic compounds such as tris-(pentafluorophenylthio)-arsen (Figure 1.5.a) and 1,2-bis-dithiarsolan-2-ylmercapto-ethane (Figure 1.5.b).<sup>190,191</sup>

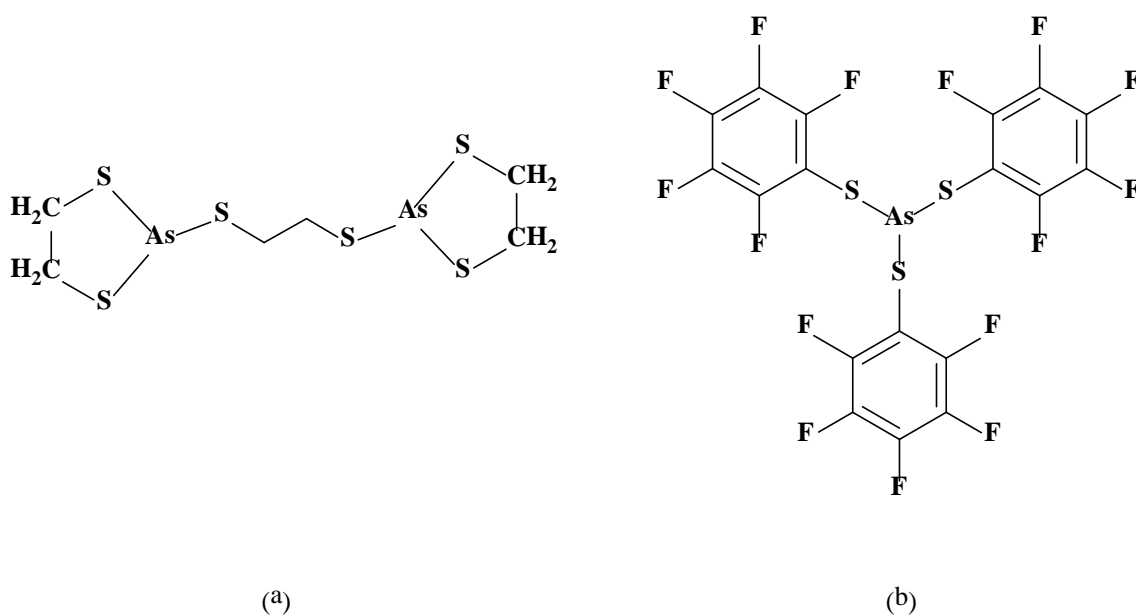


**Figure 1.5.** Tricoordinated arsenic compounds

Field studies of filtration column prepared with  $\text{BDTH}_2$  and ZVI have been conducted on 39 groundwater samples in West Bengal, India. Iron was used to oxidize As(III) to As(V) in groundwater samples. Arsenic contamination of groundwater is a serious issue in various parts of West Bengal. In these areas, arsenic concentration varies from  $8.82 \pm 0.19$  ppb to  $220.47 \pm 4.85$  ppb. No detectable concentration of arsenic after

the filtration of water samples through a BDTH<sub>2</sub> column, but iron level in the effluent samples increased in the range of  $2.23 \pm 0.00$  ppm to  $95.09 \pm 16.96$  ppm after column filtration. Elevated levels of iron can be an issue as it causes changes in the color of water to an orange, rusty hue and also negatively affects the taste and odor of water.

### 1.10. Conclusion

The primary goal of this dissertation research is to explore the extension of ligand utility of BDTH<sub>2</sub> in column filtration for the removal of As(III) from drinking water.

Remediation of arsenic from groundwater and drinking water often requires precipitation/coprecipitation, coagulation and flocculation followed by filtration of hazardous solids formed to obtain arsenic free water. Surface adsorption by various metal oxides and oxyhydroxides is an alternative technology for the remediation process. However, although these metal oxides and oxyhydroxides are often excellent adsorbents for As(V), they are ineffective for removal of As(III) from water. Membrane filtration on the other hand, is not economically viable for application in small scale.

BDTH<sub>2</sub> has been successfully applied in the batch remediation of different soft, divalent metals such as Pb(II), Cd(II), Cu(II), Mn(II), Zn(II), Fe(II) and Hg(II) from ground water, coal refuse, gold ore, lead battery recycling plant wastewater and contaminated soils.<sup>172,174-177,179,180,182,183,192-196</sup> However, application of BDTH<sub>2</sub> requires dissolution in organic solvent or the metallated form BDTH<sub>2</sub>, which limits the applicability of the compound. The batch treatment of arsenic contaminated water by BDTH<sub>2</sub> in large scale water treatment systems works out perfectly well. The problem lies in the application of BDTH<sub>2</sub> as a low cost, portable, lightweight column in homes and

arsenic affected areas of developing countries, where large water treatment systems and cost of remediation technologies are issues. This requires the development of alternative methods of ligand application. While the application of BDTH<sub>2</sub> as an ethanolic solution limits its environmental application, potassium or sodium salt of BDTH<sub>2</sub> needs immediate application to avoid the formation of disulfide products. The application of BDTH<sub>2</sub> as filtration column material with ZVI and sand as inert solid support for arsenic removal is found to be effective. However the leaching of BDTH<sub>2</sub> and iron from filtration column limits its applicability, thus requiring the search for alternative methods of BDTH<sub>2</sub> application as arsenic removal agent in filtration columns.<sup>189</sup> Immobilization of BDTH<sub>2</sub> on solid support by covalent bonding can eliminate the ligand washing out of the column, as well as it will increase the dispersion of ligand with increased surface area, decrease ligand loading and increase better ligand arsenic interaction. The presence of reactive functional groups on the side chain of BDTH<sub>2</sub> will increase the possibility of immobilizing the ligand on a solid support.

The focus of the dissertation is the design and synthesis of the acid derivative of BDTH<sub>2</sub> (ABDTH<sub>2</sub>) that can be immobilized on silica. Following the synthesis and characterization of ABDTH<sub>2</sub>, the As(III) complex of the compound will be synthesized and characterized to determine the binding nature followed by leaching study over a pH range of 5-9 to determine the stability of the As(III) complex. This work further focuses on the immobilization of newly synthesized ligand on silica support followed by its application in batch study over a pH range of 5-9 and column study for the removal of As(III) from water. The current research work will also focus on the development of



more robust and inexpensive means of remediation of arsenic by designing solid supported ligands for filtration columns.

## CHAPTER 2

### ABDTH<sub>2</sub>: A Functional Reagent for As(III)

#### 2.1. Introduction

The new dithiol compound, 2,2'-(isophthaloylbis(azanediyl))bis(3-mercaptopropanoic acid) (Figure 2.1b), is designed to incorporate the metal-bonding capability of cysteine, an essential, naturally occurring, hydrophobic amino acid, in a framework similar to BDTH<sub>2</sub> (Figure 2.1a). The compound is conventionally abbreviated ABDTH<sub>2</sub> to show that it is similar to BDTH<sub>2</sub> but with two carboxylic acid (“A”) groups. Cysteine (CSH) is an integral part of many metal-binding enzymes including the metallothioneins. It is potentially a trifunctional amino acid with the ability to coordinate metals through its carboxyl, amino and thiol functional groups. The pK<sub>a</sub> values for these groups are: 1.69-2.44 (COOH), 8.17-8.78 (NH<sub>2</sub>) and 10.29-10.71 (SH). In aqueous solutions cysteine exists as the ammonium zwitterion.<sup>197-201</sup> Cysteine forms covalent compounds with Hg, Cd, Pd, and several other metals. These metal complexes have been used to study the bonding interactions between metals and the thiol group of cysteine as a model for cysteine containing protein and peptide.<sup>202</sup>

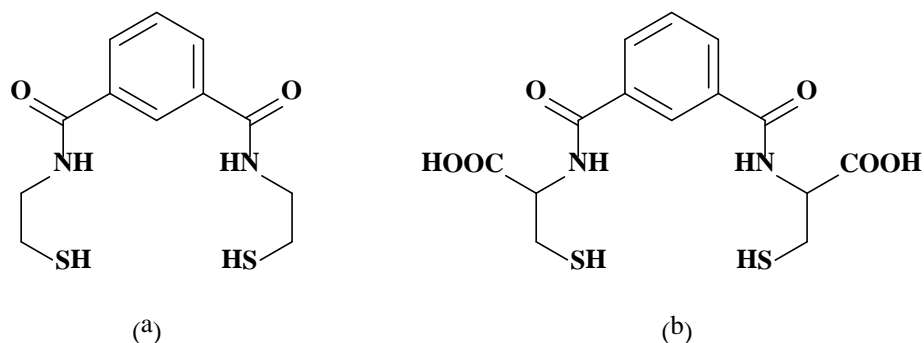


**Figure 2.1.** The molecular structures of (a) BDTH<sub>2</sub> and (b) ABDTH<sub>2</sub>

The Cd(II) compound of cysteine was studied at two different alkaline pH (7.5 and 11.0) with ligand to metal molar ratios varying from 2.0 to 20. A distorted tetrahedral CdS<sub>2</sub>N(N/O) (Figure 2.2.a) coordination geometry was observed at pH 7.5 for the molar ratio of 2.0 indicating that both ligands bond to Cd(II). This was confirmed by a single <sup>113</sup>Cd NMR resonance at 509-527 ppm. The average Cd-S and Cd-N(N/O) bond distances, measured by Cd K-edge EXAFS (Extended X-ray Absorption Fine Structure) spectroscopy, were  $2.54 \pm 0.02$  and  $2.34 \pm 0.04$  Å, respectively. On the other hand, at pH 11.0 the dominating species was [Cd(S,N-Cys)<sub>2</sub>]<sup>2-</sup> (Figure 2.2.b) due to deprotonation of the amine groups. Consequently the metal-ligand bond distances are shortened slightly. An increase in ligand concentration in the solution at pH 7.5 caused a corresponding increase in the number of thiolate ligands in the cadmium (II) complexes with [Cd(S-cysteinate)<sub>4</sub>]<sup>n-</sup> complex being the predominant species.<sup>202</sup>

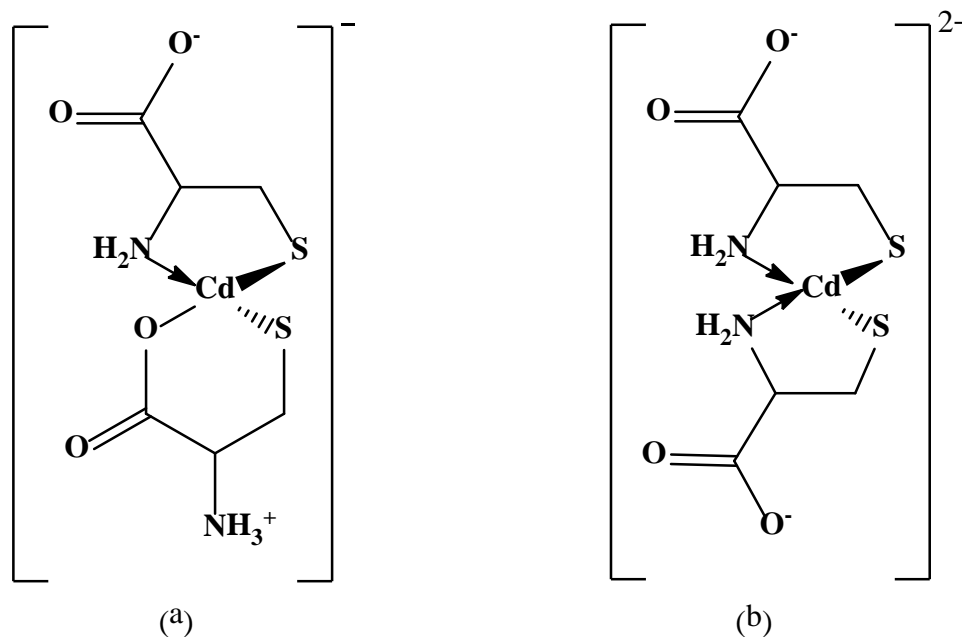


**Figure 2.2.** Cd(II)-Cysteine complexes in solution at pH 7.5 (a) and pH 11 (b)

Cysteine formed two, three and four coordinated complexes with mercury through metal-sulfur coordination ( $\text{Hg}(\text{SC})_n$  ( $n = 2, 3, 4$ )) in alkaline aqueous solutions. Different species of mercury-cysteine complexes were obtained in solution at varying Cys/Hg ratios of 2.2, 3.3, 4.3, 5.3 and 10.1 with adjustment of the pH (by NaOH) to 7.7.<sup>203</sup> EXAFS spectroscopy confirmed the presence of a linear two-coordinated complex of mercury-cysteine in alkaline condition at low concentration of cysteine to mercury with an average Hg-S bond distance of 2.36 Å. Increasing cysteine concentrations in solution led to the formation of three and four coordinated mercury-cysteine complexes with an average Hg-S bond distance of 2.44 Å and 2.50 Å, respectively.<sup>203</sup> The Hg-S bond distance decreases with decreasing coordination number of mercury thiolate complex.

Cysteine-arsenic complexes have been studied due to the strong affinity of arsenic towards the sulfur moiety of cysteine rich proteins. Coordination of arsenic with cysteine

produces a 1:3 arsenic:cysteine complex ( $\text{As}(\text{SC})_3$ ) through sulfur-arsenic bonding.<sup>204-206</sup>

A biosorbent containing cysteine has been developed from chicken feathers that captures  $\text{As}(\text{III})$  species from aqueous solutions. XANES study indicates the presence of arsenic bonded to three sulfurs of cysteine units on the biosorbent. The interatomic distance between arsenic and sulfur is  $2.26 \pm 0.01 \text{ \AA}$ .<sup>207</sup> Raman spectroscopy demonstrating the absence of a sharp band at  $2556 \text{ cm}^{-1}$  (S-H vibrational mode) and the presence of an intense band at  $401.5 \text{ cm}^{-1}$  indicates the formation of As-S bonds in  $\text{As}(\text{III})$ -cysteine complex.<sup>157</sup>

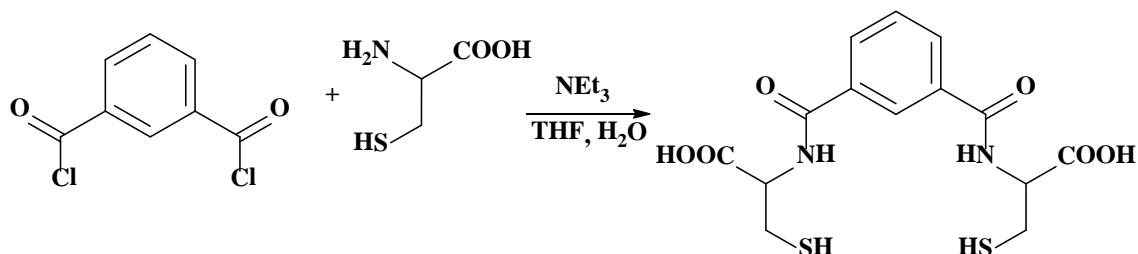
BDTH<sub>2</sub> binds with Cd, Hg, Pb and As by forming insoluble metal-ligand complexes containing strong, non-polar, covalent M-S bond within metal-ligand framework.<sup>172,179</sup> One of the major advantages of BDTH<sub>2</sub> over cysteine is that BDTH<sub>2</sub> does not form disulfide bond through oxidation.<sup>172,208-210</sup> As a result, thiol groups of BDTH<sub>2</sub> are available for bonding with metals. It would be ideal to have cysteine units in a molecular framework similar to BDTH<sub>2</sub> in order to synthesize ABDTH<sub>2</sub> by combining cysteine and isophthaloyl chloride together, so that it can be immobilized on solid supports like silica without forming disulfide bonds. The solid-supported ABDTH<sub>2</sub> thus formed can be used as a filtration column material for heavy metal remediation. This chapter will demonstrate the synthesis and characterization of ABDTH<sub>2</sub>.

## **2.2. Results and Discussion**

### **2.2.1. Synthesis and Characterization**

A yellow microcrystalline thiol ligand was synthesized according to scheme 2.1 using isophthaloyl chloride and L-cysteine in 1:2 ratio as starting material. Synthesis of

ABDTH<sub>2</sub> was carried out in various quantities of 20 g to 100 g. Characterization data of ABDTH<sub>2</sub> from different batches of synthesis showed similar values.



**Scheme 2.1.** Synthesis of ABDTH<sub>2</sub>

The melting point of ABDTH<sub>2</sub> was in the range 105-109<sup>o</sup>C. The melting point of the compound was higher than monothiol compounds and was consistent with the range of melting point of dithiol compounds reported in literature.<sup>180,211,212</sup> However, the melting point of ABDTH<sub>2</sub> was lower than the melting point of BDTH<sub>2</sub> (133-135<sup>o</sup>C). This is most likely due to the presence of H-bonded solvent. In IR spectra, a strong and broad absorption band at 3337 cm<sup>-1</sup> was due to the presence of carboxylic acid group in the ligand. The bands for aromatic C-H, methylene C-H, acid carbonyl (C=O), amide carbonyl (C=O) and amide N-H bending at 3066, 2962, 1734, 1647 and 1533 cm<sup>-1</sup>, respectively were also seen in the spectra of the synthesized compound. The bands for aromatic C-H, methylene C-H, amide carbonyl (C=O) and amide N-H bending were similar to the IR bands observed in BDTH<sub>2</sub>.<sup>180,213</sup> The absorption peak in IR spectra at 2568 cm<sup>-1</sup> confirmed the presence of a characteristic thiol peak in the molecule. The observed IR band was consistent with the reported IR value of S-H bond in other compounds such as N-acetyl-L-cysteine (2551 cm<sup>-1</sup>), ethanediol bismercaptoacetate

(2560  $\text{cm}^{-1}$ ), bis(2-mercaptoethyl) malonate (2560  $\text{cm}^{-1}$ ), BDTH<sub>2</sub> (2557  $\text{cm}^{-1}$ ).<sup>213,214</sup> ABDTH<sub>2</sub> has a similar molecular framework to BDTH<sub>2</sub> including the presence of carboxyl groups on the  $\alpha$ -carbon next to NH (Figure 2.1b).<sup>181</sup> The presence of amide carbonyl and amide N-H bending suggested that L-cysteine was bonded to the isophthaloyl chloride through amide bond formation. <sup>1</sup>H NMR (400 MHz) of the compound in DMSO-*d*<sub>6</sub> showed triplets at  $\delta$  2.60 ppm (2H) attributed to thiol proton. The proton signals at  $\delta$  7.60 ppm, 8.06 ppm and 8.41 ppm corresponded to aromatic protons. Other signals at  $\delta$  2.90 ppm, 4.50 ppm, and 8.90 ppm corresponded to methylene protons at  $\alpha$  and  $\beta$  carbons and amide NH, respectively. ESI (electrospray ionization) mass spectrum showed the molecular fragment C<sub>14</sub>H<sub>16</sub>N<sub>2</sub>O<sub>6</sub>S<sub>2</sub> peak at *m/e* 373, which corresponded to the parent ion of the molecule. The characterization data from IR, NMR and mass spectroscopy demonstrated the synthesis of ABDTH<sub>2</sub> similar to the molecular framework of BDTH<sub>2</sub>. BDTH<sub>2</sub> had shown excellent heavy metal capture ability from different waste waters. It is also expected that with similar molecular structure ABDTH<sub>2</sub> will have the similar chemical properties and will be used to support on silica to remove arsenic and other heavy metals from drinking water.

### 2.2.2. pK<sub>a</sub> Determination of ABDTH<sub>2</sub>

The pK<sub>a</sub> of ABDTH<sub>2</sub> was determined by volumetric titration (Figure 2.3) of ABDTH<sub>2</sub> (in triplicate) in water with dilute sodium hydroxide (NaOH). A slurry of ABDTH<sub>2</sub> in water was used for the titration. The initial pH of a saturated solution of ABDTH<sub>2</sub> in water was determined to be in the range of 2.55-2.85. The titration experiment indicated that the average pK<sub>a</sub>'s of ABDTH<sub>2</sub> were pK<sub>a1</sub> = 2.98 ± 0.23 and

$pK_{a2} = 4.67 \pm 0.08$ . These values are comparable to the  $pK_a$  values of other dicarboxylic acid such as terephthalic acid (3.51, 4.82) and *m*-phthalic acid (3.50, 4.50) containing two carboxylate groups connected to a benzene ring (Figure 2.4.a and b, respectively).<sup>215</sup> The higher  $pK_a$  value of the carboxylic acid groups in ABDTH<sub>2</sub> as compared to  $pK_a$  of carboxylic acid in cysteine ( $pK_a$  1.7)<sup>216</sup> suggested that cysteine was connected to a benzene ring in ABDTH<sub>2</sub> and thus the acidity of carboxylic acid in ABDTH<sub>2</sub> was lower than in cysteine.

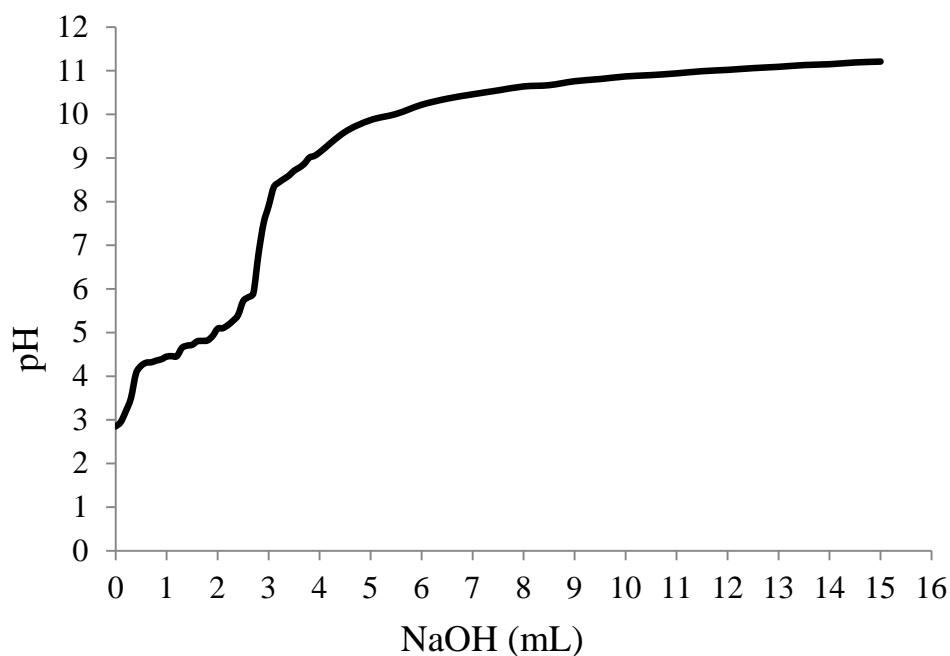


**Figure 2.3.** Titration of ABDTH<sub>2</sub> with 0.025 M sodium hydroxide (NaOH) ( $pK_{a1}$  3.20 and  $pK_{a2}$  4.60)



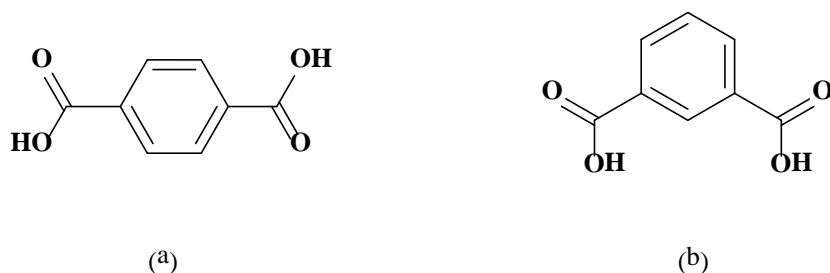


**Figure 2.4.** Structure of (a) terephthalic acid and (b) *m*-phthalic acid

## 2.3. Experimental

### 2.3.1. Materials and Techniques

All the reactions were carried out at room temperature. The following reagents were used as received from the indicated vendors: L-cysteine hydrochloride (98% purity, Sigma), triethylamine (> 99.5%, Mallinckrodt Chemicals), isophthaloyl chloride (> 99%, TCI America), tetrahydrofuran (Acros Organics) and ethyl acetate (Fisher Scientific). DMSO- $d_6$  (99.9%), obtained from Cambridge Isotope Laboratories Inc., was used as NMR solvent. ABDTH<sub>2</sub> was characterized by nuclear magnetic resonance (NMR), infrared (IR) spectroscopy, mass spectroscopy (MS) and melting point. <sup>1</sup>H NMR of ABDTH<sub>2</sub> was produced in DMSO- $d_6$  using tetramethoxy silane (TMS) as internal solvent on a Varian INOVA instrument at room temperature at an operating frequency of 399.78 MHz with a pulse of 71.2 deg. Mass spectra was obtained on a Finnigam LTQ instrument. IR of compounds was produced using KBr pellets with a model Nicolet Avatar 370 DTGS IR spectrophotometer (Thermo Electron Corporation).

### 2.3.2. Synthesis

Triethylamine (114 mL, 83.5 g, 826 mmol) was added to a stirring solution of L-cysteine (100.2 g, 826 mmol) in water (800 mL, DI) under nitrogen at 25°C. The resulting clear solution was stirred for 5 min. Isophthaloyl chloride (80 g, 394 mmol) in THF (800 mL) was then added dropwise to the reaction and stirred for 12 h. The solution was divided into two equal parts and each extracted with ethylacetate (400 mL; 800 mL total). The ethylacetate extracts were combined and dried over Na<sub>2</sub>SO<sub>4</sub> before the solvent was removed under vacuum to produce ABDTH<sub>2</sub> as a light yellow solid (113 g, 76% yield). Mp: 105-109°C; IR (KBr, cm<sup>-1</sup>): 3337 (broad, acid OH and secondary NH), 3066 (aromatic CH), 2962 (methylene CH), 2568 (SH), 1734 (CO, acid), 1647 (CO, amide), 1533 (NH), 689 (CS); <sup>1</sup>H NMR (DMSO-*d*<sub>6</sub>, 400 MHz): δ (ppm) - 2.60 [t, 2H, SH], 2.90 [m, 4H, CH<sub>2</sub>], 4.50 [m, 2H, CH], 7.60 [t, 1H, C<sub>6</sub>H<sub>4</sub>], 8.06 [d, 2H, C<sub>6</sub>H<sub>4</sub>], 8.41 [s, 1H, C<sub>6</sub>H<sub>4</sub>], 8.90 [d, 2H, NH]; MS (+ESI, Finnigam LTQ): 373 (C<sub>14</sub>H<sub>16</sub>N<sub>2</sub>O<sub>6</sub>S<sub>2</sub>).

### 2.3.3. Titration

The titration of ABDTH<sub>2</sub> was conducted in triplicate using a low concentration of NaOH solution. ABDTH<sub>2</sub> (49.5 mg, 0.13 mmol; 51.9 mg, 0.14 mmol; 49.6, 0.13 mmol) was dissolved in 200 mL beaker with D.I. water (100 mL) each time providing a slurry of ABDTH<sub>2</sub> solution with an initial pH of 2.85, 2.55 and 2.61, respectively. The solutions were titrated with 0.025 M NaOH by dispensing both 100 μL and 500 μL from a 1000 μL pipette to yield the titration curves shown in Figure 2.3. From this data, the average values of pKa<sub>1</sub>, 2.98 (± 0.23) and pKa<sub>2</sub>, 4.67 (± 0.08) were calculated.

## 2.4. Conclusion

A dithiol organic compound ABDTH<sub>2</sub> was synthesized from isophthaloyl chloride and L-cysteine which has similar molecular framework as BDTH<sub>2</sub>. IR, <sup>1</sup>H NMR and mass spectroscopy indicated the formation of ABDTH<sub>2</sub>. IR showed the characteristic thiol peak at 2568 cm<sup>-1</sup>. The thiol peak at 2.60 ppm was observed in <sup>1</sup>H NMR. Due to presence of the thiol group, ABDTH<sub>2</sub> can be applied in removing toxic heavy metals and metalloids like mercury, cadmium, lead and arsenic. The applicability of attaching ABDTH<sub>2</sub>, containing carboxylic acid group, on solid support such as polystyrene, silica gel through formation of amide linkages will be explored and such ABDTH<sub>2</sub> solid supports can be used as filtration column material for water purification.

## CHAPTER 3

### Synthesis of ABDT-As(III)

#### 3.1. Introduction

Arsenic is a metalloid element which exists in various oxidation states in nature.<sup>11,108,110</sup> Arsenic and its compounds have been used as antimicrobial agents in the treatment of syphilis and trypanosomiasis, promyelocytic leukemia and many other diseases.<sup>217-220</sup> Inorganic arsenic is also carcinogenic causing acute toxicity to humans and animals due to accumulation of arsenic through drinking water and other sources.<sup>221-223</sup> Toxicity of arsenic is dependent on the species of arsenic present in the environment. Arsenite (As(III)) is more toxic than arsenate (As(V)) due to its strong affinity towards thiol moiety in biological system. Arsenic binds with sulfur or sulphhydryl moiety of thiol containing proteins such as enzymes inhibiting the activity of the protein by forming covalent As-S bond thus causing the toxicity.<sup>98,157,224-226</sup>

Mononuclear As(III)-thiolate compounds have been known over the decades. Dimethylarsinic acid,  $(\text{CH}_3)_2\text{AsO}(\text{OH})$ , reacted with cysteine (CSH) *in vitro* to give S-(dimethylarsino)-DL-cystein  $((\text{CH}_3)_2\text{As}(\text{SC}))$  (SC = monoanionic cysteine unit) complex (Figure 3.1).<sup>204</sup> The synthesis of  $(\text{CH}_3)_2\text{As}(\text{SC})$  from water had also been demonstrated. It inhibited the growth of the Gram positive bacteria, *S. aureus* 209.<sup>204,227</sup> Arsenic(III) coordinated with three cysteine units  $(\text{As}(\text{SC})_3)$  had also been reported.<sup>205</sup>

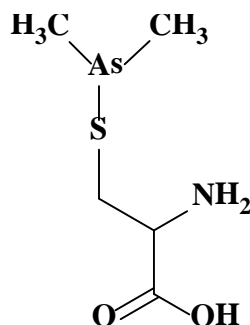


**Figure 3.1.** S-(Dimethylarsino)-DL-cysteine

As(SC)<sub>3</sub> (Figure 3.2.a) was formed in an aqueous solution when H<sub>3</sub>AsO<sub>3</sub> was combined with three equivalents of cysteine in the pH range of 2.5 to 7. As the pH of the solution was increased, the hydroxyl groups displaced two of the cysteine molecules to form the negatively charged compound, [As(SC)(OH)<sub>2</sub>]<sup>-</sup> (Figure 3.2.b) which is predominate in the pH range of 8.0 to 9.5.<sup>217</sup> Cysteine-rich biomass was found to adsorb As(III) by coordinating As(III) to three cysteine units to form As(SC)<sub>3</sub> confirmed by X-ray absorption fine structure (XAFS).<sup>156,157</sup> Arsenic dithiolate and trithiolate have also been reported in literature. In 1,2-bis-dithiarsolan-2-ylmercapto-ethane, arsenic forms dinuclear complex with 1,3-dithiopropene having one 1,3-dithiopropene unit bridging between two arsenic centers.<sup>228-230</sup> Arsenic also formed compound with glutathione (GSH). Glutathione plays an important role in the detoxification of arsenic. Arsenic coordinates with sulfur from three glutathione units to form As(SG)<sub>3</sub>.<sup>231-233</sup> ABDTH<sub>2</sub> containing cysteine units in the molecular framework has been synthesized for the removal of As(III) from water. This chapter will discuss the interaction of As(III) with ABDTH<sub>2</sub> and the structural features of ABDT-As(III).

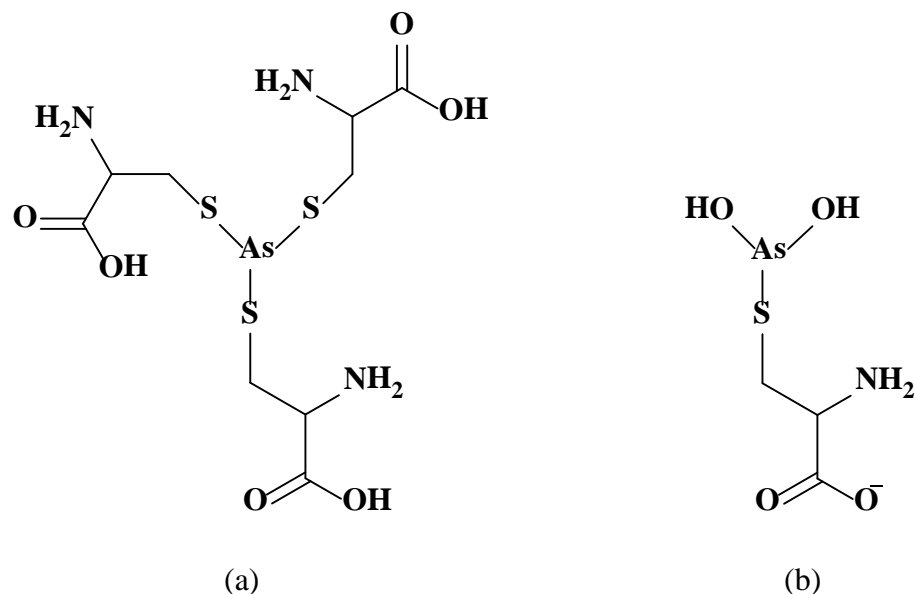


**Figure 3.2.** Structure of (a)  $\text{As}(\text{SC})_3$  and (b)  $[\text{As}(\text{SC})(\text{OH})_2]^-$

### 3.2. Results and Discussion

#### 3.2.1. Synthesis and Characterization

ABDT-As(III) was synthesized in water to a 66% yield by reacting  $\text{NaAsO}_2$  and  $\text{ABDTH}_2$  as starting material. The compound was characterized by melting point (MP), IR,  $^1\text{H}$  NMR and mass spectra. The material was decomposed in the temperature range of  $195\text{--}198^\circ\text{C}$ . The decomposition temperature was significantly higher than the melting point ( $105\text{--}109^\circ\text{C}$ ) of  $\text{ABDTH}_2$ . The high decomposition temperature is similar to the melting point of various dithiol-metal complexes ( $\text{BDET-Hg}$ ,  $\text{BDET-Cd}$  and  $\text{BDET-Pb}$ ) reported in literature.<sup>179</sup> IR data showed all the important peaks. The bands corresponding to OH (carboxylic acid), carbonyl I (carboxylic  $\text{C}=\text{O}$ ), carbonyl II (amide  $\text{C}=\text{O}$ ) and amide (N-H bending) were observed at  $3385$ ,  $1719$ ,  $1654$  and  $1534\text{ cm}^{-1}$ , respectively. The characteristic band for S-H stretching at  $2568\text{ cm}^{-1}$  was absent in ABDT-As(III) suggesting the formation of As-S bonds. The absence of S-H peak in IR spectroscopy

was also observed in BDT-M (M = Hg, Cd, Pb) compounds (Figure 1.3) where metal was bonded to BDTH<sub>2</sub> through M-S bond. ABDTH<sub>2</sub> had bonding ability with metal that was very similar to BDTH<sub>2</sub> due to its structural similarity with BDTH<sub>2</sub>. <sup>1</sup>H NMR of ABDT-As(III) in DMSO-*d*<sub>6</sub> indicated the formation of As-S bonds. The proton signal for SH in ABDT-As(III) was absent in <sup>1</sup>H NMR. However, the proton signals at  $\delta$  7.64 ppm, 8.02 ppm and 8.39 ppm were observed for aromatic protons. Similarly proton signals for  $\alpha$  and  $\beta$  methylene protons, and amide NH were found at  $\delta$  2.87 ppm, 4.52 ppm and 8.91 ppm, respectively. IR and proton NMR suggested that As(III) was bonded to ABDTH<sub>2</sub> through formation of As(III)-S bond.

### 3.2.2. XAFS Study

To examine the As bonding environment in ABDT-As(III), XAFS study was performed at the K-edge of arsenic on ABDT-As(III) along with BDT-As(III). Synthetic orpiment (As<sub>2</sub>S<sub>3</sub>) was used as the reference material. Figure 3.3 shows the arsenic K-edge X-ray absorption near edge spectroscopy (XANES) spectra of As<sub>2</sub>S<sub>3</sub> (orpiment), BDT-As(III) and ABDT-As(III). The absorption energy of As(III) in BDT-As(III) and ABDT-As(III) was very similar to the peak position of As<sub>2</sub>S<sub>3</sub>. The K-edge value (energy, eV) for both BDT-As(III) and ABDT-As(III) was found as 11866 eV close to the reported literature values, which was similar to the K-edge value obtained for the arsenite standard sample of As<sub>2</sub>S<sub>3</sub>. This result suggests that arsenic in BDT-As(III) and ABDT-As(III) is in trivalent oxidation state.<sup>156</sup> XANES was carried out as a tool to determine the rapid oxidation of As(III) to As(V) by magnetite and ferrihydrite in presence of oxygen via Fe<sup>2+</sup> mediated reactions. The XANES peak for As(III) was observed at 11871 eV,

whereas peak for As(V) was observed 11875 eV. In another experiment it was observed that the XANES value for MMA(V) and DMA(V) was observed approximately at 11875 eV. The value obtained from current experiment was in the lower range of 11866 eV indicated the presence of As(III) in the compounds.<sup>234,235</sup>

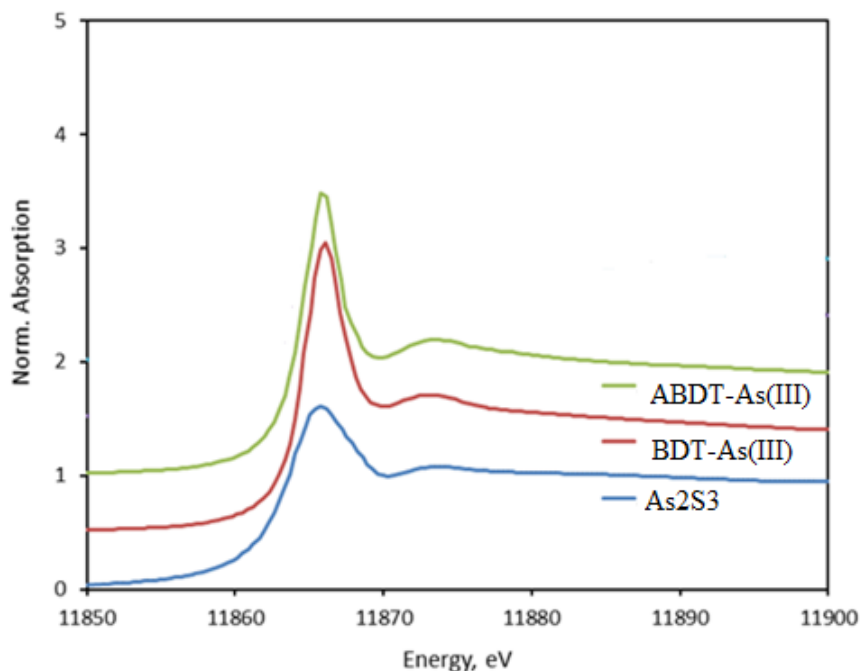


**Figure 3.3.** Arsenic *K*-edge spectra for As<sub>2</sub>S<sub>3</sub> (orpiment), BDT-As(III) and ABDT-As(III)

Figure 3.4 compares the EXAFS region of the arsenic XAFS spectra for As<sub>2</sub>S<sub>3</sub> (orpiment), BDT-As(III) and ABDT-As(III). EXAFS oscillations were converted to reciprocal space (*k*-space, chi spectrum in Å<sup>-1</sup>) representation and weighted by *k*<sup>3</sup>. These oscillations occurred at regular intervals in *k*-space and the amplitude of the oscillations was almost similar for all three materials.



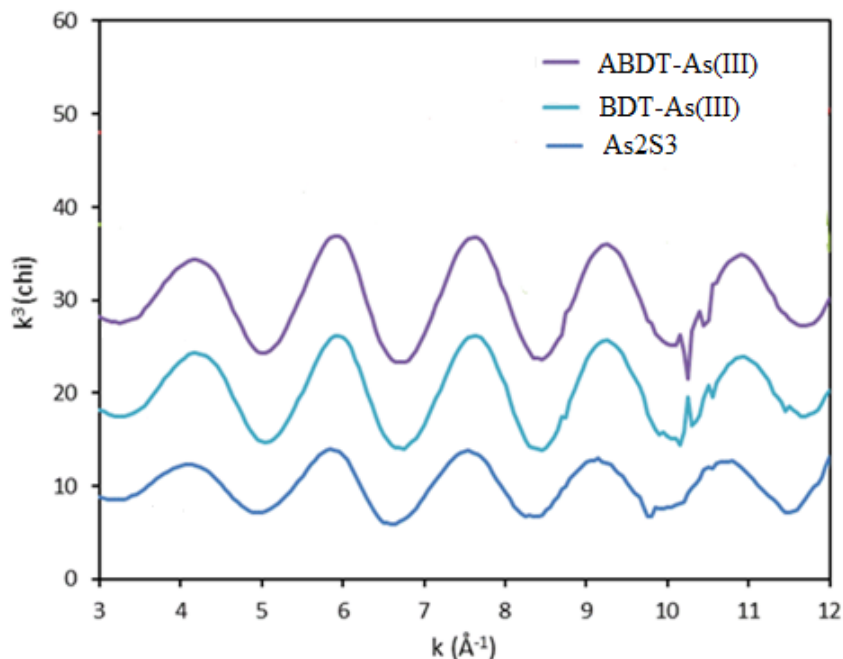


**Figure 3.4.** Arsenic EXAFS ( $k^3\chi$ ) spectra for  $\text{As}_2\text{S}_3$  (orpiment), BDT-As(III) and ABDT-As(III)

The radial structure function (RSF) is shown in Figure 3.5. An RSF spectrum was obtained by applying Fourier transform to the spectra in Figure 3.4. The RSF can be considered a one-dimensional representation of the structure local to the absorbing atom which is arsenic. It is possible to estimate the bond distance ( $R$  in Å) between As and S and the coordination number (CN) by applying TKAtoms fitting procedure, one of the programs in the IFEFFIT XAFS data analysis package.<sup>236,237</sup> This was achieved by using  $\text{As}_2\text{S}_3$  (orpiment) as a model compound to compare the XAFS data of ABDT-As(III). In  $\text{As}_2\text{S}_3$ , each  $\text{As}^{3+}$  cation is coordinated by three  $\text{S}^{2-}$  anions at a distance of 2.283 Å.<sup>238</sup> Least-squares fitting of  $\text{As}_2\text{S}_3$ , summarized in Table 3.1, can be obtained using all three modes: R mode ( $\text{FT}[k^3\chi]$  over the region 1.2 to 2.4 Å), q mode (back-transform of the FT region) and k mode ( $k^3\chi$ , over the range 3 to 12 Å<sup>-1</sup>). In the least-square fitting for

As<sub>2</sub>S<sub>3</sub>, the coordination number, N, was fixed at 3 in order to obtain a value of 0.57 for the coordination parameter, S<sub>0</sub><sup>2</sup>. The values listed in Table 3.1 for the energy zero shift, e<sub>0</sub>, the As-S distance, R, and the Debye-Waller factor, σ<sup>2</sup>, were also obtained by least-squares fitting of the EXAFS data to the calculated equation derived for the As-S photoelectron back-scattering. The R<sub>factor</sub> is a statistical measure of the goodness of the fitting. Good agreement was obtained for the As-S distance derived from the FEFF EXAFS analysis (2.29 ± 0.01 Å) compared to that (2.283 ± 0.005 Å) obtained from the crystal structure analysis.

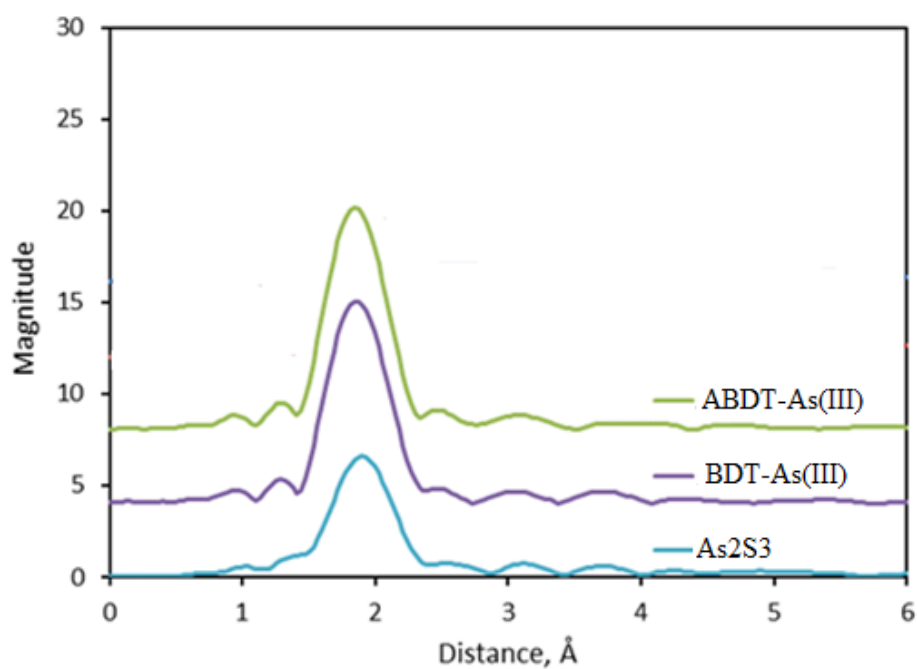


**Figure 3.5.** Arsenic RSF spectra for As<sub>2</sub>S<sub>3</sub> (orpiment), BDT-As(III) and ABDT-As(III)

**Table 3.1:** Least-squares fitting parameters derived for As<sub>2</sub>S<sub>3</sub>

Mode	Range	$e_0$	$S_0^2$	CN	$R, \text{\AA}$	$\sigma^2, \text{\AA}^2$	$R_{\text{factor}}$
R	1.2 - 2.4 $\text{\AA}$	9.1	0.59	(3)	2.29	0.0037	0.0088
q		9.8	0.57	(3)	2.29	0.0035	0.0060
k	3 - 12 $\text{\AA}^{-1}$	9.7	0.54	(3)	2.29	0.0030	0.0292
	errors (q)	$\pm 1.3$	$\pm 0.06$		$\pm 0.01$	$\pm 0.0008$	

These values were then used to model the EXAFS region for BDT-As(III) and ABDT-As(III). The resulting least-squares fitting values are shown in Table 3.2 and 3.3 and the comparison of data and fit obtained by this method is shown in Figure 3.6 (As<sub>2</sub>S<sub>3</sub>) and 3.7 (ABDT-As(III)). Using a fixed value of 0.57 for  $S_0^2$ , similar analysis was carried out for the EXAFS data ( $k^3\chi$ ) obtained for arsenic in BDT-As(III) and ABDT-As(III). In these cases, the coordination number, CN, and other parameters were derived from the least-squares fitting. Figure 3.6 and Figure 3.7 have also shown the close correspondence of the  $k$ -space EXAFS spectrum for arsenic derived from back-transform of the As-S shell in the RSF and the  $k$ -space EXAFS spectrum for As in ABDT-As(III).

**Table 3.2.** Least-squares fitting parameters derived for BDT-As(III)

Mode	Range	$e_0$	$S_0^2$	CN	$R, \text{\AA}$	$\sigma^2, \text{\AA}^2$	$R_{\text{factor}}$
R	1.2 - 2.4 $\text{\AA}$	9.1	(0.57)	4.9	2.26	0.0037	0.0185
Q		9.9	(0.57)	4.9	2.27	0.0036	0.0118
k	3 - 12 $\text{\AA}^{-1}$	9.6	(0.57)	4.8	2.26	0.0034	0.0278
	errors (q)	$\pm 1.8$		$\pm 0.75$	$\pm 0.01$	$\pm 0.0011$	

**Table 3.3.** Least-squares fitting parameters derived for ABDT-As(III)

Mode	Range	$e_0$	$S_0^2$	CN	$R, \text{\AA}$	$\sigma^2, \text{\AA}^2$	$R_{\text{factor}}$
R	1.2 - 2.4 $\text{\AA}$	7.6	(0.57)	5.3	2.26	0.0035	0.0144
q		8.3	(0.57)	5.3	2.26	0.0036	0.0097
k	3 - 12 $\text{\AA}^{-1}$	8.0	(0.57)	5.2	2.26	0.0032	0.0279
	errors (q)	$\pm 1.7$		$\pm 0.75$	$\pm 0.01$	$\pm 0.0010$	

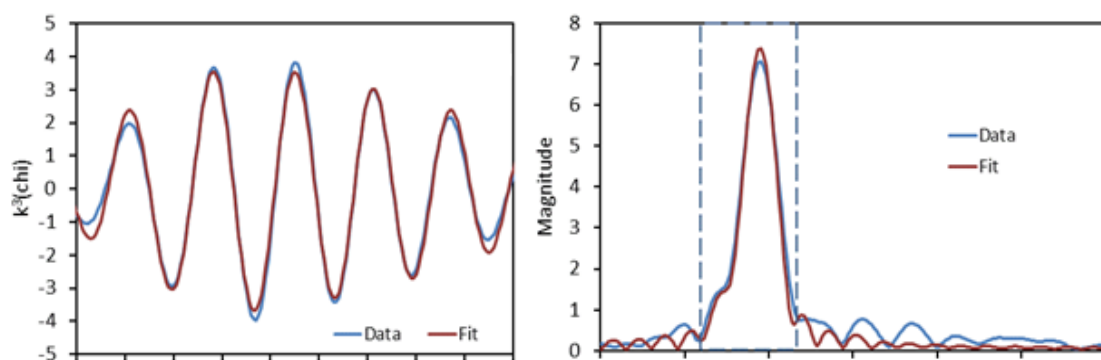


**Figure 3.6.** Comparison of FEFF model function and least-squares fitting for  $\text{As}_2\text{S}_3$ . Left: q-mode fits; right: R-mode fits over the range 1.2 – 2.4  $\text{\AA}$

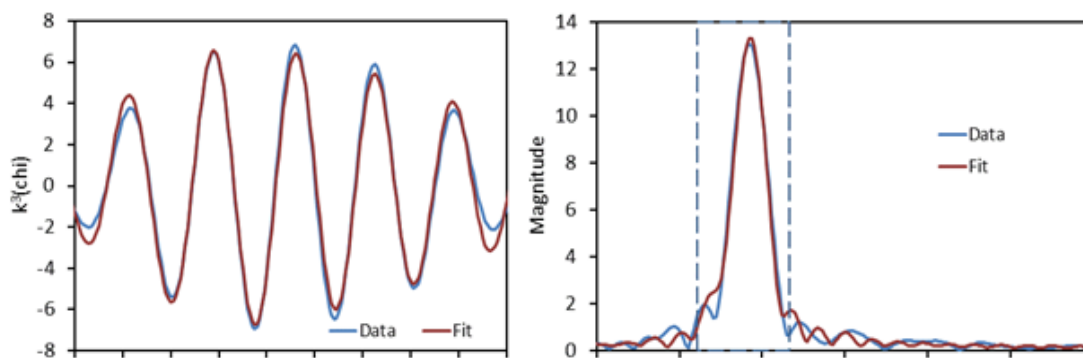


**Figure 3.7.** Comparison of FEFF model function and least-squares fitting for ABDT-As(III). Left: q-mode fits; right: R-mode fits over the range 1.2 – 2.4 Å

The As-S bond distance ( $R$ , Å) in both BDT-As(III) and ABDT-As(III) was estimated to be 2.26 Å obtained by FEFF fitting of BDT-As(III) and ABDT-As(III) which is about 0.03 Å shorter than the obtained value for  $As_2S_3$  while the Debye-Waller factor ( $\sigma^2$ ) is similar. The estimated As-S bond distance falls within the range of 2.24 – 2.28 Å reported in literature and is in good agreement with published trithiol ligation distance.<sup>206,238,239</sup> The As-S bond distance in ABDT-As(III) was comparable with the As-S distance in tris(phenylthio)arsine (Figure 3.8.a) 2.24 Å.<sup>239</sup> Whereas the As-S bond distance was estimated to be 2.28 Å in  $As_2S_3$  (Figure 3.8.b).<sup>238</sup> The coordination numbers obtained for the As-S shell in BDT-As(III) and ABDT-As(III) from FEFF EXAFS analysis falls in the range between 4.8 and 5.3 with high experimental error. These values are significantly greater than that for  $As_2S_3$  structure which may indicate additional secondary interaction with other ligands presumably because of their nonsystematic nature.<sup>156,206,240</sup> This result suggested that the BDT-As(III) and ABDT-As(III) complexes are being polymeric rather than crystalline. XAFS study also suggested the bonding

nature in ABDT-As(III) was similar to the  $\text{As}_2\text{S}_3$ . This result indicated that ABDTH<sub>2</sub> can be used as silica supported reagent to remove As(III) in filtration column applications.

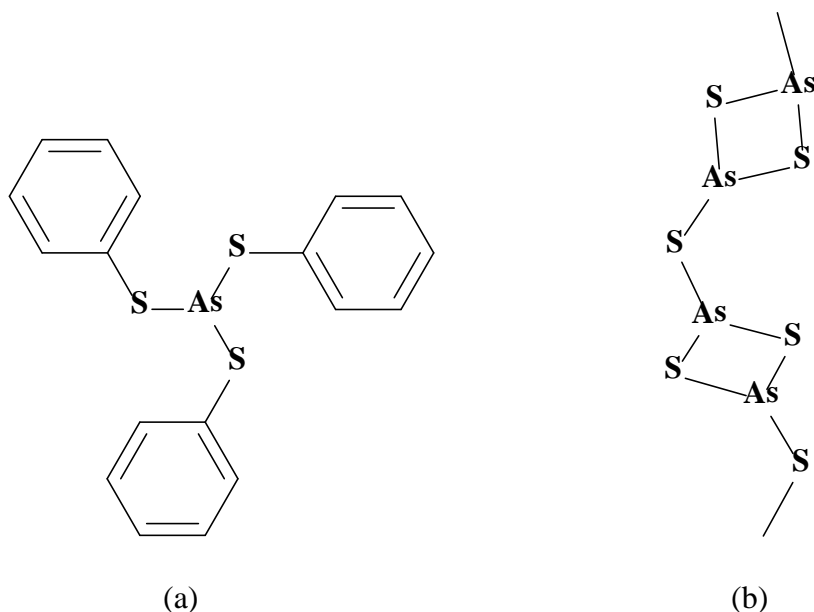
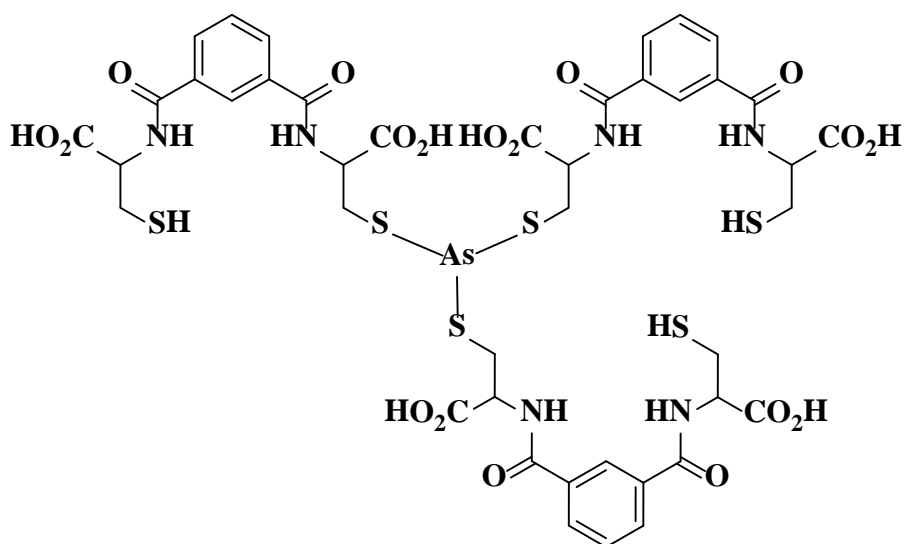


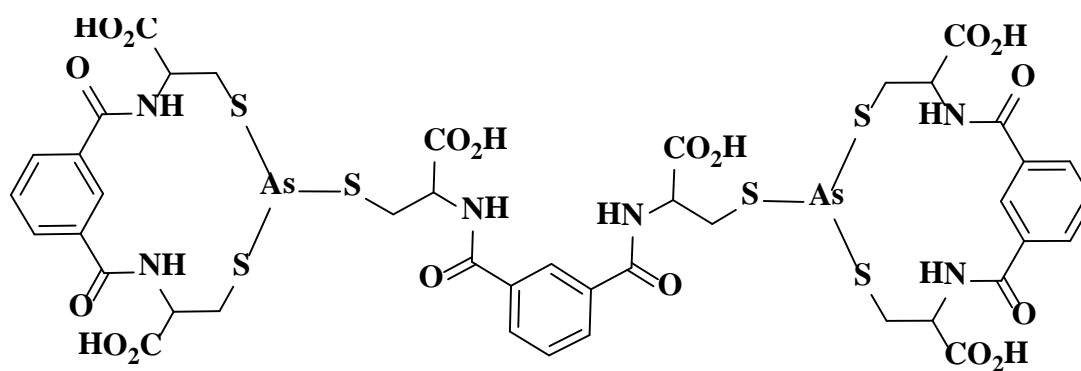
**Figure 3.8.** Structure of (a) tris(phenylthiol)arsine and (b)  $\text{As}_2\text{S}_3$

The experimental K-edge absorption energy of As(III) in  $\text{As}_2\text{S}_3$  was 11866 eV. This was very close to the values reported in the literatures for As(III) bonded to three sulfurs. The similar absorption energy of arsenite was observed at 11869 in  $\text{As}(\text{Glu})_3$ , where arsenic is bonded to three glutathione unit through sulfurs.<sup>235</sup> As(III) is also bonded to three sulfur unit in  $\text{As}_2\text{S}_3$ . The XANES and EXAFS spectra indicated that the As(III) absorption energy of ABDT-As(III) was very close to the value of  $\text{As}_2\text{S}_3$  and  $\text{As}(\text{Glu})_3$  and the As-S bond distance in ABDT-As(III) was similar to trithiol coordinated As(III) compounds. However the coordination number obtained from least-squares fitting parameters for ABDT-As(III) was higher than the coordination number in  $\text{As}_2\text{S}_3$ . This suggested that arsenite in ABDT-As(III) is coordinated to three sulfurs. However secondary coordination to arsenite was present in ABDT-As(III). The proposed structures

of ABDT-As(III) are shown in Figure 3.9. It was possible that either As(III) was bonded to three sulfurs from three ABDTH<sub>2</sub> (Figure 3.9.a) or ABDTH<sub>2</sub> was bridging between two arsenite units (Figure 3.9.b).



(a)



(b)

**Figure 3.9.** Proposed structure of ABDT-As(III)

### 3.2.3. Leaching Study

ABDT-As(III) was set for arsenic leaching at pH 5, 7 and 9 for 24 h, 1, 2 and 3 weeks. The filtrate of the solution was analyzed by ICP-OES to determine the arsenic concentration leached out from the compound. The pH range of 5-9 was used for the experiment as pH of groundwater varies in the range of 6-8 depending on the condition of soil and sediments. The experimental data is shown in Table 3.4. The study demonstrated that about 6.25-7.04% of arsenic was leached out in water after 24 h. After 1, 2 and 3 weeks, arsenic had been leached out in the range between 12.63% - 18.62%. The study showed that the percentage of leaching was almost remained same over the period of 1, 2 and 3 weeks. However the percentage of arsenic leaching from ABDT-As(III) was higher than leaching observed in BDT-As(III).<sup>189</sup> The leaching study of arsenic from the solid BDT-As(III) showed relatively low leaching of arsenic (up to 0.77%) over the course of several weeks over the range of pH 5-9. The higher leaching of arsenic from ABDT-As(III) is most likely due to presence of physisorbed arsenic on solid. The presence of carboxylic acid group on the molecule was possibly also contributing the increased solubility of solid ABDT-As(III) aqueous solution. However the percentage of arsenic leaching is substantially less than the arsenic leaching from granular ferric hydroxide (GFH). It was observed that arsenic and iron leaching was 80% and 65%, respectively, under anaerobic and reducing conditions.<sup>241</sup> The relatively high leaching of arsenic from ABDT-As(III) could also be attributed to the oxidation of As(III) to As(V) followed by its release in water.



**Table 3.4.** As leaching from 10 mg of ABDT-As(III) after 24 h, 1, 2 and 3 weeks

<b>Time</b>	<b>pH</b>	<b>[As], ppm (in 50 mL)</b>	<b>As (mg)/10 mg ABDT-As(III)</b>	<b>As (mg) Leached</b>	<b>% As Leached</b>
<b>As Stock</b>		93.95 $\pm$ 0.27	4.69		
<b>24 h</b>	5	5.93 $\pm$ 0.17		0.30	6.30
	7	5.87 $\pm$ 0.16		0.29	6.25
	9	6.62 $\pm$ 0.13		0.33	7.04
<b>1 week</b>	5	11.87 $\pm$ 0.36		0.59	12.63
	7	14.35 $\pm$ 0.48		0.71	15.28
	9	14.43 $\pm$ 0.32		0.72	15.36
<b>2 weeks</b>	5	15.11 $\pm$ 0.38		0.76	16.08
	7	14.68 $\pm$ 0.32		0.73	15.63
	9	15.63 $\pm$ 0.35		0.78	16.64
<b>3 weeks</b>	5	16.01 $\pm$ 0.27		0.80	17.05
	7	15.52 $\pm$ 0.24		0.77	16.52
	9	17.49 $\pm$ 0.56		0.87	18.62

### **3.3. Experimental**

#### **3.3.1. Materials and Techniques**

The experimental was carried out with ethanol and DI water as solvents. Sodium metaarsenite ( $\text{NaAsO}_2$ , >99%) was purchased from Sigma-Aldrich and used as received. Hydrochloric acid (HCl, omnie trace) was obtained from EMD and diluted to obtain the desired pH of solution. The melting point of the compound was taken by MEL-TEMP instrument manufactured by Laboratory Devices. The mass spectrum was obtained on Finnigam LTQ in the University of Kentucky Mass Spectroscopy Facility. IR of compounds was produced using KBr as pellets with a model Nicolet Avatar 370 DTGS IR spectrophotometer manufactured by Thermo Electron Corporation. NMR spectra were taken using a Varian 400 MHz INOVA instruments in the University of Kentucky Nuclear Magnetic Resonance Facility. X-ray absorption fine structure (XAFS) spectroscopy of ABDT-As(III) was obtained at beam-line X-18B of the National Synchrotron Light Source (NSLS), Brookhaven National Laboratory, NY. Leaching study of arsenic from ABDT-As(III) was carried out in DI water and the corresponding arsenic concentration in aqueous solution was analyzed by Varian Vista Pro CCD Simultaneous Inductive Coupled Plasma Optical Emission Spectrometer (ICP-OES) at a wavelength of 193.7 nm at 1.20 kW power, 4.0 second replicate read time with default values for all other parameters.

#### **3.3.2. Synthesis of ABDT-As(III)**

ABDTH<sub>2</sub> (1g, 2.69 mmol) in EtOH (10 mL) was added to a stirring solution of NaAsO<sub>2</sub> (350 mg, 2.70 mmol) in DI water (40 mL) and the resulting solution stirred

for 2 h. A white colloidal suspension formed. Precipitation was induced by adding diluted HCl dropwise until the pH reached 5 - 6 (~10 mL). The white precipitate was isolated by filtration and then washed with water (200 mL total). The solid was dried in air obtaining to yield 0.82 g (66%) of product. Mp: 195-198 °C (dec); IR (cm<sup>-1</sup>, KBr): 3385 (OH from carboxylic acid), 3067 (sp<sup>2</sup> CH), 2934 (sp<sup>3</sup> CH), 1719 (carboxylic CO), 1654 (amide CO), 1534 (amide NH); <sup>1</sup>H NMR (DMSO-*d*<sub>6</sub>, 400 MHz):  $\delta$  (ppm) - 2.87 [m, 4H, CH<sub>2</sub>], 4.52 [m, 2H, CH], 7.64 [t, 1H, C<sub>6</sub>H<sub>4</sub>], 8.02 [d, 2H, C<sub>6</sub>H<sub>4</sub>], 8.39 [s, 1H, C<sub>6</sub>H<sub>4</sub>], 8.91 [d, 2H, NH].

### 3.3.3. XAFS

The coordination environment in ABDT-As(III) and BDT-As(III) was analyzed by X-ray absorption fine structure (XAFS) spectroscopy. The sample was scanned from 100 eV below the arsenic K absorption edge at 11,867 eV to as much as 800 eV above the edge. The energy scale for the spectra was calibrated to an arsenate absorber whose peak position was assumed to occur at 11,871 eV. The spectra were collected both in absorption and fluorescence geometries using conventional gas-filled ionization detectors and a PIPS detector, respectively, for the two different modes. A reference absorption spectrum of As<sub>2</sub>S<sub>3</sub> (synthetic orpiment) was also obtained using a pressed pellet of the sulfide diluted to 2-3 wt% and mixed well in SOMAR, an organic pelletizing substance for comparison. All other samples were received as powders and exposed to the synchrotron X-ray beam by suspending them in ultrathin polypropylene baggies. The XAFS spectra were first calibrated with the reference energy point defined by the major peak in the spectrum of the arsenate standard followed by dividing into

separate X-ray absorption near-edge structure (XANES) and extended X-ray absorption fine structure (EXAFS) regions. The EXAFS region was then converted to a reciprocal space (k-space, chi spectrum) representation and a Fourier transform was applied to the  $k^3$ -weighted chi spectrum to produce a radial structure function (RSF). The RSF can be considered a one-dimensional representation of the structure local to the absorbing atom, which is arsenic.

#### **3.3.4. Leaching Study**

Arsenic leaching from ABDT-As(III) was studied at a pH of 5, 7 and 9 for 24 h, 1, 2 and 3 weeks. The study was conducted by setting up 10 mg of ABDT-As(III) in 50 mL of DI water in the above mentioned pH. Diluted HCl (0.5 M) and diluted KOH (0.5 M) were used to adjust the pH of water. Blanks were also analyzed for the same pH and time intervals. After each time period, solutions were filtered through the 0.2  $\mu$ m PTFE filter to remove solid particulate. Samples were then acidified with 2.5 mL concentrated  $\text{HNO}_3$  followed by digestion of samples in polypropylene digestion vessel at  $95^\circ\text{C}$  for 6 h. Samples were then cooled down and the volume of the samples was marked up to 50 mL again with DI water. ABDT-As(III) (10 mg) was also digested in 50 mL DI water with 2.5 mL of concentrated  $\text{HNO}_3$  and 2.5 mL of  $\text{H}_2\text{O}_2$  at  $95^\circ\text{C}$  for 10 h to determine the concentration of arsenic in the stock solution. The stock solution was diluted 8 times prior to analysis to fit into the calibration curve. All other samples were analyzed without dilution of solution. Due to arsenic concentration in solutions in the ppm range, solutions were analyzed by ICP-OES at 193.7 nm to determine the arsenic concentration in samples. For quality control purposes, a duplicate sample (0.59% relative difference), a

matrix spiked with 2 ppm As (99% Recovery) and a As standard (5 ppm at 109% recovery) were included at the beginning of the analysis. The analyzed data are shown in Table 3.4. The blank samples contained no As and are not included in the table.

### 3.4. Conclusions

The binding of As(III) with ABDTH<sub>2</sub> was demonstrated by synthesizing ABDT-As(III). As(III) was bonded with ABDTH<sub>2</sub> through formation of As-S bonds. ABDT-As(III) showed higher decomposition temperature in comparison to the melting point of ABDTH<sub>2</sub>. IR and <sup>1</sup>H NMR indicated the formation of ABDT-As(III) compound. XAFS analysis showed the coordination of arsenic with three sulfur units similar to As<sub>2</sub>S<sub>3</sub>. The average bond distance was estimated to be  $2.26 \pm 0.01 \text{ \AA}$ , which was in the range of reported As-S bond distance of 2.24-2.28  $\text{\AA}$ .<sup>206,238,239</sup>

This was an excellent indication of the ABDTH<sub>2</sub>'s capabilities to bind and capture As(III) as an alternative to BDTH<sub>2</sub>. It would be ideal to attach ABDTH<sub>2</sub> on a solid-support for the application as a remediation column. Binding the ligand to a solid surface will prevent the release of ABDTH<sub>2</sub> as well as will increase the interaction of ligand with As(III) in solid/liquid interphase. Binding of ABDTH<sub>2</sub> on solid-support would also prove beneficial by maximizing the surface area of the thiol binding sites and allowing for higher-flow scenarios that could not be achieved with a simpler column prepared by dispersing BDTH<sub>2</sub> solid in quartz sand.

## CHAPTER 4

### Preparation of Silica-Supported ABDTH<sub>2</sub> (SiABDTH<sub>2</sub>)

#### 4.1. Introduction

Silica gels are of great interest due to the presence of silanol groups which have importance in interface interaction in chromatography, as substrate adsorption in the catalytic process, and as composite filler into polymer matrix. Surface silanol groups can also be chemically modified by the reaction of surface hydroxyl groups with silane coupling agents which will improve physical and chemical properties. Further treatment is also possible to immobilize new organic functional molecules as chelating agents. Modified silica bonded with various chelating ligand have been widely used in preconcentration and removal of several metals such as mercury, copper, zinc, cadmium, lead, gold and silver.<sup>242,243</sup> Thiol based compounds such as cysteine and cysteine-rich proteins showed promise for separation and preconcentration of heavy metals as selective chelating agents. The thiol group of these compounds interacts strongly with many soft heavy metals forming a strong M-S bond (M = Hg, Cd, Pb, As). Metallothionein (MT) is a family of cysteine-rich, low molecular weight (MW ranging from 500 to 14000 Da) proteins which has the capacity to bind both physiological (such as zinc, copper, selenium) and xenobiotic (such as cadmium, mercury, silver, arsenic) heavy metals through the thiol group of its cysteine residues.<sup>244</sup> Due to its metal binding ability, cysteine and polycysteine immobilized on silica support have been synthesized as sorbent for heavy metal capture from aqueous and gas phases.<sup>161,245,246</sup> Makkuni et. al. have designed cysteine and polycysteine based silica as shown in Figure 4.1 and 4.2, which

showed excellent mercury uptake from aqueous media.<sup>161</sup> It was also observed that smaller particle size (0.015 mm) adsorbent had high dynamic capacity of ~ 50 mg/g Hg adsorbed in 1 min as compared to larger particle size (0.75 mm) which showed only ~5 mg/g Hg adsorbed in 1 min.

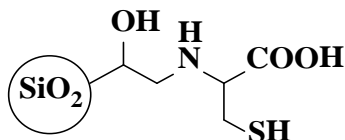


**Figure 4.1.** Cysteine functionalized silica

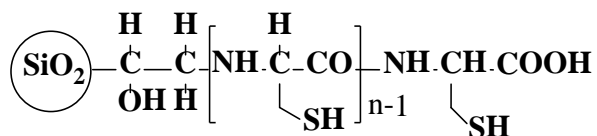


**Figure 4.2.** Poly-L-Cysteine functionalized silica

Ethylene sulfide was immobilized on silica using 3-(trimethoxysilyl)propylamine as molecular linker between silica and active thiol (Figure 4.3). This solid supported thiol showed improved mercury removal than cadmium and lead as thiol has strong affinity towards mercury.<sup>247,248</sup>

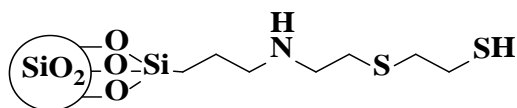


**Figure 4.3.** Ethylene sulfide immobilized silica

The silica support is widely accepted for its high surface area, high thermal stability, cheap and easy availability. Silica contains a network of Si-O covalent bonds. The bond energy of Si-O in molecular lattice of silicon dioxide is 452 kJ/mol and the melting point is 1600°C. Depending on the particle size of silica, the surface area can be in the range of 500-800 m<sup>2</sup>/g.<sup>249,250</sup> There are various methods available such as thermal gravimetric analysis, reaction with organometallic compound, spectroscopic analysis and solid state NMR for determining the concentration of hydroxyl groups on the silica surface. The amount of hydroxyl group on the surface depends on the method of measurement as it is difficult to separate total silanol groups and hydroxyl groups of adsorbed or ligated water. A deuterio-exchange experiment with mass spectrometric analysis was done for determining small amounts of water and hydroxyl groups on the surface of dispersed oxide adsorbents where it showed that there were 5.0 OH per nm<sup>2</sup> independent of the origin and structural characteristics (specific surface area, type of the pores, size distribution of the pores, particle packing density, structure of SiO<sub>2</sub> skeleton).<sup>251</sup> Other experiments were conducted to confirm the presence of 3.3 OH per 100 Å<sup>2</sup> of Si60.<sup>252</sup> This corresponds to 2.54 mmol SiOH per gram of material. Furthermore, the silanol reaction can utilize one, two, or three SiOH groups to introduce the amine group, with bonding to three SiOH being the most stable. This would allow the introduction of a maximum of 0.847 mmol ABDTH<sub>2</sub> per gram of Si60.

Functionalization or immobilization of active thiol molecule on silica surface is widely done using spacer molecule such as aminopropyltriethoxysilane (APTES). Surface modification is commonly carried out to introduce reactive groups on the silica particle surface by grafting organosilanes onto silica.<sup>253</sup> APTES is a well known silane



coupling agent that is used in affinity-based application because of the silane group that can strongly bind to silicon or glass substrates having its amine group available for forming covalent bonds with carboxyl groups (functional groups that are commonly found in bio-molecules). This is also used as a silane coupling agent for fiber-glass reinforced plastics by improving the adhesion of resin matrix to the fiber.<sup>254,255</sup>

This chapter explores the surface modification of silica gel (Si60) with APTES followed by the immobilization of ABDTH<sub>2</sub> on modified silica through amide linkage.

## 4.2. Results and Discussion

SiABDTH<sub>2</sub> was prepared in a two step synthetic pathway. The first step was the modification of the Si60 surface hydroxide groups with  $\gamma$ -aminopropyltriethoxysilane to form Si-O-Si siloxane linkage with pendant propylamine groups. The material was then treated with chlorotrimethylsilane to protect the potentially reactive silanol groups by converting them to trimethylsiloxy groups. With the application of ABDTH<sub>2</sub> in heated ethanol, the carboxyl groups of ABDTH<sub>2</sub> condensed with the free propylamines, forming amide (-CONH-) linkages.

This synthesis resulted in ABDTH<sub>2</sub> attached to the siloxane cage where Si-O-Si is very stable towards hydrolysis. It was found that SiO-Si bond in Si<sub>8</sub>O<sub>20</sub>[Si(CH<sub>3</sub>)<sub>2</sub>H]<sub>8</sub> was prone to hydrolysis because Si was attached to hydrogen and the dimethylsilyl group of Si<sub>8</sub>O<sub>20</sub>[Si(CH<sub>3</sub>)<sub>2</sub>H]<sub>8</sub> was readily removed from the Si<sub>8</sub>O<sub>20</sub><sup>8-</sup> silicate core by the reaction with methanol or H<sub>2</sub>O, while SiO-Si bond in Si<sub>8</sub>O<sub>20</sub>[Si(CH<sub>3</sub>)<sub>3</sub>]<sub>8</sub> did not hydrolyze under the same condition due to the Si-C bond as all the coordination sites of Si are covalently bonded to either oxygen or carbon. This showed that trimethylsilyl group was strongly

attached to the  $\text{Si}_8\text{O}_{20}^{8-}$  silicate core. The stability of the Si–O–Si bond against alcoholysis or hydrolysis depended on the type of functional group attached to the silicon atom.<sup>256</sup> SiABDTH<sub>2</sub> was prepared by crosslinking of silanol group on silica surface and  $\gamma$ -aminopropyltriethoxy silane. In this case Si of  $\gamma$ -aminopropyltriethoxy silane was attached to the silica surface through three Si–O–Si linkages and it was also connected to the methylene carbon from aminopropyl group. The amide linkage on the silica surface is less likely to be hydrolyzed at neutral pH. The acid hydrolysis rate constant of amide decreased with the degree of substitution. In contrast, the base hydrolysis rate constant of amide increased with increased degree of substitution.<sup>257</sup>

Prior to the surface modification, Si60 obtained from manufacturer was analyzed by particle size analyzer to obtain the size distribution of these particles (Figure 4.4). Particle size was varied widely in the range of 0.375  $\mu\text{m}$  to 2000  $\mu\text{m}$  with the average standard deviation of 643.9 when analyzed in triplicate. However the average mean particle size was 925.2  $\mu\text{m}$ .

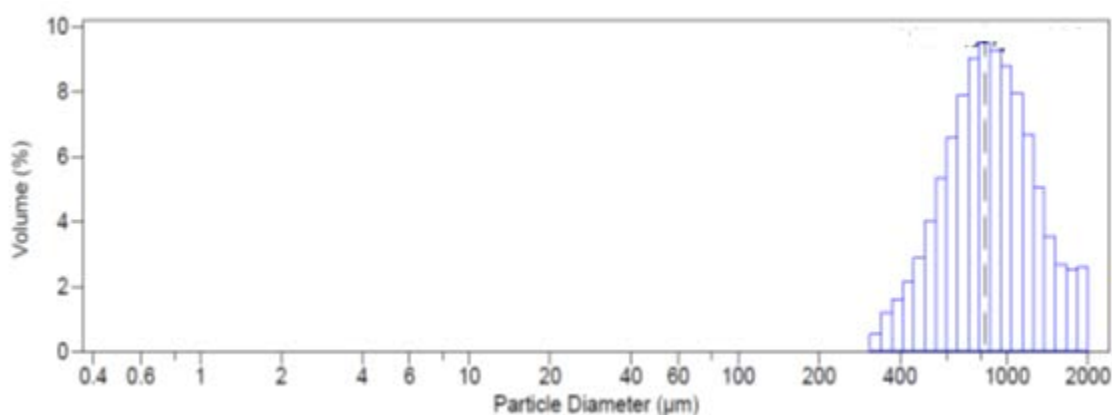


**Figure 4.4.** Particle size distribution of Si60

The IR spectra of SiABDTH<sub>2</sub> showed the characteristic absorption for SH at 2545 cm<sup>-1</sup>. A broad peak was observed at 3399 cm<sup>-1</sup> attributed to the remaining COOH group on ABDTH<sub>2</sub>. Si60 had a sharp absorbance at 3447 cm<sup>-1</sup> for the O-H bond. The peak was absent in SiABDTH<sub>2</sub>. This confirmed that the SiOH group had been displaced by formation of Si-O-Si linkage through APTES treatment followed by treatment with Me<sub>3</sub>SiCl to create Si-O-SiMe<sub>3</sub> linkages.

Elemental analysis (EA) of both SiNH<sub>2</sub> and Si ABDTH<sub>2</sub> was conducted to determine presence of nitrogen and sulfur on SiNH<sub>2</sub> and SiABDTH<sub>2</sub>, respectively. The nitrogen content in SiNH<sub>2</sub> was determined to be 1.94 mmol/g of solid support which was higher than the reported value in literature.<sup>258</sup> This suggested increased surface coverage by  $\gamma$ -aminopropyltriethoxy silane. The sulfur content in Si ABDTH<sub>2</sub> was also determined to be 0.24 mmol/g of solid support suggesting the presence of 0.14 mmol of ABDTH<sub>2</sub> per gram of solid support as 2 mmol of sulfur can be obtained from 1 mmol of ABDTH<sub>2</sub>.

Silica particles modified with organic content on the surface of particles were analyzed by thermogravimetric analysis (TGA). Figure 4.5 shows the percent weight loss of Si60, SiNH<sub>2</sub> and Si ABDTH<sub>2</sub> with temperature. The percent weight loss of Si60 was very low compared to SiNH<sub>2</sub> and Si ABDTH<sub>2</sub>. The curve showed initial 5.0% weight loss of Si60 (Figure 4.5 a) in the range of 30<sup>0</sup>–200<sup>0</sup> C which was attributed to the release of water and hydrocarbon contamination that were physically adsorbed on the surface. The molecular formula was derived to be SiO<sub>2</sub>.(H<sub>2</sub>O)<sub>0.18</sub> based on the TGA curve. The following loss of mass of 1.50% at 411<sup>0</sup>C is related to the condensation of free silanol groups on the surface to form siloxane groups. The APTES modified Si60 (SiNH<sub>2</sub>) (Figure 4.5 b) showed a total mass loss of 21% without any definitive steps

corresponding to the decomposition of organic groups indicating the binding of APTES on the silica surface.<sup>247,253</sup> The experiment was conducted in presence of air. The possible decomposition products of organic fraction in SiNH<sub>2</sub> are CO<sub>2</sub>, NO<sub>2</sub> and H<sub>2</sub>O. When organic fraction was heated at high temperature in presence of air, oxides of elements were produced. ABDTH<sub>2</sub> immobilized Si60 (SiABDTH<sub>2</sub>) showed largest weight loss, a total of 26%, without any definitive steps, which was about 5% increase in mass loss compared to SiNH<sub>2</sub> corresponding to further derivatization by ABDTH<sub>2</sub> on SiNH<sub>2</sub> (Figure 4.5 c).<sup>253,259</sup>

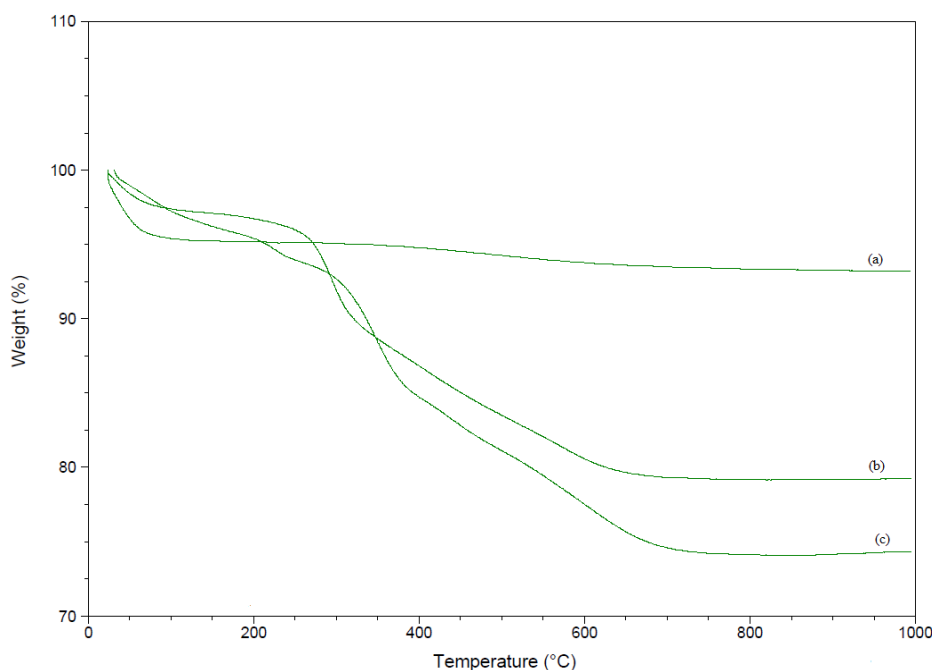


**Figure 4.5.** Thermogravimetric analysis for (a) Si60, (b) SiNH<sub>2</sub> and (c) SiABDTH<sub>2</sub>

The ABDTH<sub>2</sub> loading on SiABDTH<sub>2</sub> was also determined by inductive coupled plasma-optical emission spectroscopy (ICP-OES). SiABDTH<sub>2</sub> was digested in aqueous media in presence of strong acid and peroxide to break down organic content present on

the surface of SiABDTH<sub>2</sub> and analyzed for sulfur concentration of aqueous solution by ICP-OES. As determined by ICP-OES analysis, sulfur content (Table 4.1) was be 0.270 – 0.273 mmol S per gram SiABDTH<sub>2</sub> beads or an ABDTH<sub>2</sub> loading of 0.135 – 0.137 mmol per gram of beads for the 20 g scale preparations.

**Table 4.1.** Sulfur concentration and ABDTH<sub>2</sub> loading per g of SiABDTH<sub>2</sub> in different batches

Sample	Raw [S] (ppm)	Final [S] (ppm)	mmol S/ g beads	mmol ABDTH <sub>2</sub> /g
<b>9 g SiABDTH<sub>2</sub></b>	8.69 ± 0.19	86.9 ± 1.9	0.271 ± 0.006	0.136 ± 0.003
<b>48 g SiABDTH<sub>2</sub></b>	29.95 ± 1.14	299.5 ± 11.4	0.468 ± 0.017	0.234 ± 0.009
<b>93 g SiABDTH<sub>2</sub></b>	4.78 ± 0.33	478.0 ± 33.8	0.747 ± 0.052	0.373 ± 0.026
<b>131 g SiABDTH<sub>2</sub></b>	2.93 ± 0.12	146.2 ± 5.9	0.229 ± 0.009	0.114 ± 0.005

The titration of SiABDTH<sub>2</sub> was carried out using dilute sodium hydroxide to arrive at the average pK<sub>a</sub> value of 3.30 for SiABDTH<sub>2</sub> (Figure 4.6), which was very close to the first pK<sub>a</sub> of ABDTH<sub>2</sub>. This suggested that the second carboxylate group of ABDTH<sub>2</sub> was connected to the silica surface through a amide linkage. Having a free carboxylate group on SiABDTH<sub>2</sub> will be advantageous to arsenic removal during column study as the arsenic species such as [H<sub>2</sub>AsO<sub>3</sub>]<sup>-</sup>, [HAsO<sub>3</sub>]<sup>2-</sup> in water will interact with the carboxylate group through hydrogen bonding and bring the arsenic species in close proximity to the sulfur of ABDTH<sub>2</sub>.

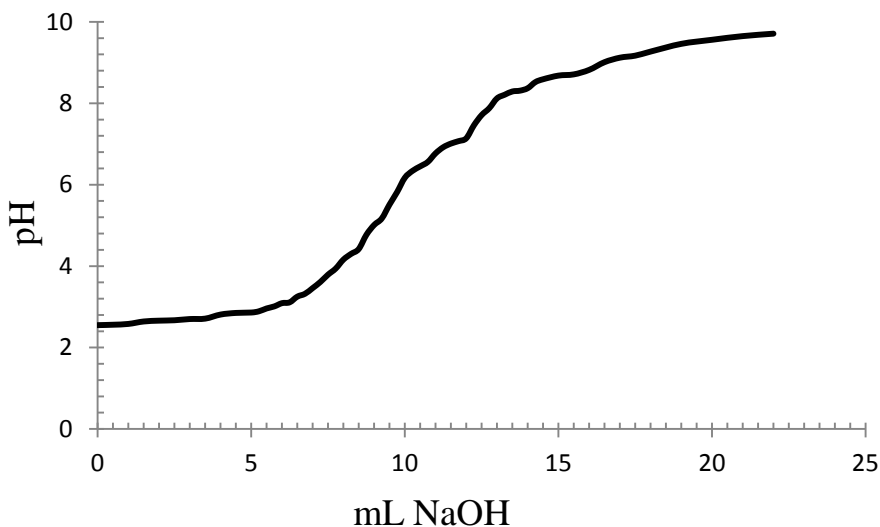


**Figure 4.6.** Titration of SiABDTH<sub>2</sub> with NaOH

Immobilization of ABDTH<sub>2</sub> on silica was carried out in different batches with various amount of starting materials to compare the variation of ABDTH<sub>2</sub> loading on modified silica. It was observed that initially ABDTH<sub>2</sub> loading per gram of solid support was increased with increasing amount of SiNH<sub>2</sub> for the reaction. Though, further increase in amount of SiNH<sub>2</sub> did not increase the ABDTH<sub>2</sub> loading per gram of solid. ABDTH<sub>2</sub> loading per gram of modified silica increased from 0.136 mmol to 0.234 mmol (Table 4.1) when the preparation batch was increased from 20 g to 50 g with increasing solvent content. It was further increased to 0.373 mmol (Table 4.1) with increased batch content to 60 g. However, the increase in the batch content of Si60 to 90 g without increasing the solvent content for the reaction did not improve ABDTH<sub>2</sub> loading per gram of modified silica, it decreased the ABDTH<sub>2</sub> loading to 0.114 mmol (Table 4.1). The characterization data indicated that ABDTH<sub>2</sub> had been immobilized on silica support with modification of silica surface with  $\gamma$ -aminopropyltriethoxysilane. The preparation of SiABDTH<sub>2</sub> in

different batches indicated that it can be prepared in large scale. However different parameters need to be optimized to obtain best results.

### **4.3. Experimental**

#### **4.3.1. Materials and Techniques**

All chemicals were obtained from the commercial sources and used as received. Solvents were obtained in reagent grade for the reaction purpose. Silica gel (Si60) with surface area of  $500 \text{ m}^2 \text{ g}^{-1}$ , pore size  $\sim 60 \text{ \AA}$ , pore volume  $\sim 0.75 \text{ ml g}^{-1}$  was obtained from Macherey Nagel. The particle size of silica gel was in the range of 0.5 to 1.0 mm (18-35 mesh, ASTM grade).  $\gamma$ -Aminopropyltriethoxysilane and chlorotrimethylsilane ( $\text{Me}_3\text{SiCl}$ , 98%) were purchased from MP Biomedicals, LLC as laboratory grade and Acros Organics, respectively. Chloroform from Acros Organics, ethyl alcohol from Fisher Scientific and toluene from EM science were used as received. DI water was used for the analytical purpose as mentioned in the experimental. Omni trace hydrochloric acid ( $\text{HCl}$ ) and nitric acid ( $\text{HNO}_3$ ) were purchase from EMD. Infrared (IR) spectra of the compounds were produced with a model Nicolet Avatar 370 DTGS IR spectrophotometer manufactured by Thermo Electron Corporation. Solid samples were scanned using KBr. Elemental analysis was obtained in the Center for Advanced Energy Research Facility at the University of Kentucky. Thermogravimetric analysis of samples were obtained on TA instrument 2950 TGA HR V5.4A by heating from  $30^\circ\text{C}$  to  $1000^\circ\text{C}$  at a heating rate of  $20^\circ\text{C}/\text{min}$ . Samples were scanned at high resolution dynamic method on a platinum pan under air with varying sample size of 3.5-6.0 mg during analysis. Sulfur concentration in aqueous solution was determined by Varian Vista Pro CCD

Simultaneous Inductive Coupled Plasma Optical Emission Spectrometer (ICP-OES).

Particle size of silica was analyzed in Beckman Coulter LS 13 320 instrument.

#### **4.3.2. Scale-up Procedure**

##### **4.3.2.1. 9 g SiABDTH<sub>2</sub>**

**SiNH<sub>2</sub>:** A suspension of silica-60 (20 g) in toluene (500 mL) was refluxed with  $\gamma$ -aminopropyltriethoxysilane (15.70 g, 71.36 mmol) in chloroform (40 mL) at  $\sim 100^{\circ}\text{C}$  for 48 h. After refluxing, the solid was filtered and washed with  $\text{CHCl}_3$  (5 x 80 mL), and dried under vacuum for 12 h. The dried solid was then soaked in a solution of  $\text{Me}_3\text{SiCl}$  (31.28 g, 286.97 mmol) in toluene (350 mL) at room temperature for 24 h. After soaking, the solid was filtered and washed with acetone (10 x 40 mL) and diethyl ether (10 x 15 mL) and dried under vacuum at  $100^{\circ}\text{C}$  for 5 h. This resulted in isolation of 25.81 g of solid.  $\text{Me}_3\text{SiCl}$  will bind with any unreacted  $-\text{OH}$  on the solid to form  $-\text{OSiMe}_3$  to block the reactivity of the hydroxyl groups on the silica surface.

**SiABDTH<sub>2</sub>:** Silica-NH<sub>2</sub> (9.0 g) was refluxed in a solution of ABDTH<sub>2</sub> (22.78 mmol, 8.50 g) in ethanol (500 mL) for 24 h. After refluxing, the solid was filtered and washed with ethanol (12 x 50 mL) and dried under vacuum yielding 8.6 g.

**Characterization:** The surface modification of the silica particle with amine followed by thiol functional groups was characterized by infrared spectroscopy (IR), elemental analysis (EA) and thermogravimetric analysis (TGA). Particles were also analyzed for particle size distribution. EA provided nitrogen content and also sulfur content on the



silica particle. ICP-OES analysis of sulfur element on modified silica particle was also conducted to determine the loading of thiol chelator (ABDTH<sub>2</sub>) on silica.

**Infrared Spectroscopy:** IR was carried out for both SiNH<sub>2</sub> and SiABDTH<sub>2</sub> to determine the functionality (-NH<sub>2</sub>, -CH<sub>2</sub>-, -OH) on the silica surface. A peak at 3434 cm<sup>-1</sup> was observed for N-H in SiNH<sub>2</sub>. The peak intensity of O-H in Si60 at 3459 cm<sup>-1</sup> was decreased drastically after treatment of Si60 particles with APTES. A broad peak at 3440 cm<sup>-1</sup> for carboxylic acid and a peak at 3050 cm<sup>-1</sup> for sp<sup>2</sup> C-H were observed in SiABDTH<sub>2</sub>. There was also a peak at 1538 cm<sup>-1</sup> (N-H) that was observed due to the formation of amide linkage.

**Elemental Analysis (%):** The experimental EA of SiNH<sub>2</sub> showed the presence of elements as follows C 7.71; H 2.42; N 2.72; O 9.37; Si 32.87; S 0.03; (Si60: C 0.05; H 1.26; N 0.01; O 7.22; Si 42.60; S <0.01). From the experimental analysis, nitrogen content was 1.94 mmol/g SiNH<sub>2</sub>. Similarly EA of SiABDTH<sub>2</sub> was as follow - C 10.33; H 2.68; N 2.89; O 12.04; Si 26.88; S 0.76; (Si60: C 0.05; H 1.26; N 0.01; O 7.22; Si 42.60; S <0.01) and the sulfur content was 0.24 mmol/g of SiABDTH<sub>2</sub>.

**Thermogravimetric Analysis (TGA):** Thermogravimetric curve of Si60 and modified silica (SiNH<sub>2</sub> and SiABDTH<sub>2</sub>) was obtained in Universal V3.9A TA instrument in the temperature range between 30<sup>0</sup>C and 1000<sup>0</sup>C with the rate of increase of 20<sup>0</sup>C/min at air flow rate of 110/55 mL/min. The thermogravimetric curve is shown in Figure 4.5.

**ICP-OES analysis of Sulfur:** SiABDTH<sub>2</sub> beads (500 mg) were digested at 110<sup>0</sup>C for 20 h by addition of 10 mL water, 10 mL 1:1 HNO<sub>3</sub>:H<sub>2</sub>O, 5 mL conc. HNO<sub>3</sub> and 10 mL conc. HCl. After digestion, the sample was diluted to 50 mL by addition of DI water and the solutions were filtered through a 0.2 μm Teflon filter to isolate the beads in order to analyze the filtrate. The solutions were then analyzed by ICP to determine the sulfur content (Table 4.1). The sulfur content was determined by ICP-OES analysis at a wavelength of 181.972 nm with an operating power of 1.20 kW and sample replicate read time of 2.00 s. Yttrium measured at 371.029 nm was used as an internal standard for the analysis. Samples were diluted by a factor of 10 prior to analysis. Quality control of the analysis was maintained by conducting the analysis of duplicate sample (0.57% RSD), matrix spike (98% recovery) and sulfur standards (5 ppm, 105% recovery and 10 ppm, 102% recovery at 181.972 nm)

**Particle Size Distribution of Si60:** Particle size distribution of Si60 was analyzed by a Beckman Coulter LS 13 320 particle size analyzer in triplicate. The mean particle size of the triplicate samples was 920.4 μm, 928.8 μm and 926.4 μm, respectively. Particle size distribution of three analyses was in the range of 0.375 μm to 2000 μm with standard deviation of 357.8 μm, 396.0 μm and 360.3 μm. The distributions are shown in Figures 4.4.

#### **4.3.2.2. 48 g SiABDTH<sub>2</sub>**

**SiNH<sub>2</sub>:** A suspension of silica-60 (Si60, 50 g, 18-35 mesh; 0.5-1.0 mm) in toluene (700 mL) was refluxed with γ -aminopropyltriethoxysilane (39.25 g, 178.4 mmol) in

chloroform (60 mL) at 100°C for 48 h before the solid was isolated by filtration, washed with  $\text{CHCl}_3$  (7 x 100 mL) and dried under vacuum for 12 h. The solid was then suspended in a solution of  $\text{Me}_3\text{SiCl}$  (42.5 g, 389.90 mmol) in toluene (500 mL) at room temperature for 24 h, filtered, washed with acetone (10 x 60 mL) and diethyl ether (10 x 25 mL), and dried under vacuum at 100°C for 5 h resulting in 61.21 g of  $\text{SiNH}_2$ .

**SiABDTH<sub>2</sub>:**  $\text{SiNH}_2$  (50 g) was refluxed in a solution of ABDTH<sub>2</sub> (50.08 g, 134.26 mmol) in ethanol (700 mL) for 24 h before filtration, washing with ethanol (15 x 50 mL) and drying under vacuum to yield 48.2 g of SiABDTH<sub>2</sub>.

**Characterization:** SiABDTH<sub>2</sub> beads (1.0 g) were digested at 110°C for 20 h by sequential addition of 10 mL water, 10 mL 1:1  $\text{HNO}_3\text{:H}_2\text{O}$ , 5 mL concentrated nitric acid and 10 mL concentrated HCl. Post-digestion, the sample was diluted to 50 mL by addition of DI water and the solution was filtered through 0.2  $\mu\text{m}$  Teflon filter to isolate the beads. The sulfur content was determined by ICP-OES analysis at a wavelength of 180.669 nm with an operating power of 1.20 kW and sample replicate read time of 2.00 s. Yttrium measured at 371.029 nm was used as internal standard for the analysis.

Duplicate samples (0.23% RSD), matrix spike (101% recovery) and sulfur standards (20 ppm, 100% recovery and 40 ppm, 102% recovery at 180.669 nm) were included in the analysis for quality control. Samples were diluted by a factor of 10 prior to analysis.

ABDTH<sub>2</sub> loading was calculated from sulfur analysis of SiABDTH<sub>2</sub> to be 0.235 mmol g<sup>-1</sup>.

<sup>1</sup>. Raw data and calculated values are shown in Table 4.1.

#### 4.3.2.3. 93 g SiABDTH<sub>2</sub>

**SiNH<sub>2</sub>:** A suspension of Si60 (60 g) in toluene (1500 mL) was refluxed with  $\gamma$ -aminopropyltriethoxysilane (47.10 g, 212.76 mmol) in chloroform (120 mL) at 130°C for 48 h. After refluxing, the solid was isolated by filtration, washed with CHCl<sub>3</sub> (5 x 100 mL) and dried under vacuum for 12 h. The solid was then suspended in a solution of Me<sub>3</sub>SiCl (100 mL) in toluene (500 mL) at room temperature for 24 h. The solid was filtered, washed with acetone (5 x 100 mL) and diethyl ether (5 x 100 mL), and dried under vacuum at 100°C for 5 h resulting in the isolation of 83 g of solid SiNH<sub>2</sub>.

**SiABDTH<sub>2</sub>:** SiNH<sub>2</sub> (83g) was combined with ABDTH<sub>2</sub> (83g, 223 mmol) in ethanol (1500 mL) and refluxed for 24 h. The solid was isolated by filtration, washed with ethanol (4 x 500 mL) and dried under vacuum for 12 h to yield 92.5 g solid SiABDTH<sub>2</sub>.

**Characterization:** SiABDTH<sub>2</sub> was analyzed by ICP-OES to determine the ABDTH<sub>2</sub> loading on silica. SiABDTH<sub>2</sub> was digested in triplicate with 1.0 g of material by addition of water (50 mL, DI), nitric acid (2.5 mL, concentrated, Omnitrace), hydrochloric acid (2.5 mL, concentrated, Omnitrace) and heating to 100°C for 20 h. The longer time caused complete digestion of the organic component from the insoluble solid support as hydrogen peroxide could not be used as an oxidizing agent due to the presence of considerable amount of sulfur. After digestion, the volume was brought to 50 mL with DI water and the suspension was syringe filtered (0.2  $\mu$ m, Teflon, Environmental Express) prior to analysis by ICP-OES for sulfur content at a wavelength of 181.972 nm. The ICP was operated at 1.20 kW and with a sample replicate read time of 2.00 s.

Yttrium measured at 371.029 nm was used as an internal standard. Duplicate samples (1.39% RSD), matrix spike (101% recovery) and sulfur check standards (2 ppm, 100% recovery and 5 ppm, 101% recovery at 181.972 nm) were included in the analysis for quality control. Samples were diluted 100-fold prior to analysis. Raw data and calculated values are shown in Table 4.1.

#### **4.3.2.4. 131 g SiABDTH<sub>2</sub>**

**SiNH<sub>2</sub>:** A suspension of Si60 (90 g) in toluene (1500 mL) was refluxed with  $\gamma$ -aminopropyltriethoxysilane (70 g, 316.2 mmol) in chloroform (120 mL) in a 3 L round bottom flask at 130°C for 48 h. After refluxing, the solid from each batch was isolated by filtration, washed with CHCl<sub>3</sub> (5 x 100 mL) and dried under vacuum for 12 h separately. The solid was then suspended in a solution of Me<sub>3</sub>SiCl (150 mL) in toluene (500 mL) at room temperature for 24 h. The solid was filtered, washed with acetone (5 x 100 mL) followed by washing with diethyl ether (5 x 100 mL) and dried under vacuum at 100°C for 5 h resulting in the isolation of 115 g of solid SiNH<sub>2</sub>.

**SiABDTH<sub>2</sub>:** SiNH<sub>2</sub> (115 g) was combined with ABDTH<sub>2</sub> (86 g, 231 mmol) in ethanol (1500 mL) and refluxed for 24 h separately. The solid was then isolated by filtration followed by a combination of washing (4 x 500 mL) and soaking (2 x 500 mL) with ethanol over a period of 4 h and then dried under vacuum for 12 h to yield 131 g of solid SiABDTH<sub>2</sub>.

**Characterization:** Sulfur content in SiABDTH<sub>2</sub> was determined by ICP-OES. Samples were digested in triplicate by taking 1.0 g of sample with addition of water (50 mL, DI), nitric acid (2.5 mL, concentrated, Omnitrace), hydrochloric acid (2.5 mL, concentrated, Omnitrace) and heating to 100°C for 20 h. The longer time was provided for complete digestion of the organic part from the insoluble solid support as hydrogen peroxide could not be used as an oxidizing agent due to presence of considerable amount of sulfur. After digestion, the volume was brought to 50 mL with DI water and the suspension was syringe filtered (0.2 µm, Teflon, Environmental Express) prior to analysis by ICP-OES for sulfur content at a wavelength of 181.972 nm. The ICP was operated at 1.20 kW and with a sample replicate read time of 2.00 s. Yttrium measured at 371.029 nm was used as an internal standard. Duplicate samples (0.35% RD), matrix spike (103% recovery) and sulfur standards (2 ppm, 101% recovery and 5 ppm, 101% recovery at 181.972 nm) were included in the analysis for quality control. Samples were diluted 50-fold prior to analysis. Raw data and calculated values are shown in Table 4.1. The ICP analysis of sulfur content of SiABDTH<sub>2</sub> confirms the binding of about 0.114 mmol of ABDTH<sub>2</sub> per gm of SiABDTH<sub>2</sub> in both batches.

#### 4.3.3. Titrations of SiABDTH<sub>2</sub>

SiABDTH<sub>2</sub> (1.02 g, 37 mmol ABDTH<sub>2</sub>) was slurried in 100 mL DI water and allowed to stir for 10 min before titrating with dilute NaOH (0.024 M, 978.9 mg in 1000 mL). The initial pH of the SiABDTH<sub>2</sub> slurry was 2.90 and increased with the addition of NaOH to generate the curve shown in Figure 4.4. From the titration curve a pK<sub>a</sub> of 3.30 was calculated for SiABDTH<sub>2</sub> which was close to pK<sub>a1</sub> of ABDTH<sub>2</sub> (3.60). A second and

third titration was conducted for triplicate measurements of pKa. SiABDTH<sub>2</sub> (0.99 g and 1.01 g) was slurried again in DI water (100 mL) with an initial pH of 2.55 and 2.78, respectively, followed by titration with NaOH (0.026 M) by dispensing either 100  $\mu$ L and 500  $\mu$ L to yield the titration curves. From these data, the average pKa value of 3.10 ( $\pm$  0.26) was calculated.

#### **4.4. Conclusions**

ABDTH<sub>2</sub> was immobilized on Si60 by modifying the silica surface with APTES. The higher decomposition temperature of organic component in TGA analysis of SiABDTH<sub>2</sub> indicated the immobilization of ABDTH<sub>2</sub> on the silica surface. Elemental analysis and ICP-OES analysis also confirmed the presence of ABDTH<sub>2</sub> on silica. SiABDTH<sub>2</sub> was prepared in different batches of various amounts of starting materials. ABDTH<sub>2</sub> loading on silica surface was increased until 60 g scale preparation. However, with increasing the batch scale to 90 g of Si60 did not improve the ABDTH<sub>2</sub> loading on silica. SiABDTH<sub>2</sub> would be an excellent solid-supported thiol to apply as filtration column material for the removal of arsenic from water.

## CHAPTER 5

### Arsenic and Mercury Removal Using SiABDTH<sub>2</sub>

#### 5.1. Introduction

The contamination of surface and ground water with heavy metals and metalloids is one of the major environmental concerns at present. Heavy metals and metalloids such as cadmium (Cd), mercury (Hg), lead (Pb) and arsenic (As) adversely affect human health and the natural ecosystem due to their acute and long term toxicity.<sup>260</sup> Amongst all these elements released into the environment, particular concern has been raised about the transport and accumulation of arsenic and mercury. Both As and Hg are ubiquitous in nature, non-biodegradable and toxic to the environment. Arsenic contamination of groundwater in several parts of the world poses severe health concern as groundwater is extensively used for drinking water, household and agricultural use. As mercury is released into environment from both natural and anthropogenic sources, in these areas mercury bioaccumulation is another major health concern effecting neurons, heart, lungs, and muscles causing chronic mercury toxicity.<sup>181,261</sup> Due to the high toxicity of these elements, the U.S. Environmental Protection Agency (EPA) has set the maximum contaminant level (MCL) of 10 µg/L (ppb) arsenic and 2 µg/L (ppb) mercury in drinking water.<sup>177,178,262</sup>

Extensive research needs to be carried out to develop new materials and technology to remove these toxic metals from contaminated drinking water, groundwater and various other media. Several common mitigation and remediation methods such as phytoremediation, bioremediation, activated carbon, adsorption, ion-exchange resin,



electrolytic or liquid extraction, electrodialysis, reverse osmosis, chelating fiber and precipitating agents are available that can be employed separately or in combination to remove arsenic and mercury from drinking water and wastewater. Coagulation and precipitation of the toxic metals with sulfur containing reagents is perhaps the most effective way for large scale treatment process. This method however leads to the additional issue of handling large amounts of toxic sludge. Low-cost solid supported adsorbent could be an attractive alternative means of removing toxic metal by adsorption. Many researchers have used silica coated with cysteine, polycysteine and other sulfur containing reagents to remove and/or recover heavy metals in aqueous and gas phase.<sup>246</sup> BDTH<sub>2</sub> is an inexpensive and effective precipitating agent of soft heavy metals from aqueous media by forming stable metal ligand complexes. It can reduce arsenic and mercury concentrations in the ppm to ppb range by complete precipitation of the BDT-metal compound, to below instrumental detection limits.<sup>172</sup> Due to the absence of reactive functional groups other than thiol, it cannot be immobilized on solid support like silica for use as filtration column material for removing arsenic and other toxic metals. As a result, an acid derivative of BDTH<sub>2</sub> (ABDTH<sub>2</sub>) has been synthesized and immobilized on silica to prepare SiABDTH<sub>2</sub>. This chapter discusses the arsenic and mercury uptake ability of SiABDTH<sub>2</sub> from aqueous media through chemisorption. Chemisorption is a process where adsorption is occurring through chemical reactions on the exposed surface of the adsorbent.

## 5.2. Results and Discussion

### 5.2.1. Arsenic Removal Batch Study

Aqueous solutions of arsenic at pH 5, 7 and 9 were treated with SiABDTH<sub>2</sub>. The pH range of 5-9 was used for the experiment as pH of groundwater varies in the range of 6-8 depending on the condition of soil and sediments. Approximately 200 ppb aqueous arsenic solution was prepared at desired pH by mixing 8.70 mg, 8.66 mg and 8.66 mg of NaAsO<sub>2</sub>, respectively, in 50 mL DI water to obtain 100 ppm solution followed by serial dilutions to prepare desired concentration of 200 ppb arsenic solution. NaAsO<sub>2</sub> form anionic arsenious acid species Na[H<sub>2</sub>AsO<sub>3</sub>] in water. NaAsO<sub>2</sub> is a oxide donor which acts as Lux-Flood base, whereas H<sub>2</sub>O is a oxide acceptor and acts as acid. Arsenic stock solutions at different pH values were analyzed by graphite furnace atomic absorption (GFAA) spectroscopy to determine the actual concentration of arsenic in the stock solutions as 222.1, 233.1 and 196.9 ppb at pH 5, 7 and 9, respectively. Aqueous arsenic solution was then treated with SiABDTH<sub>2</sub> in the respective pH solutions for 24 h, followed by filtration through 0.2 µm Teflon filter to remove particulate from solutions. Filtrate was then digested at 95<sup>0</sup>C with concentrated nitric acid and analyzed by GFAA to detect low level concentration of arsenic in aqueous solution. GFAA spectroscopy instrument has a detection range of 5 – 50 ppb arsenic. As a result higher concentration solutions were diluted in order to measure the arsenic concentration within the instrumental limit. Arsenic stock solution of 50 mL 222.1 ppb arsenic aqueous solution at pH 5 was stirred with 0.6 g of SiABDTH<sub>2</sub> for 24 h before the analysis of arsenic concentration in the SiABDTH<sub>2</sub> treated solution by GFAA. The instrumental and calculated values of spectroscopic analysis for pH 5 solution are shown in Table 5.1.

GFAA analysis showed that arsenic concentration in the treated solution was less than 5 ppb which is the lower detection limit of the instrument indicating 100% arsenic capture by 0.6 g of SiABDTH<sub>2</sub>. Arsenic stock solution of 50 mL of 222.1 ppb at pH 5 was also stirred with 0.4 g and 0.2 g of SiABDTH<sub>2</sub>, respectively, for 24 h prior to analysis. In both cases arsenic concentration in treated aqueous solution was less than 5 ppb.

Aqueous arsenic solutions at pH 7 and 9 were also treated with SiABDTH<sub>2</sub> and a similar trend was observed as shown in Table 5.1. When 50 mL of 213.0 ppb aqueous arsenic solution at pH 7 was stirred with 0.6, 0.4 and 0.2 g of SiABDTH<sub>2</sub> separately, arsenic concentration in solution was decreased to below 5 ppb with as low as 0.2 g of SiABDTH<sub>2</sub>. Similarly, SiABDTH<sub>2</sub> also removed 100% arsenic from 50 mL of 233.1 ppb arsenic solution at pH 9 when stirred with 0.6, 0.4 and 0.2 g of SiABDTH<sub>2</sub>.

**Table 5.1.** Determination of As removal by SiABDTH<sub>2</sub> at pH 5, 7 and 9

	<b>pH 5</b>	<b>% Capture</b>	<b>pH 7</b>	<b>% Capture</b>	<b>pH 9</b>	<b>% Capture</b>
<b>As stock</b>	222.1 ± 5.9	N/A	213.0 ± 6.2	N/A	233.1 ± 5.1	N/A
<b>0.2 g SiABDTH<sub>2</sub></b>	< 5.0	100%	< 5.0	100%	< 5.0	100%
<b>0.4 g SiABDTH<sub>2</sub></b>	< 5.0	100%	< 5.0	100%	< 5.0	100%
<b>0.6 g SiABDTH<sub>2</sub></b>	< 5.0	100%	< 5.0	100%	< 5.0	100%

A time dependent arsenic removal by SiABDTH<sub>2</sub> from aqueous solution study was also carried out to explore the effectiveness of SiABDTH<sub>2</sub> in a shorter period of

time. In this study, SiABDTH<sub>2</sub> was treated with approximately 200 ppb of 50 mL aqueous arsenic solution at pH 5, 7 and 9. SiABDTH<sub>2</sub> of 0.2 and 0.6 g was stirred with solutions contain arsenic for 1, 2 and 5 h, respectively, (Table 5.2, 5.3 and 5.4). Desired aqueous arsenic solutions were obtained by dilution of stock solution prepared by mixing NaAsO<sub>2</sub> in DI water. The study showed that at pH 5, 0.2 g of SiABDTH<sub>2</sub> captured 25% of arsenic within 1 h of contact time. But percentage of arsenic capture was increased to 37% and 74% by increasing the contact time to 2 and 5 h, respectively. When SiABDTH<sub>2</sub> loading was increased to 0.6 g at same pH, percentage of arsenic binding was increased to 34% within 1 h followed by 69% and 93% after 2 h and 5 h, respectively. At pH 7 and 9, a similar trend was observed. At pH 7, 0.2 g of SiABDTH<sub>2</sub> removed 41%, 56% and 79% of arsenic in 1, 2 and 5 h, respectively. Whereas 0.6 g of SiABDTH<sub>2</sub> removed 54%, 86% and 100% of arsenic in the same time periods. Similarly at pH 9, 0.2 and 0.6 g of SiABDTH<sub>2</sub> captured 31%, 41% and 72%, and 50%, 67% and 92% in 1, 2 and 5 h, respectively. Lower percent binding of arsenic in shorter period of time was attributed to the presence of non-anionic species of arsenious acid. However the percentage of arsenic removal with time reaches plateau at very low and high concentration as reaction equilibrium reaches with time. A deuterium exchange kinetic study can be conducted to determine the availability of ABDTH<sub>2</sub> ligand at different concentration of deuterium. The adsorption of arsenic by SiABDTH<sub>2</sub> was also dependent on pH. Figure 5.1 and 5.2 illustrates the adsorption of As(III) by SiABDTH<sub>2</sub> at different pH for 1, 2 and 5 h. Maximum adsorption of arsenic was observed at pH 7. Adsorption of arsenic was increased when pH was increased from 5 to 7 but decreased at pH 9. At lower pH, H<sub>3</sub>AsO<sub>3</sub> is the predominant species. Thiol of SiABDTH<sub>2</sub> is also present in

protonated form. This resulted in poor binding interaction between As(III) species and thiol group of SiABDTH<sub>2</sub> at pH 5. As pH of solution increases, [H<sub>2</sub>AsO<sub>3</sub>]<sup>-</sup> species starts to appear in solution which resulted in increase in percentage of As(III) at pH 7. However as the pH of solution increases, deprotonation of thiol groups present on the solid surface leads to the formation of thiolates. Also at higher pH arsenious acid is present in the form of anionic species of [H<sub>2</sub>AsO<sub>3</sub>]<sup>-</sup> and [HAsO<sub>3</sub>]<sup>2-</sup>. As a result of the electrostatic repulsion between the anionic arsenious species and thiolates, arsenic capture at higher pH decreases.<sup>103,104,167,231</sup>

As(III) removal study indicated that SiABDTH<sub>2</sub> has demonstrated excellent capture ability of As(III) from aqueous solutions compared to other existing arsenic sorbents. It removed 100% As(III) over the pH range of 5-9 under laboratory conditions. Activated alumina (AA), activated carbon and iron based materials showed arsenic capture ability. However, these materials can only remove As(V) in the range of 80% - 96% depending on the pH of solutions, the effect of dissolved oxygen and the nature of surface of the sorbents.<sup>128,131,147</sup> On the other hand these materials showed poor As(III) capture capability. As a result, preoxidation of As(III) is required in most cases for the removal of As(III). Membrane filtration processes are other absorption techniques that showed complete arsenic removal capacity, but the operating cost and small scale applications are remain issues.<sup>152</sup> The extensive use of the ground water in many countries leads to the prolonged exposure of arsenic present in the ground water. As(III) is also the major oxidation of state of arsenic species present in the ground water. As a result, easy and inexpensive removal of As(III) is remain focus of research. In this regard, SiABDTH<sub>2</sub> has demonstrated complete removal of As(III) from 50 mL 200 ppb

aqueous solutions over the pH range of 5-9. Use of silica as solid support also makes it cost effective due to its abundance in nature.

**Table 5.2.** Time dependent As removal by SiABDTH<sub>2</sub> at pH 5

<b>Sample ID</b>	<b>Time</b>	<b>Conc. (µg/L)</b>	<b>Stdev.</b>	<b>% Remed.</b>
<b>As stock</b>		196.9	± 3.21	N/A
<b>0.2 g SiABDTH<sub>2</sub></b>	1 h	146.8	± 0.84	25%
	2 h	123.6	± 2.18	37%
	5 h	51.4	± 0.40	74%
<b>0.6 g SiABDTH<sub>2</sub></b>	1 h	129.4	± 2.10	34%
	2 h	60.1	± 0.57	69%
	5 h	14	± 0.05	93%

**Table 5.3.** Time dependent As removal by SiABDTH<sub>2</sub> at pH 7

<b>Sample ID</b>	<b>Time</b>	<b>Conc. (µg/L)</b>	<b>Stdev.</b>	<b>% Remed.</b>
<b>As stock</b>		249.4	± 0.60	N/A
<b>0.2 g SiABDTH<sub>2</sub></b>	1 h	146.6	± 0.23	41%
	2 h	109.8	± 1.90	56%
	5 h	53.2	± 0.57	79%
<b>0.6 g SiABDTH<sub>2</sub></b>	1 h	114.5	± 0.98	54%
	2 h	33.9	± 0.24	86%
	5 h	< 5.0	N/A	100%

**Table 5.4.** Time dependent As removal by SiABDTH<sub>2</sub> at pH 9

Sample ID	Time	Conc. (µg/L)	Stdev.	% Remed.
As stock		192.1	± 1.42	N/A
<b>0.2 g SiABDTH<sub>2</sub></b>	1 h	131.7	± 1.53	31%
	2 h	112.4	± 1.76	41%
	5 h	54.5	± 0.15	72%
<b>0.6 g SiABDTH<sub>2</sub></b>	1 h	96.2	± 0.84	50%
	2 h	63.5	± 0.55	67%
	5 h	14.6	± 0.14	92%

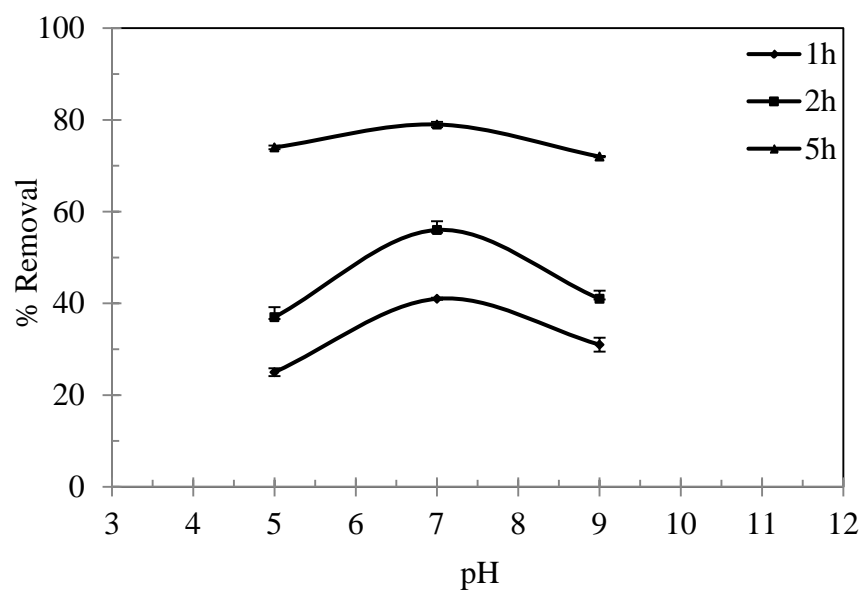


**Figure 5.1.** Removal of As(III) from water by 0.2 g of SiABDTH<sub>2</sub> as a function of pH

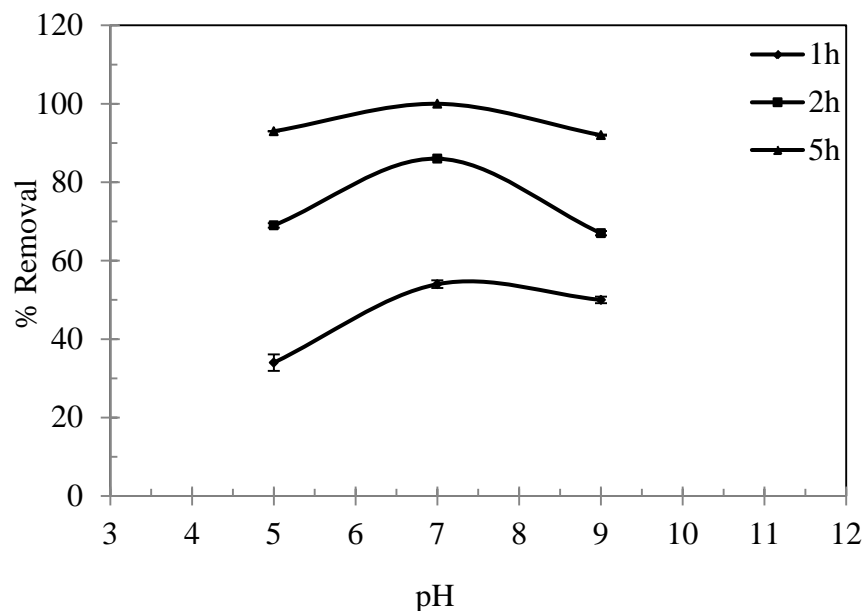


**Figure 5.2.** Removal of As(III) from water by 0.6 g of SiABDTH<sub>2</sub> as a function of pH

### 5.2.2. Arsenic Leaching Study of SiABDT-As(III)

A leaching study of arsenic from SiABDT-As(III) was carried out by putting the material at pH 5, 7 and 9 for 24 h, 1, 2, 3 and 4 weeks and the results are shown in Table 5.5. Arsenic concentration in solutions was analyzed by GFAA spectroscopic analysis at a wavelength of 193.7 nm. Leaching study showed that 12-29% of arsenic leached back into water at pH 5, 7 and 9. The percentage of leaching remained almost constant over several weeks suggesting that certain percent of arsenic was bonded to physisorbed ABDTH<sub>2</sub> on solid surface which was leaching back to water. The leaching of arsenic is most likely due to presence of physisorbed arsenic as well as oxidation of As(III) to As(V) and its subsequent release from ABDT-As(III) in aqueous solution. As a result ABDTH<sub>2</sub> will be regenerated for further As(III) binding.



**Table 5.5.** As leaching from 0.2 g of SiABDT-As(III) after 24 h, 1, 2, 3 and 4 weeks

<b>Time</b>	<b>pH</b>	<b>Final [As] ppb</b>	<b>As (mg)/0.2 g SiABDT- As(III)</b>	<b>As (mg) Leached</b>	<b>% As Leached</b>
<b>As Stock</b>		9144 ± 528	0.45		
<b>24 h</b>	5	1937.0 ± 43.0		0.10	21
	7	1735.0 ± 23.0		0.09	19
	9	1678.0 ± 32.0		0.08	18
<b>1 week</b>	5	1715.0 ± 26.0		0.09	19
	7	1576.0 ± 30.0		0.08	17
	9	1449.0 ± 29.0		0.07	16
<b>2 weeks</b>	5	16.81 ± 30.0		0.08	18
	7	2279.0 ± 21.0		0.11	25
	9	1948.0 ± 107.0		0.10	21
<b>3 weeks</b>	5	2431.0 ± 89.0		0.12	27
	7	2219.0 ± 6.0		0.11	24
	9	1086.0 ± 41.0		0.05	12
<b>4 weeks</b>	5	2687.0 ± 61.0		0.13	29
	7	2634.0 ± 42.0		0.13	29
	9	1621.0 ± 48.0		0.08	18

### 5.2.3. XAFS Study of Arsenic Sorbents

The arsenic binding environment in SiABDT-As(III) and SiABDT-As(III)<sub>LCH</sub> was determined by performing XAFS spectroscopy on the arsenic sorbents. SiABDT-As(III)<sub>LCH</sub> was obtained by leaching off arsenic from SiABDT-As(III) in aqueous solution. As a result any physisorbed arsenic should be leached back to water. The study was conducted at the K-edge of arsenic in SiABDT-As(III), SiABDT-As(III)<sub>LCH</sub> with synthetic orpiment (As<sub>2</sub>S<sub>3</sub>) as reference material. The spectra for arsenic in SiABDT-As(III) and SiABDT-As(III)<sub>LCH</sub> were very similar to the spectrum of As<sub>2</sub>S<sub>3</sub>. The overall shape and position of the major peaks in the XANES and RSF spectra of all four materials are virtually same. Although the corresponding spectrum of As<sub>2</sub>S<sub>3</sub> showed different intensity in spectral features, it exhibited major peaks at about the same positions as sorbent samples. This similarity implies strongly that the bonding for arsenic in the sorbent samples is similar to that in arsenic sulfide. The arsenic K-edge XANES spectra of the compounds are shown in Figure 5.3. The absorption energy of arsenic in SiABDT-As(III) and SiABDT-As(III)<sub>LCH</sub> was very similar to the arsenic K-edge absorption peak position in As<sub>2</sub>S<sub>3</sub>. In all these compounds, the K-edge value (eV) was 11866 eV in close agreement with the K-edge value observed in As<sub>2</sub>S<sub>3</sub> suggesting that the oxidation state of arsenic in SiABDT-As(III) and SiABDT-As(III)<sub>LCH</sub> was +3.<sup>156</sup> Figure 5.4 shows the EXAFS region of XAFS spectra for As<sub>2</sub>S<sub>3</sub> and SiABDT-As(III) and SiABDT-As(III)<sub>LCH</sub>. The oscillations in EXAFS were converted to reciprocal space (*k*-space, chi spectrum in Å<sup>-1</sup>) representation and weighted by *k*<sup>3</sup>.

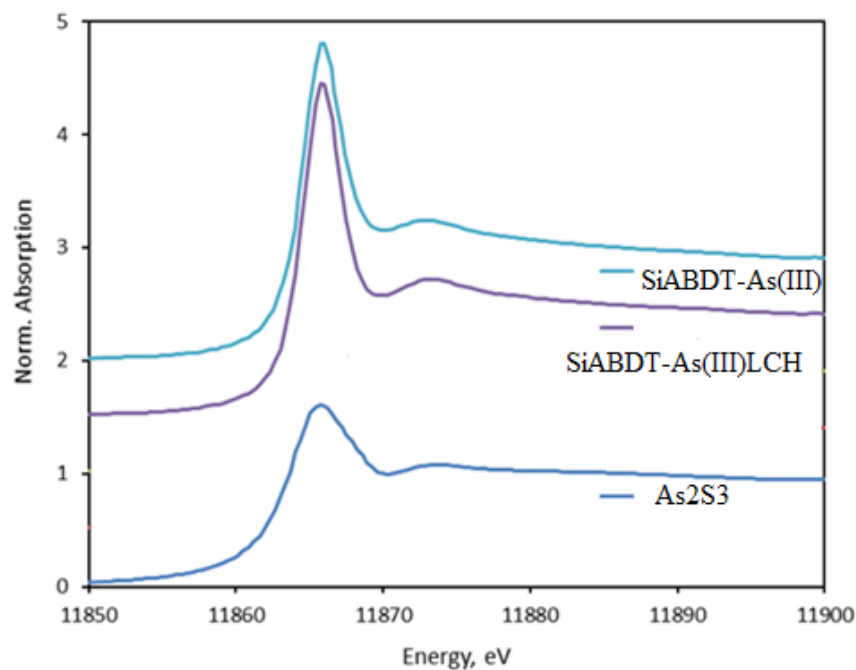


**Figure 5.3.** Arsenic *K*-edge spectra for As<sub>2</sub>S<sub>3</sub>, SiABDT-As(III)<sub>LCH</sub> and SiABDT-As(III)

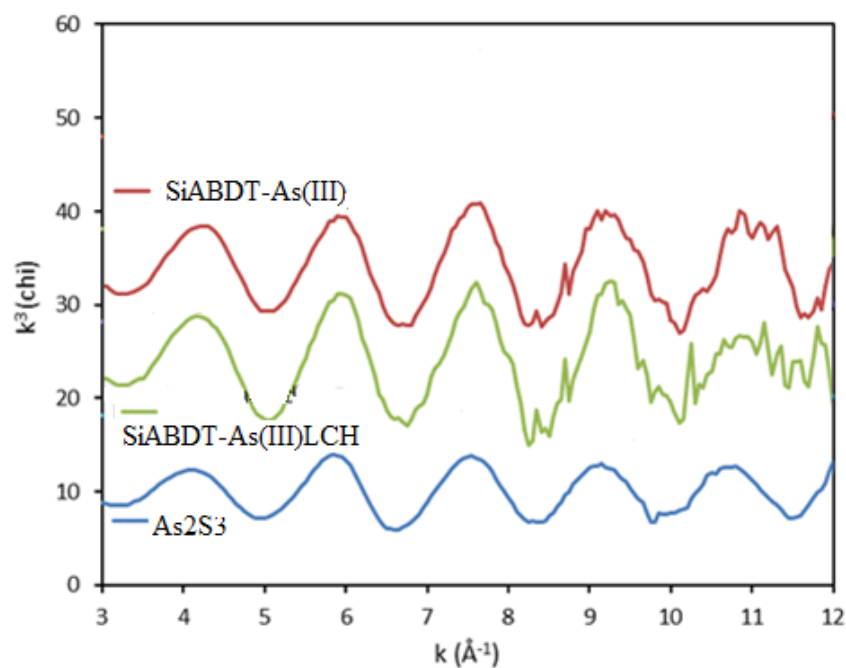


**Figure 5.4.** Arsenic EXAFS ( $k^3\chi$ ) spectra for As<sub>2</sub>S<sub>3</sub> and arsenic sorbents SiABDT-As(III)<sub>LCH</sub> and SiABDT-As(III)

The radial structure function (RSF) of arsenic sorbents is shown in Figure 5.5. RSF spectrum was obtained by applying Fourier Transform to the spectra in Figure 5.4. It is considered as a one-dimensional representation of the structure local to the absorbing atom which is arsenic in these materials. It is possible to estimate the distance ( $R$  in Å) of As-S bond and the coordination number (CN) by applying data fitting procedures in the IFEFFIT XAFS data analysis package. The crystal structure of orpiment, naturally occurring  $\text{As}_2\text{S}_3$ , was refined by Mullen and Nowacki and the details were published in 1972 in *Z. Kristallographie*.<sup>238</sup> The structure consists of continuous As-S layers in the a-c plane, in which each As atom is coordinated to three S atoms at an average distance of 2.283 Å. The distance between adjacent layers is much larger, approximately 3.3 Å. Hence, the major peak in the RSF corresponds to the threefold As-S coordination within the layers. Using the program TKAtoms<sup>236</sup>, one of the programs in the IFEFFIT XAFS data analysis package<sup>237</sup>, the As-S coordination shell was modeled based on the crystallographic details given in the paper by Mullen and Nowacki to obtain XAFS parametric data for As-S coordination. Using these parametric data and a second program, SixPack, in the same data analysis package, least-squares fitting of the EXAFS data was carried out for  $\text{As}_2\text{S}_3$ .<sup>237,263</sup> The results for  $\text{As}_2\text{S}_3$  are summarized in Table 5.6. In the fitting, the coordination number,  $N$ , was fixed at 3 in order to obtain a value of 0.57 for the coordination parameter,  $S_0^2$ . The values listed in Table 5.6 for the energy zero shift,  $e_0$ , the As-S distance,  $R$ , and the Debye-Waller factor,  $\sigma^2$ , were also obtained by least-squares fitting of the EXAFS data to the calculated equation derived for the As-S photoelectron back-scattering. As shown in Table 5.6, the least-squares fitting was done in all three modes: R mode ( $\text{FT}[k^3\chi]$  over the region 1.2 to 2.4 Å),  $q$

mode (back-transform of the FT region) and k mode ( $k^3\chi$ , over the range 3 to 12  $\text{\AA}^{-1}$ ) and reasonably consistent results were found in all three modes. The  $R_{\text{factor}}$  is a statistical measure of the fitting. The As-S distance derived from the FEFF EXAFS analysis ( $2.29 \pm 0.01$   $\text{\AA}$ ) was in good agreement with to that ( $2.283 \pm 0.005$   $\text{\AA}$ ) obtained from the crystal structure analysis.

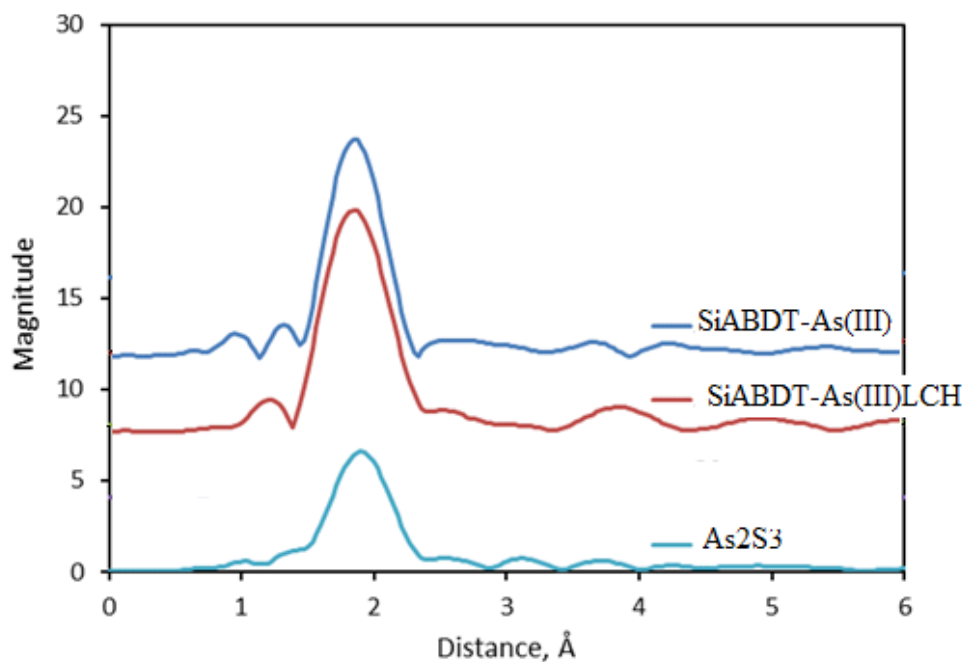


**Figure 5.5.** Arsenic RSF spectra for  $\text{As}_2\text{S}_3$ ,  $\text{SiABDT-As(III)}_{\text{LCH}}$  and  $\text{SiABDT-As(III)}$

**Table 5.6.** Least-squares fitting parameters derived for As<sub>2</sub>S<sub>3</sub> (Values in parentheses were held fixed during fitting)

Mode	Range	$e_0$	$S_0^2$	CN	R, Å	$\sigma^2$ , Å <sup>2</sup>	R <sub>factor</sub>
R	1.2 - 2.4 Å	9.1	0.59	(3)	2.29	0.0037	0.0088
q		9.8	0.57	(3)	2.29	0.0035	0.0060
k	3 - 12 Å <sup>-1</sup>	9.7	0.54	(3)	2.29	0.0030	0.0292
	errors (q)	±1.3	±0.06		±0.01	±0.0008	

These values were used in photoelectron backscattering to model the EXAFS region of SiABDT-As(III) and SiABDT-As(III)<sub>LCH</sub> for calculating the coordination number. Using a fixed value of 0.57 for  $S_0^2$ , similar analyses were carried out for the EXAFS data ( $k^3\chi$ ) obtained for arsenic in the sorbent samples. In these cases, the coordination number, CN, was derived from the least-squares fit, along with the other unconstrained parameters. The results are summarized in Table 5.7 and 5.8. The comparison of data and fit obtained for SiABDT-As(III) is shown in Figure 5.6. The comparison of data and fit for the reference sample, As<sub>2</sub>S<sub>3</sub>, can be found in Figure 3.6 in chapter III. The close correspondence of the  $k$ -space EXAFS spectrum for arsenic derived from back-transform of the As-S shell in the RSF and the  $k$ -space EXAFS spectrum for arsenic in SiABDT-As(III) can be observed in Figure 5.6. The fitting errors are larger for these samples as a result of the weaker EXAFS signal/noise ratios obtained for these samples.

**Table 5.7.** Least-squares fitting parameters of EXAFS data derived for SiABDT-As(III)

Mode	Range	$e_0$	$S_0^2$	CN	$R, \text{\AA}$	$\sigma^2, \text{\AA}^2$	$R_{\text{factor}}$
R	1.2 - 2.4 $\text{\AA}$	8.2	(0.57)	4.4	2.26	0.0024	0.0457
Q		8.7	(0.57)	4.6	2.26	0.0028	0.0303
K	3 - 12 $\text{\AA}^{-1}$	8.6	(0.57)	4.2	2.26	0.0020	0.0719
	errors (q)	$\pm 3.1$		$\pm 1.1$	$\pm 0.015$	$\pm 0.0018$	

**Table 5.8.** Least-squares fitting parameters of EXAFS data derived SiABDT-As(III)<sub>LCH</sub>

Mode	Range	$e^0$	$S_0^2$	CN	$R, \text{\AA}$	$\sigma^2, \text{\AA}^2$	$R_{\text{factor}}$
R	1.2 - 2.4 $\text{\AA}$	8.9	(0.57)	6.1	2.265	0.0045	0.0485
q		10.0	(0.57)	6.0	2.27	0.0041	0.0317
k	3 - 12 $\text{\AA}^{-1}$	9.4	(0.57)	6.1	2.27	0.0045	0.1160
	errors (q)	$\pm 3.0$		$\pm 1.5$	$\pm 0.015$	$\pm .0019$	

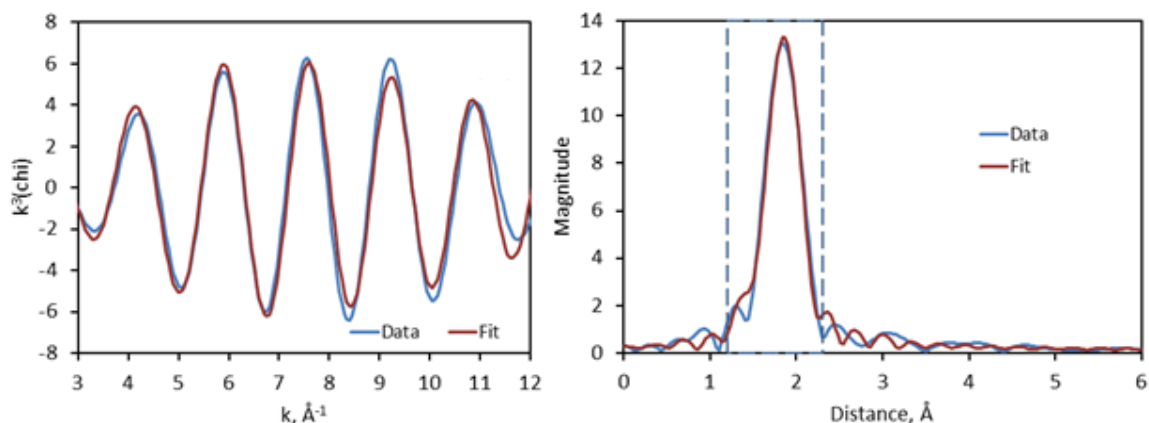


**Figure 5.6.** Comparison of FEFF model function and least-squares fitting for SiABDT-As(III). Left: q-mode fits; right: R-mode fits over the range 1.2 -2.4 \text{\AA}

The estimated bond distance ( $R$ , \text{\AA}) in SiABDT-As(III) and SiABDT-As(III)<sub>LCH</sub> was 2.26 and 2.27, respectively, which was in the range of reported As-S bond distance of 2.24-2.28 \text{\AA} for trithiol compounds while the Debye-Waller factor ( $\sigma^2$ ) was similar.<sup>206,238,239</sup> Similar As-S bond distance was also observed in tris(phenylthio)arsine (Figure 3.8.a) and As<sub>2</sub>S<sub>3</sub> (Figure 3.8.b) with a bond distance of 2.24 \text{\AA} and 2.28 \text{\AA}, respectively.<sup>238,239</sup> The coordination numbers obtained for the As-S shell in the sorbent sample from the FEFF EXAFS analysis range between 4.2 and 6.1. These values were significantly greater than that for the arsenic sulfide structure with high experimental error. Such findings suggest that the As-S coordination in the sorbents may vary between tetrahedral coordination (CN = 4) and octahedral coordination (CN = 6) with additional secondary interaction.

XAFS spectroscopy of SiABDT-As(III) and SiABDT-As(III)<sub>LCH</sub> showed only sulfur bound arsenic. No evidence was found for the bonding of As to any other element in the examined materials. XAFS of all the materials was compared with the As



bonding environment in  $\text{As}_2\text{S}_3$  which showed obvious similarities; however, the coordination of As by S in the arsenic containing materials exhibits a small reduction in the As-S distance (less than 0.03 Å) and a significant increase in coordination number from 3 to between 4 and 6.

#### **5.2.4. Batch Study of Hg Removal by SiABDTH<sub>2</sub>**

Studies of mercury capture ability of SiABDTH<sub>2</sub> in aqueous solution were also conducted. At pH 5, 7 and 9, 0.2 and 0.6 g of SiABDTH<sub>2</sub> was mixed with 4.98, 4.70 and 4.45 ppm aqueous mercury solution, respectively, for 24 h. After 24 h, samples were analyzed by ICP-OES to determine the remaining concentration of mercury in solution. SiABDTH<sub>2</sub> captured 72.8, 55.8 and 74.1% of mercury at pH 5, 7 and 9, respectively, when 0.2 g of SiABDTH<sub>2</sub> was added to the mercury solutions at different pHs (Table 5.9). When the amount of SiABDTH<sub>2</sub> increased to 0.6 g, the percentage of mercury capture increased to 92.8, 74.8 and 84.1% at pH 5, 7 and 9, respectively. This is likely due to all the ABDTH<sub>2</sub> binding sites are not available for the capture of mercury as certain percentage of ABDTH<sub>2</sub> is bonded on the surface of smaller pore size making it inaccessible for mercury capture. However SiABDTH<sub>2</sub> showed improved mercury removal capacity from aqueous solutions compared to commercially available mercury precipitating agents like sodium trithiocarbonate (STC), sodium dithiocarbamate (SDTC) and 2,4,6-trimercaptotriazine (TMT) (Figure). STC and SDTC showed comparable mercury binding ability, whereas TMT was unable to reduce mercury concentration significantly from 50 ppm aqueous mercury solution when applied in

stoichiometric ratio. However significant leaching of mercury was observed from the precipitant of STC, SDTC and TMT due to unstable nature of precipitating agents.<sup>192,264</sup>

**Table 5.9.** Hg concentration in supernatant solution after treatment with SiABDTH<sub>2</sub>

	<b>0.2 g</b>			<b>0.6 g</b>	
	<b>Initial (ppm)</b>	<b>Final (ppm)</b>	<b>% Remediation</b>	<b>Final (ppm)</b>	<b>% Remediation</b>
<b>pH 5</b>	4.98 ± 0.11	1.35 ± 0.01	72.8	0.46 ± 0.01	92.8
<b>pH 7</b>	4.70 ± 0.08	2.08 ± 0.03	55.8	1.18 ± 0.02	74.8
<b>pH 9</b>	4.45 ± 0.08	1.15 ± 0.03	74.1	0.71 ± 0.03	84.1

### 5.2.5. Leaching Study of SiABDT-Hg

A leaching study of mercury from SiABDT-Hg was carried out to determine the binding stability of mercury with SiABDTH<sub>2</sub>. The study was conducted for 24 h, 1, 2, 3 and 4 weeks at pH 5, 7 and 9. The percentage of mercury leaching was in the range of 1.47-3.67% for different conditions (Table 5.10). The percent of mercury leaching remained almost the same over several weeks. This was most likely due to either very low percentage of mercury was physisorbed on the particle surface or mercury was bonded to the physisorbed ABDTH<sub>2</sub>. It was also possible that at high pH Hg(OH)<sup>+</sup> and/or Hg(OH)<sub>2</sub> were being released in aqueous solutions.

**Table 5.10.** Hg leaching study of SiABDT-Hg

<b>Time</b>	<b>pH</b>	<b>Final [Hg] ppm</b>	<b>Hg (mg)/0.2 g SiABDT-Hg</b>	<b>Hg (mg) Leached</b>	<b>% Hg Leached</b>
<b>Stock</b>		137.6 ± 3.2	6.88		
<b>24 h</b>	5	5.04 ± 0.04		0.25	3.67
	7	4.39 ± 0.04		0.22	3.19
	9	4.98 ± 0.02		0.24	3.62
<b>1 week</b>	5	4.17 ± 0.02		0.20	3.00
	7	4.12 ± 0.05		0.20	3.00
	9	4.28 ± 0.04		0.21	3.11
<b>2 weeks</b>	5	2.85 ± 0.02		0.14	2.07
	7	2.76 ± 0.03		0.13	2.00
	9	3.24 ± 0.04		0.16	2.35
<b>3 weeks</b>	5	2.75 ± 0.02		0.13	2.00
	7	2.44 ± 0.04		0.12	1.77
	9	2.72 ± 0.02		0.13	2.00
<b>4 weeks</b>	5	2.74 ± 0.02		0.13	2.00
	7	2.02 ± 0.04		0.10	1.47
	9	2.45 ± 0.02		0.12	1.78

### 5.2.6. XPS Study of SiABDT-Hg

X-ray Photoelectron Spectroscopy (XPS) binding energies are reported with fwhm in parantheses. Figure 5.7 shows a narrow scan region where both the Hg 4f and Si 2p core levels emanate from the solid surface. The spectrum for SiABDTH<sub>2</sub> showed a peak at 103.2 (1.9) eV denoting Si 2p from SiABDTH<sub>2</sub> consistent with a SiO<sub>2</sub> structure. With the introduction of Hg in the sample at a 1:0.5 SiABDTH<sub>2</sub>:Hg ratio, core levels of the Hg<sub>4f7/2</sub> and Hg<sub>4f5/2</sub> appeared at 100.8 (1.5) and 104.8 (1.6) eV, respectively, consistent with Hg in a +2 oxidation state. At a higher loading of Hg in the sample with a 1:1 SiABDTH<sub>2</sub>:Hg ratio, there was little change in the chemical oxidation states present. The binding energy for Hg<sub>4f7/2</sub> lower than 101.0 eV was absent, which suggests that no elemental mercury [Hg(0)] was present on the solid surface as binding energy for Hg<sub>4f7/2</sub> of Hg(0) should be around 99.9 eV.<sup>265</sup> Similar binding energies for Hg<sub>4f7/2</sub> and Hg<sub>4f5/2</sub> were observed for mercury adsorbed on thiol impregnated activated carbon. Thiol impregnated activated carbon had shown mercury capture ability. The binding energy of mercury on the thiol impregnated activated carbon was observed at 101 and 105 eV for Hg<sub>4f7/2</sub> and Hg<sub>4f5/2</sub>, respectively.<sup>266</sup> In another study, thiol impregnated activated carbon was obtained by treating with thionyl chloride. When mercury was adsorbed on the surface of activated carbon through Hg-S bond, the binding energy of mercury was observed at 102 and 104 for Hg<sub>4f7/2</sub> and Hg<sub>4f5/2</sub>, respectively.<sup>267</sup> Narrow scan of the S 2p core levels is shown in Figure 5.8. The peak at 169.8 (3.5) eV was consistent with a short chain thiol group in the unreacted SiABDTH<sub>2</sub>. After the reaction with Hg, a marked shift to 163.4 (2.2) eV was observed with a marked increase in signal intensity. Increasing the Hg loading did not affect the overall S 2p line shape. The binding energy

shift accompanied by the increase in S 2p intensity suggested the formation of more ionic sulfur mercury bond after reaction of SiABDTH<sub>2</sub> with Hg.<sup>268-274</sup>

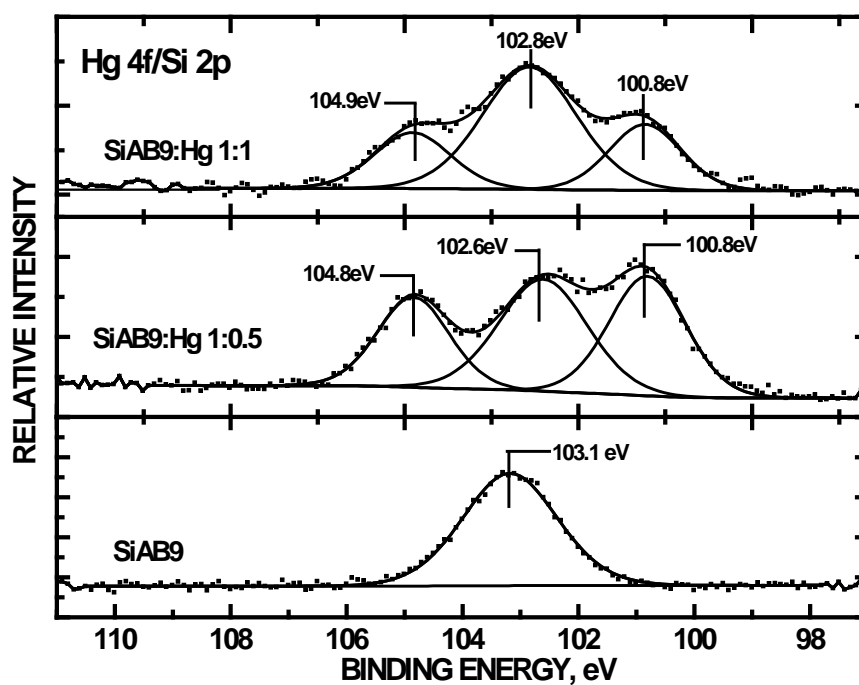


**Figure 5.7.** XPS of Hg 4f and Si 2p in SiABDT-Hg

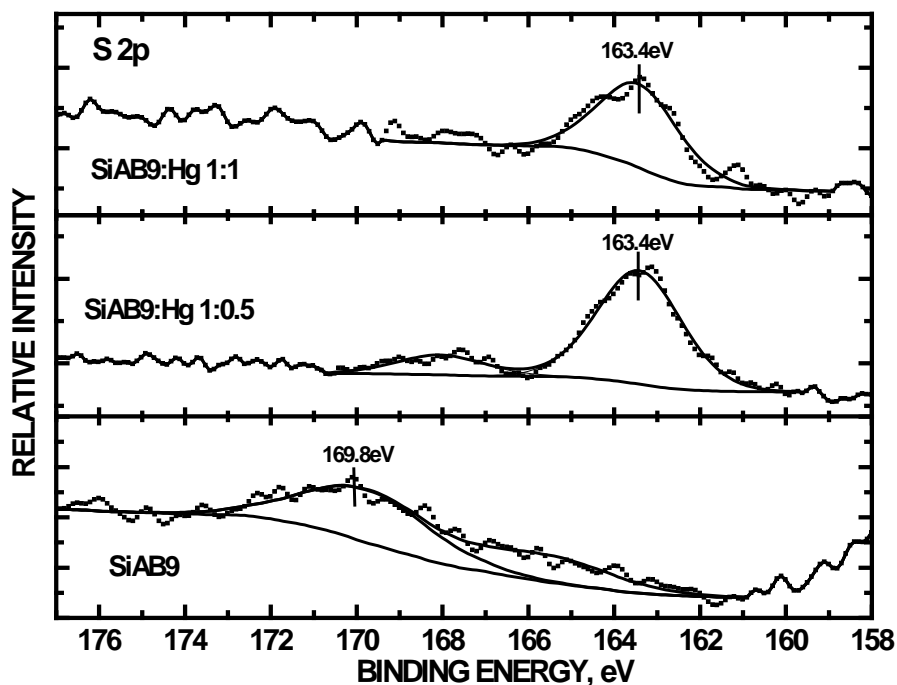


**Figure 5.8.** XPS of sulfur 2p in SiABDT-Hg

### 5.3. Experimental

#### 5.3.1. Materials and Techniques

Metal removal and leaching studies of arsenic and mercury were carried out in aqueous media using DI water. The arsenic stock solution was prepared using sodium meta arsenite ( $\text{NaAsO}_2$ , >99%) purchased from Sigma-Aldrich. A mercury stock solution was prepared from mercuric(II)chloride ( $\text{HgCl}_2$ , > 99.8%) obtained from Baker Analyzed Reagents. Omni trace HCl and  $\text{HNO}_3$  (EMD) were used for analytical purposes. The arsenic concentration was analyzed using a Varian SpectraAA 880Z Zeeman Graphite Furnace Atomic Absorption (GFAA) spectrometer at 193.7 nm wavelength. Mercury concentrations in aqueous solution were analyzed using a Varian Vista Pro CCD Simultaneous Inductive Coupled Plasma Optical Emission Spectrometer (ICP-OES) at a wavelength of 253.6 nm at 1.20 kW power. X-ray absorption fine

structure (XAFS) spectroscopy of arsenic samples was obtained at beam-line X-18B of the National Synchrotron Light Source (NSLS), Brookhaven National Laboratory, NY. XPS of mercury samples was carried out using a Kratos 165 XPS system with a hemispherical analyzer.

### **5.3.2. As(III) Binding Study by SiABDTH<sub>2</sub>**

#### **5.3.2.1. Batch Study of As(III) Removal at pH 5, 7 and 9**

**As(III) Removal at pH 5 by SiABDTH<sub>2</sub>:** A solution of arsenic (221 ppb) was prepared at pH 5 by dilution of 100 ppm arsenic stock solution made of NaAsO<sub>2</sub> (8.70 mg) in 50 mL water (DI) for treatment with SiABDTH<sub>2</sub>. SiABDTH<sub>2</sub> (0.2 g, 0.4 g and 0.6 g) from 20 g batch was treated with 50 mL of 221 ppb solution in triplicate by stirring for 24 h before filtering through a 0.2 µm Teflon filter. Aliquots (20 mL) from each sample were digested along with corresponding stock solution of 221 ppb (20 mL x 3) at 95°C for 6 h with addition of 1 mL concentrated HNO<sub>3</sub> before analysis by GFAA to determine the arsenic content in solution. Arsenic stock solutions were diluted 10 times prior to analysis by GFAA. All batch study samples were analyzed without dilution prior to analysis. All arsenic samples were analyzed at a wavelength of 193.7 nm using a GFAA spectrometer. Samples were combined with a 1% Pd modifier, ashed for 8.0 s at 1400°C and atomized at 2600°C for 2.6 s during analysis. A duplicate sample (1% RSD), a matrix spiked with 10 ppb As (97% recovery) and As standard (20 ppb, 100% recovery) were included for quality control at the beginning of the analysis. All samples and standards were fired three times to obtain the instrumental value. The instrumental and calculated data is shown in Table 5.1.

**As(III) Removal at pH 7 and 9 by SiABDTH<sub>2</sub> :** As(III) removal study was also conducted at pH 7 and 9. Arsenic solutions of 213 ppb and 233 ppb were prepared at pH 7 and 9, respectively, by dilution of 100 ppm arsenic stock solution made of NaAsO<sub>2</sub> (8.66 mg) in 50 mL water (DI). Arsenic solutions of different pH were then treated with SiABDTH<sub>2</sub>. SiABDTH<sub>2</sub> (0.2 g, 0.4 g and 0.6 g) from 20 g batch was mixed with 50 mL of 213 ppb and 233 ppb solutions in triplicate. Solutions were stirred for 24 h followed by filtration through a 0.2 µm Teflon filter to remove solid particulate. Aliquots (20 mL) from each sample were digested along with corresponding stock solution of 213 ppb (20 mL x 3) and 233 ppb (20 mL x 3) at 95°C for 6 h with addition of 1 mL concentrated HNO<sub>3</sub>. Arsenic concentrations in solutions were determined by analyzing in GFAA. Arsenic stock solutions were diluted 10 times prior to analysis by GFAA at a wavelength of 193.7 nm. All other samples were analyzed without dilution. Samples were combined with a 1% Pd modifier, ashed for 8.0 s at 1400°C and atomized at 2600°C for 2.6 s during analysis. Duplicate samples (0.94% and 3% RSD for pH 7 and 9, respectively), matrix spiked with 10 ppb As (100% and 96% recovery at pH 7 and 9, respectively) and As standards (10 ppb, 99.5% recovery; 20 ppb, 103% recovery) were included for quality control at the beginning of the analysis. The analyzed data are shown in Table 5.1.

#### **5.3.2.2. As(III) Removal by SiABDTH<sub>2</sub> as a Function of Time**

Aqueous arsenic stock was first prepared from NaAsO<sub>2</sub> at pH 5, 7 and 9 followed by application of SiABDTH<sub>2</sub> to carry out the experiment. Before preparing the arsenic



stock solution, the pH of DI water was adjusted to  $7.0 \pm 0.05$  by adding 0.5 M HCl and/or 0.5 M KOH solution. pH of DI water was also adjusted to  $5.0 \pm 0.03$  and  $9.0 \pm 0.06$  using 0.5 M HCl and/or 0.5 M KOH solution. Initial stock solution of 23.64 ppm arsenic was prepared by adding 4.10 mg of  $\text{NaAsO}_2$  in 100 mL DI water at pH 7. This stock solution was then diluted to approximately 200 ppb arsenic with dilution of 4 mL of 23.64 ppm solution to 500 mL solution. The exact concentration of arsenic in the solution was determined by GFAA to be 196.9, 249.4 and 192.1 ppb at pH 5, 7 and 9, respectively.  $\text{SiABDTH}_2$  (0.2 g and 0.6 g) was added to 50 mL of above solution separately and agitated by shaking for 1, 2 and 5 h at room temperature. After each time interval, the solid was isolated by syringe filtration through a  $0.45 \mu\text{m}$  Teflon filter and the filtrates were digested for GFAA analysis. Digestion was conducted at  $95^\circ\text{C}$  for 6 h by adding 2.5 mL concentrated  $\text{HNO}_3$  to the filtrates. After digestion, the samples were diluted to 50 mL again with DI water. Samples were diluted 10 times prior to analysis except for samples for 5 h (0.6 g  $\text{SiABDTH}_2$ ) at pH 5, 2 h (0.6 g  $\text{SiABDTH}_2$ ) and 5 h samples (0.6 g  $\text{SiABDTH}_2$ ) at pH 7, and 5 h (0.6 g  $\text{SiABDTH}_2$ ) at pH 9. Samples of 5 h for 0.2 g  $\text{SiABDTH}_2$  at pH 5, 7 and 9 were only diluted 2 times prior to analysis. Samples were analyzed at 193.7 nm using a Varian SpectrAA 880Z Zeeman GFAA spectrometer to determine arsenic concentration in solution. Samples were combined with a 1% Pd modifier, ashed for 8.0 s at  $1400^\circ\text{C}$  and atomized at  $2600^\circ\text{C}$  for 2.6 s during analysis. A duplicate sample (5.9% RSD), a matrix spiked with 20 ppb As (92% Recovery) and As standard (20 ppb, 88% recovery) were included for quality control at the beginning of the analysis. All samples and standards were fired three times to obtain the instrumental value. The experimental values are shown in Table 5.2, 5.3 and 5.4.

### 5.3.2.3. Leaching Study of SiABDT-As(III)

SiABDT-As(III) was first prepared to conduct a leaching study of arsenic.

Aqueous arsenic solution was made by adding 110.4 mg of sodium metaarsenite ( $\text{NaAsO}_2$ ) to 25 mL of DI water at pH 7. pH of water was adjusted using 0.5 M HCl and/or 0.5 M KOH. SiABDTH<sub>2</sub> (5.0 g) obtained from 20 g batch of synthesis was added to the arsenic solution and the reaction media was agitated by constant shaking on a shaker for 24 h. After the reaction, the solid was separated by gravity filtration. The solid was then washed thoroughly with 200 mL DI water followed by drying under air.

SiABDT-As(III) was analyzed by GFAA for arsenic content per gram of solid. Prior to analysis by GFAA, SiABDT-As(III) (0.2 g) was digested at 95<sup>0</sup>C for 24 h with 50 mL DI water and 5 mL HNO<sub>3</sub> in a polypropylene digestion vessel. The solution was then cooled down to room temperature and final volume of the solution was marked upto 50 mL again by adding DI water before syringe filtration through 0.2  $\mu\text{m}$  Teflon filter in order to remove solid from the solution. Sample was diluted 400 times prior to analysis to bring down the concentration of sample within the instrumental analysis range of 5 ppb to 50 ppb in GFAA. The arsenic content was 0.45 mg in 0.2 g of SiABDT-As(III) which corresponds to 2.29 mg of arsenic per gram of SiABDT-As(III).

The leaching study was conducted by setting up 0.2 g SiABDT-As(III) in 20 mL DI water separately for 1 day, 1, 2, 3, and 4 weeks for three different pH values of 5, 7 and 9. pH of DI water was adjusted by using 0.5 M HCl and/or 0.5 M KOH. After each time interval, samples were filtered through a 0.2  $\mu\text{m}$  filter to remove solid particles. Blanks (with SiABDTH<sub>2</sub> only) were also analyzed at the same time intervals and pH values. After filtration, all the samples were diluted to 50 mL and digested by adding 2.5

mL concentrated  $\text{HNO}_3$  in a polypropylene digestion vessel at  $95^\circ\text{C}$  for 6 h. After digestion, volume of the samples was raised to 50 mL again with DI water. All samples except blank samples were diluted 100 times prior to analysis. All arsenic samples were analyzed at a wavelength 193.7 nm using a Varian SpectrAA 880Z Zeeman GFAA spectrometer. Samples were combined with a 1% Pd modifier, ashed for 8.0 s at  $1400^\circ\text{C}$  and atomized at  $2600^\circ\text{C}$  for 2.6 s during analysis. A duplicate sample (1.9% RSD), a matrix spiked with 8 ppb As (96% Recovery) and As standard (20 ppb, 109% recovery) were included for quality control at the beginning of the analysis. All samples and standards were fired three times to obtain the instrumental value. The analyzed data are shown in the Table 5.5. The blank samples contained no As and are not included in the table.

#### **5.3.2.4. XAFS Spectroscopy of Arsenic Sorbents**

Bonding of Arsenic in  $\text{SiABDT-As(III)}$  and  $\text{SiABDT-As(III)}_{\text{LCH}}$  sorbents was analyzed by X-ray absorption fine structure (XAFS) spectroscopy at beam-line X-18B of the National Synchrotron Light Source (NSLS), Brookhaven National Laboratory, NY. XAFS spectra of arsenic were collected from 100 eV below the arsenic K absorption edge at 11,867 eV to 800 eV above the edge. The energy scale for the spectra was calibrated to an arsenate absorber whose peak position was assumed to occur at 11,871 eV. A reference absorption spectrum of  $\text{As}_2\text{S}_3$  (synthetic orpiment) was also obtained for comparison. The XAFS spectra were first calibrated with a reference energy point defined by the major peak in the spectrum of the arsenate standard followed by dividing into separate X-ray absorption near-edge structure (XANES) and extended X-ray

absorption fine structure (EXAFS) regions. The EXAFS region was then converted to a reciprocal space (k-space, chi spectrum) representation and a Fourier transform was applied to the  $k^3$ -weighted chi spectrum to produce a radial structure function (RSF). The RSF can be considered a one-dimensional representation of the structure local to the absorbing atom, which in this case is arsenic.

### **5.3.3. Mercury Binding Study by SiABDTH<sub>2</sub>**

#### **5.3.3.1. Batch Study of Hg Removal at pH 5, 7 and 9**

Aqueous mercury stock was prepared by adding 11.0 mg of HgCl<sub>2</sub> in 50 mL DI water at pH 7 giving 162 ppm of mercury solution. The mercury stock solution was then diluted to the desired concentration of approximately 5 ppm by diluting 15 mL of 162 ppm solution to 500 mL aqueous solution at pH 5, 7 and 9. pH of water was adjusted with 0.5 M HCl and/or 0.5 M KOH prior to preparation of solution. The exact concentration of mercury in the solution was determined by analyzing the solution with ICP-OES and found to be 4.98, 4.70 and 4.45 ppm at pH 5, 7 and 9, respectively. SiABDTH<sub>2</sub> (0.2 g and 0.6 g) was then added to 50 mL of above solution at each pH separately and agitated by shaking for 24 h at room temperature. After agitation, the solid was isolated by syringe filtration through a 0.45  $\mu$ m Teflon filter and the filtrates were digested for ICP-OES analysis. Mercury stock solution and filtrates were digested at 100<sup>0</sup>C for 10 h by addition of 2.5 mL concentrated HNO<sub>3</sub> and 2.5 mL concentrated HCl to the solution. After digestion, volume of the samples was marked upto 50 mL again with DI water. Samples were analyzed at a wavelength of 253.6 nm using ICP-OES to determine mercury concentration in solution. A duplicate sample (0.9% RSD), a

matrix spiked with 2 ppm Hg (95.2% Recovery) and Hg standard (2 ppm and 5 ppm, 98 and 102% recovery, respectively) were included for quality control at the beginning of the analysis. The experimental values are shown in Table 5.9.

### **5.3.3.2. XPS Study of SiABDT-Hg**

X-ray photoelectron spectroscopy (XPS) scans of the SiABDTH<sub>2</sub> and SiABDT-Hg (SiABDTH<sub>2</sub> treated with Hg) samples were taken using a Kratos 165 XPS spectrometer equipped with a hemispherical analyzer and a Mg K $\alpha$  anode ( $h\nu = 1253.6$  eV) operated at 225 W. The system pressure during analysis did not exceed  $1.0 \times 10^{-8}$  Torr. High resolution scans were performed with a 20 eV pass energy and charge referenced to adventitious carbon at C 1s = 284.7 eV. The samples were mounted onto double sided tape (Scotch 3M) and outgassed using a turbomolecular pump prior to introduction into ultrahigh vacuum for analysis. A 70:30 Gaussian/Lorentzian line shape and Shirley background subtractions were used to curve fit all of the XPS peaks using CasaXPS software version 2.2.107 (Casa Software Ltd., U.K.).<sup>275-277</sup>

### **5.3.3.3. Hg Leaching Study from SiABDT-Hg**

Mercury leaching studies were conducted using SiABDT-Hg obtained from mixing aqueous mercury solution of 311.6 mg of mercuric chloride (HgCl<sub>2</sub>) in 25 mL of DI water at pH 7. pH of water was adjusted using 0.5 M HCl and/or 0.5 M KOH. SiABDTH<sub>2</sub> (5.0 g) was added to the mercury solution and the reaction media was agitated by constant shaking on a shaker for 24 h. After the reaction was over, the solid was separated by gravity filtration followed by washing with 200 mL DI water and dried

under air. SiABDT-Hg was analyzed by ICP-OES for mercury content per gram of solid. Prior to analysis by ICP-OES, SiABDT-Hg (0.2 g) was digested at 100<sup>0</sup>C for 24 h with 5 mL concentrated HNO<sub>3</sub>, 5 mL concentrated HCl and 40 mL DI water in a polypropylene digestion vessel. Solution was then cooled down to room temperature before syringe filtration through 0.2 µm Teflon filter to remove solid from the solution. Final volume of the solution was marked upto 50 mL by adding DI water. Solution was diluted 25 times prior to analysis by ICP-OES to determine the mercury content in solution obtained from 0.2 g of SiABDT-Hg. The mercury content was 6.88 mg in 0.2 g of SiABDT-Hg which corresponds to 34.42 mg of mercury per gram of SiABDT-Hg.

The leaching study was conducted by setting up 0.2 g SiABDT-Hg in 20 mL DI water separately for 24 h, 1, 2, 3 and 4 weeks in different pH values of 5, 7 and 9. pH of DI water was adjusted by using 0.5 M HCl and 0.5 M KOH. After each time interval, samples were filtered through a 0.2 µm Teflon filter to remove solid particles. Blanks (with SiABDTH<sub>2</sub> only) were also analyzed at the same time intervals and pH values. After filtration, all the samples were diluted to 50 mL and digested by addition of 2.5 mL concentrated HNO<sub>3</sub> and 2.5 mL concentrated HCl in a polypropylene digestion vessel at 100<sup>0</sup>C for 10 h. After digestion, volume of the samples was marked upto 50 mL with DI water. All mercury samples were analyzed at a wavelength of 253.6 nm using a ICP-OES. A duplicate sample (1.2% RSD), a matrix spiked with 2 ppm Hg (101% Recovery) and Hg LCS (2 ppm, 97% recovery) were included for quality control at the beginning of the analysis. The analyzed data is shown in table 5.10. The blank samples contained no Hg and are not included in the table.

#### 5.4. Conclusions.

The study demonstrated the ability of SiABDTH<sub>2</sub> to capture arsenic from aqueous solution at pH 5, 7 and 9. SiABDTH<sub>2</sub> showed 100% As(III) binding ability from aqueous solution at different pH values after 24 h when 0.2 - 0.6 g of SiABDTH<sub>2</sub> was added to the arsenic solutions. The percentage of As(III) removal was increased in case of both 0.2 g and 0.6 g of SiABDTH<sub>2</sub> as the contact time between SiABDTH<sub>2</sub> and As(III) solutions was increased from 1 h to 5 h. The study also showed that higher percentage of As(III) removal was observed at pH 7 within short period of time. However, with longer period of time, 100% of As(III) was captured by SiABDTH<sub>2</sub> at pH 5, 7 and 9. XFAS study of SiABDT-As(III) indicated the presence of sulfur bound arsenic. However, additional secondary interaction was also observed. Leaching study indicated the leaching of arsenic in the range of 12-29% after 24 h in pH 5, 7 and 9. But the percentage of As leaching to aqueous medium remained same over the weeks. This was due to the fact that part of ABDTH<sub>2</sub> was physisorbed on the silica surface of SiABDTH<sub>2</sub> that was bonded with arsenic.

SiABDTH<sub>2</sub> also showed mercury binding ability in aqueous solution at pH 5, 7 and 9. SiABDTH<sub>2</sub> captured 72.8%, 55.8% and 74.1% at pH 5, 7 and 9 when 0.2 g of SiABDTH<sub>2</sub> was applied. When SiABDTH<sub>2</sub> content was increased to 0.6 g, the percentage of mercury removal was increased to 92.8%, 74.8% and 84.1% at pH 5, 7 and 9. XPS study of SiABDT-Hg indicated the formation Hg-S bond. Mercury leaching study of SiABDT-Hg showed that 1.47 – 3.67% of mercury was leached into water.

## CHAPTER 6

### Arsenic Filtration Column Study by SiABDTH<sub>2</sub>

#### 6.1. Introduction

Adsorptive filtration techniques for water treatment are a popular, emerging technology due to its reduced amount of toxic sludge production and economic efficiency. Fixed-bed adsorbents are relatively simple and easy to operate. These adsorbents also have the potential to selectively and effectively remove arsenic from contaminated water. Intensive research has been carried out to develop new technologies and improve existing technologies involved in removal of arsenic from water. Various water treatment technologies such as coagulation, flotation, adsorption, ion-exchange, lime softening and reverse osmosis are available for arsenic removal at present described in chapter 1.<sup>134,278</sup> However, these techniques are predominately effective for removing As(V) as compared to As(III). As a result, these techniques are often preceded by an oxidation step to convert As(III) to As(V) for effective removal of trivalent arsenic. In recent years, adsorptive filtration has gained attention as an innovative approach to remove various contaminants from the liquid phase.<sup>279</sup>

Arsenic contamination of ground water in Bangladesh, West Bengal in India and most of the Southeast Asian countries as well as in the United States is a serious issue. Concentration of arsenic in ground water varies in the range of 8.82 – 220.47 ppb. Iron oxide immobilized on sand grains has been used to remove toxic metals by binding of these metals to the surface of iron oxide through adsorption. Use of surface modified solid matrix is advantageous as it allows the sorption of soluble metals as well as ease of



separation of adsorbent through filtration. Iron hydroxides have also been used as adsorbing agents for the purpose of arsenic removal from water. Iron hydroxide coated polymeric materials such as polystyrene and polyHIPE (poly high internal phase emulsion) prepared from styrene, divinylbenzene and sobitan monooleate have been investigated for removal As(III) and As(V). pH of water was found to affect the capacity of arsenic removal with optimum pH found to be 7.0 for the removal of mixture of As(III) and As(V).<sup>280</sup> Iron-zirconium binary oxide adsorbents have been explored as an adsorptive media for arsenic. Surface hydroxyl groups act as binding sites for the oxyanionic species of As(III) and As(V). Arsenate is bonded through formation of inner-sphere surface complexes, whereas arsenite is bonded in both inner- and outer-sphere surface complexes.<sup>281</sup>

Arsenic has strong affinity toward thiols and forms strong covalent As-S bonds. Silica-supported cysteine and polycysteine have been used for removal of heavy metals from aqueous solutions. BDTH<sub>2</sub> has demonstrated the ability to bind and remove arsenic from aqueous solutions. However application of BDTH<sub>2</sub> as a filtration material in low cost, easy to use filtration columns remains an issue. In the field studies of BDTH<sub>2</sub> filtration columns show leaching of BDTH<sub>2</sub>, which decreased the capability of filtration column. The new thiol compound, ABDTH<sub>2</sub>, an acid derivative of BDTH<sub>2</sub> has shown binding capacity towards arsenic. Silica-supported ABDTH<sub>2</sub> has been designed and synthesized for the removal of arsenic from water. Batch studies of silica immobilized ABDTH<sub>2</sub> (SiABDTH<sub>2</sub>) have shown promising results where SiABDTH<sub>2</sub> captured 100% arsenite from 200 ppb arsenic contaminated aqueous solution. Immobilization of ABDTH<sub>2</sub> on silica increases the dispersion of ligand on solid surfaces which increases

the interaction between ligand and arsenic in aqueous phase as well as decreases the ligand loss through leaching. As a result, SiABDTH<sub>2</sub> can be applied effectively as filtration column material for arsenic removal from aqueous solutions. The main aim in this chapter is to test the filtration column technology using SiABDTH<sub>2</sub> as column packing material for arsenic removal from water.

## **6.2. Results and Discussion**

### **6.2.1. ABDTH<sub>2</sub> Leaching from Filtration Column**

After construction of an arsenic filtration column with SiABDTH<sub>2</sub>, the column was tested for the presence of any physisorbed ABDTH<sub>2</sub> on the silica surface. A total of 3 L of DI water was passed through the column at a flow rate of ~20 mL/min. At this point loosely bound or physisorbed ABDTH<sub>2</sub> was washed out with water. This process prevented the binding of arsenic with physisorbed ABDTH<sub>2</sub> that leaches out to the environment. The instrumental data are shown in Table 6.1. According to the data presented in Table 6.1, an average of  $0.226 \pm 0.006$  mmol of ABDTH<sub>2</sub> leached from 16.40 g of SiABDTH<sub>2</sub>, whereas, 6.11 mmol ABDTH<sub>2</sub> was present in 16.40 g of SiABDTH<sub>2</sub>. This corresponds to about 3.71% of the total ABDTH<sub>2</sub> in the column was being leached out. By comparison ~ 18 % B9 leached from the B9/sand column. The leaching of ABDTH<sub>2</sub> was most likely due to physical adsorption of a small fraction of ABDTH<sub>2</sub> onto the silica. In order to remove physisorbed ABDTH<sub>2</sub> in future experiments, the SiABDTH<sub>2</sub> could be washed in a larger volume of EtOH with mechanical stirring to insure access of the solvent to all non-covalently bound ABDTH<sub>2</sub>. Alternatively, the

solution could be made slightly basic to displace any strongly hydrogen-bonded ABDTH<sub>2</sub>.

**Table 6.1.** ABDTH<sub>2</sub> leaching from SiABDTH<sub>2</sub> filtration column

Sample	[S] ppm	ABDTH <sub>2</sub> (mmol) Leached	% Leached
<b>1</b>	4.82 ± 0.10	0.225 ± 0.005	3.68
<b>2</b>	4.90 ± 0.04	0.229 ± 0.002	3.75
<b>3</b>	4.80 ± 0.07	0.224 ± 0.003	3.67
<b>Average</b>	4.84 ± 0.13	0.226 ± 0.010	3.70

#### 6.2.2. Column I: Low Flow Rate (20 mL/min)

As(III) capturing capability of SiABDTH<sub>2</sub> in filtration column set up was conducted at a flow rate of 20 mL/min. The 212.8 ppb arsenic stock solution was passed through the SiABDTH<sub>2</sub> column for 6 h daily for 3 days. Samples of effluent were collected every 2 h. Samples were then acidified with concentrated HNO<sub>3</sub> followed by digestion of the solution before analysis by GFAA to determine arsenic concentrations in effluent samples. GFAA analysis indicated that all of the effluent samples contained < 5 ppb As (the detection limit of the instrument) which is well below the permissible limit of 10 ppb arsenic in drinking water set by the United States Environmental Protection Agency (USEPA). At the conclusion of the three-day experiment, a total of 20 L of 212.8 ppb As was treated with the SiABDTH<sub>2</sub> filtration column. This corresponds to

0.056 mmol of As(III) being captured by 16.40 g of SiABDTH<sub>2</sub>. XAFS studies of SiABDT-As(III) showed arsenic was covalently bonded to the sulfur atom of ABDTH<sub>2</sub> immobilized on the surface of silica. Based on the ABDTH<sub>2</sub> loading on SiABDTH<sub>2</sub> and a 1:1 As(III) to ABDTH<sub>2</sub> stoichiometry, only 0.94% of the available bonding sites were used. Theoretically, the current SiABDTH<sub>2</sub> column can treat approximately 2,127 L of 200 ppb As(III)-affected water.

Leupin et al. studied the As(III) removal capacity of sand and ZVI from ground water in column filtration set up. The filtration column was prepared by mixing 4 g sand and 1.5 g ZVI with a bed height of 3.5-4 cm. ZVI binds As(V) by oxidizing As(III) to As(V). When 1 L of 500 ppb As(III) was passed through the sand/ZVI filtration column at a flow rate of 0.3 mL/s, the concentration of arsenic could be lowered to less than 15 ppb. However, up to 8 ppm dissolved Fe(II) was released in water during the process.<sup>282</sup> A study of sorption and desorption of arsenic to ferrihydrite in a sand filter indicated the removal of As(III) with preoxidation of As(III) to As(V).<sup>283</sup> Household sand filters containing iron have been investigated in Vietnam, where arsenic concentration in ground water varies in the range of 10-382 ppb As. The study indicated that Fe/As ratios of  $\geq 250$  were required for arsenic removal to desired levels.<sup>284</sup>

After completion of the filtration study, arsenic-bonded SiABDTH<sub>2</sub> material from the filtration column was analyzed to detect the presence of physisorbed arsenic on the surface of SiABDTH<sub>2</sub>. A leaching study of the material was conducted for the purpose. SiABDT-As(III) was extracted in DI water for 24 h before analyzing the aqueous solution for arsenic concentration. From the GFAA analysis of aqueous solution, only 0.014% of arsenic was leached (Table 6.2) out from 0.056 mmol of arsenic bonded to

the column material which indicated that all of the arsenic was chemically bound to the SiABDTH<sub>2</sub> through the formation of covalent As-S bond.

**Table 6.2.** Arsenic leached from SiABDT-As(III) column material

Sample	As Leached		% Leached
	ppb	Mg	
<b>1</b>	15.98 ± 0.44	0.639 ± 0.017	0.015
<b>2</b>	13.81 ± 0.58	0.552 ± 0.023	0.013
<b>3</b>	14.31 ± 0.74	0.572 ± 0.030	0.014
<b>Avg.</b>	14.70 ± 1.04	0.588 ± 0.041	0.014

### 6.2.3. Column II: High Flow Rate (500 mL/min)

Arsenic removal study by SiABDTH<sub>2</sub> filtration column was also conducted at a high flow rate of a 500 mL/min to demonstrate the applicability of the technology. The initial concentration of arsenic aqueous solution was 225 ppb as analyzed by GFAA. Water containing 225.1 ppb arsenic was passed through the column with the help of a pump at a constant flow rate of 500 mL min<sup>-1</sup>. Samples were collected from the effluent solution with the passage of every 3 L of arsenic aqueous solution through the column. Samples were then digested at 95°C followed by analysis by GFAA. The instrumental analysis data of the study is shown in Table 6.3. At the beginning only 53.7% of arsenic was captured by the column material. As more water passed through the column at high flow rate, percent capture of arsenic was increasing due to better packing of column

materials and better contact of arsenic with ABDTH<sub>2</sub> to bind. It was observed that after 27 L of arsenic containing water passed through the column, ~69% of arsenic was captured by binding materials. The average household tap water flow rate varies in between 2-6 L/min. Though the experimental flow rate (500 mL/min) was lower than the average household water flow rate, it demonstrated the applicability of SiABDTH<sub>2</sub> as filtration column material.

**Table 6.3.** Arsenic captured at a flow rate of 500 mL/min

Sample	Volume Eluted	[As] ppb	% Captured
As Stock	N/A	225.1 ± 16.4	
1	0 L	104.2 ± 9.9	53.7
3	6 L	98.4 ± 7.9	56.2
5	12 L	81.6 ± 11.8	63.7
7	18 L	84.1 ± 9.3	62.6
10	27 L	69.7 ± 6.7	69.1

## 6.3. Experimental

### 6.3.1. Materials and Techniques

All the filtration column studies were carried out at room temperature. House nitrogen was used to create pressure inside the container and inert atmosphere to prevent oxidation of arsenite to arsenate. Arsenite contaminated solutions were prepared in DI water using sodium metaarsenite (NaAsO<sub>2</sub>). NaAsO<sub>2</sub> (>99%) was obtained from Sigma

Aldrich and used as received. Glass chromatography columns (1.5 cm ID, 30 cm in length) were purchased from Kontes. Arsenic concentrations in aqueous solution were determined using Varian SpectrAA 880Z Zeeman Graphite Furnace Atomic Absorption spectrometer (GFAA) at a wavelength of 193.7 nm.

### **6.3.2. Column Preparation**

A glass chromatography column (1.5 cm ID, 30 cm in length) with a fritted disk was used to design a filtration bed for the experiment. The glass column was filled with SiABDTH<sub>2</sub> (16.40 g) to a bed height of 12 cm. Two filter papers were cut to fit the ID of the column and inserted at the 4 cm and 8 cm bed heights. Before using the column for arsenic capture, the column with the packing material (SiABDTH<sub>2</sub>) was washed with DI water to remove physisorbed ABDTH<sub>2</sub> present on the solid particle. DI water (3 L) was passed through the SiABDTH<sub>2</sub> column at a rate of 20 mL/min and samples (50 mL) were taken in triplicate. Samples were digested at 100°C with the addition of 2.5 mL concentrated HNO<sub>3</sub> and 2.5 mL concentrated HCl and diluted to a final volume of 50 mL before analyses for sulfur content by ICP in order to test the potential leaching of ABDTH<sub>2</sub> from SiABDTH<sub>2</sub>.

### **6.3.3. ABDTH<sub>2</sub> Leaching from Filtration Column**

After preparing the SiABDTH<sub>2</sub> column, 3 L of DI water was passed through the column to monitor ABDTH<sub>2</sub> leaching. The flow rate of DI water was 20 mL/min. Effluent was collected for analysis to find out the amount of ABDTH<sub>2</sub> leaching from filtration column. Three aliquots (50 mL) were taken from the total water sample and

digested followed by analysis by ICP. Samples were digested at 100°C with addition of 2.5 mL concentrated HNO<sub>3</sub> and 2.5 mL concentrated HCl for 8 h. After digestion, samples were diluted to 50 mL again before analyses for sulfur concentration in samples. The sulfur content shown in Table 6.1 was determined by ICP-OES analysis at a wavelength of 181.972 nm with an operating power of 1.20 kW and sample replicate read time of 2.00 s. Yttrium was used as an internal standard for the analysis measured at 371.029 nm. Quality control of the analysis was maintained by conducting an analysis of matrix spike (102% recovery), sulfur check standards (2 ppm, 109% recovery at 181.972 nm) and percent relative standard deviation (%RSD, 0.81%) between the duplicate samples.

#### **6.3.4. Column I: Low Flow Rate (20 mL/min)**

The column from the ABDTH<sub>2</sub> leaching study was used in the present study. A stock solution of ~200 ppb As(III) was prepared by stirring NaAsO<sub>2</sub> (10.90 mg) in water (30 L, DI) for 3 h in a 50 L Nalgene carboy. Nitrogen pressure was added to the carboy to provide a constant flow of arsenic water from the carboy and to prevent air oxidation of As(III) to As(V). The pressure was maintained at <5 psi and resulted in a flow rate of ~20 mL/min. Triplicate samples (20 mL each) of stock solution were collected at the beginning of the experiment for determination of exact initial arsenic concentration. Arsenic stock solution was then passed through the SiABDTH<sub>2</sub> column under nitrogen pressure. Samples (20 mL) of effluent were collected in triplicate in digestion tubes every two hours over a period of six hours daily for three days. A total of 20 L of arsenic(III) contaminated water (6.5 L in day 1, 6.5 L in day 2 and 7 L in day 3) was



passed through the SiABDTH<sub>2</sub> column. The samples from effluents and the stock solution were acidified with nitric acid (1 mL, concentrated, Omnitrace) immediately after collection and stored at 5°C until all the samples were collected. Samples were digested at 95°C for 30 min. Then 1 mL of H<sub>2</sub>O<sub>2</sub> was added to the samples and samples were digested for an additional 5.5 hr before cooling and dilution to 20 mL with DI water. Samples were analyzing by GFAA. Arsenic stock solution was diluted 10 times prior to analysis. Arsenic concentration of samples were analyzed at 193.7 nm using Varian Spectra AA 880Z Zeeman GFAA along with a duplicate sample (0.68% RSD), a 10 ppb As standard (96% recovery) and a matrix spiked with 10 ppb arsenic (97% recovery) for quality control.

At the completion of the As(III) removal study, the column was washed with DI water (250 mL) under continuous gravity flow and allowed to air dry. The column packing material was removed from the column and extracted for 24 h in 50 mL digestion tubes with sufficient DI water (40 mL) to submerge packing materials in order to remove loosely-bound arsenic from the SiABDTH<sub>2</sub> surface. The resultant supernatant was syringe filtered (0.2 µm, Teflon, Environmental Express), and small portions of the sample split into three parts (5 mL x 3), and acidified with 0.25 mL of concentrated HNO<sub>3</sub>. Samples were digested at 95°C for 30 min, H<sub>2</sub>O<sub>2</sub> (0.25 mL) was added, and samples were heated an additional 5.5 h with the addition of 1.5 mL DI water hourly to prevent evaporation to dryness.

Samples were analyzed for arsenic concentration (Table 6.2) at 193.7 nm using a GFAA spectrometer. Samples were combined with a 1% Pd modifier, ashed for 8.0 s at 1400°C and atomized at 2600°C for 2.6 s during analysis. A duplicate sample, a 10 ppb

spiked sample and As standards were included for quality control at the beginning of the analysis. The percent recovery from 10 ppb As standard and 10 ppb spiked sample was 98% and 92%, respectively. The %RSD between the duplicate samples was 1.78%.

#### **6.3.5. Column II: High Flow Rate (500 mL/min)**

A second filtration column for high flow rate was prepared in the same way as the column for low flow rate. A glass chromatography column (15 cm ID, 30 cm in length) with a fritted disk was filled with SiABDTH<sub>2</sub> (16.38 g) to a bed length of 12 cm. Two filter papers were cut to fit the ID of the column and inserted at the 4 cm and 8 cm bed heights. DI water (3 L) was passed through the SiABDTH<sub>2</sub> column at high flow rate for better packing of the column materials and removal of adsorbed ABDTH<sub>2</sub> from silica.

A stock solution of 225.1 ppb As(III) was prepared in a Nalgene carboy by stirring NaAsO<sub>2</sub> (11.60 mg) in 30 L of DI water for 3 h. A sample of stock solution was collected to analyze the exact arsenic concentration in the solution. A high pressure pump was used to move the arsenic containing water through the SiABDTH<sub>2</sub> column at a flow rate of 500 mL/min. A total of ten samples (50 mL each) were collected for every 3 L of As water passed through the filtration column with the initial sample being collected at the beginning of the experiment and the final sample collected after 27 L of As-water had passed through the column. Every sample was digested in triplicate (10 mL each) at 95°C for 6 h with addition of 0.5 mL concentrated HNO<sub>3</sub> and 0.5 mL H<sub>2</sub>O<sub>2</sub> (added to the digested solution after 30 min of digestion) and volume was marked up to 10 mL again prior to analysis by GFAA for arsenic concentration in eluted samples. Amongst those samples, samples 1, 3, 5, 5, 9 and 10 were analyzed by GFAA (Table

6.3). An arsenic stock solution sample was collected before the start of the run and digested and analyzed by GFAA the same way as the above eluted samples. Arsenic stock solutions were diluted 10 times and all other arsenic samples were diluted 4 times prior to analysis by GFAA. All arsenic samples were analyzed at 193.7 nm using a Varian SpectrAA 880Z Zeeman graphite furnace atomic absorption spectrometer (GFAAS). Samples were combined with a 1% Pd modifier, ashed for 8.0 s at 1400°C and atomized at 2600°C for 2.6 s during analysis. A duplicate sample, a matrix spiked with 10 ppb As and 20 ppb As standard (%) were included for quality control at the beginning of the analysis. All samples and standards were fired three times.

#### 6.4. Conclusion

An arsenic (III) filtration column has been designed using SiABDTH<sub>2</sub> as column packing material. Filtration column studies have been conducted at two different flow rates, 20 and 500 mL min<sup>-1</sup>. The concentration of the initial arsenic stock solution was 212.8 and 225.1 ppb for flow rates of 20 and 500 mL/min, respectively. At a flow rate of 20 mL/min, the study was conducted for 3 days with 6 h of solution passed through the column each day. The study has shown that the filtration column captured 100% arsenic from the 212.8 ppb arsenic solution. Leaching study of SiABDT-As(III) material from the filtration column has shown that only 0.014% of arsenic was leached out from the material suggesting the presence of covalently bonded arsenic to thiol. At high flow rate of 500 mL/min, 53.7% to 69.1% of As(III) was captured from 225.1 ppb aqueous As(III) solution with 53.7% at the beginning of the experiment and 69.1% after 27 L of solution was passed through the column. The filtration column study demonstrated that

SiABDTH<sub>2</sub> can capture arsenic from aqueous media at various flow rates when used as filtration column packing material. The filtration column study at low and high flow rate indicated the applicability of SiABDTH<sub>2</sub> as filtration column materials. This material can be used in small scale, hand-held and household applications for drinking water purification.

## CHAPTER 7

### Continued Research: HBDTH<sub>2</sub> and HABDTH<sub>2</sub>

#### 7.1. Introduction

Based on research performed with marketed metal-removal reagents, new dithiol ligands had been designed and synthesized. The merP is a metal binding protein that binds Hg<sup>2+</sup> and safely eliminates from cell by converting Hg<sup>2+</sup> to Hg<sup>0</sup> in the cytoplasm. The merP contains two cysteine units Cys-14 and Cys-17 that are essential for Hg<sup>2+</sup> binding. Based on the same type of active cysteine units present in merP, dithiol ligands such as 2,6-pyridinediamidoethanethiol (PyDTH<sub>2</sub>) and BDTH<sub>2</sub> had been synthesized for the metal removal purpose from aqueous solutions. PyDTH<sub>2</sub> had shown mercury removal capacity up to 97% from 50 ppm solution when added in stoichiometric ratio. However, PyDTH<sub>2</sub> is insoluble in water. Alkali salt of the ligand is required for aqueous mercury removal purpose.<sup>285-287</sup>

BDTH<sub>2</sub> is a preeminent reagent for the complete precipitation of arsenic, mercury and other heavy metals from water. It is an inexpensive, efficient precipitating agent designed for the removal of soft heavy metals from various aqueous media like acid mine drainage, lead battery cycling plant wastewater and gold ore processing wastewater by forming insoluble precipitates. Inorganic contaminants such as Cd, Hg, Pb and As form strong covalent bonds with the sulfur moiety of BDTH<sub>2</sub> to form BDT-M (M = Cd, Hg, Pb and As) complexes which does not release the metals back to the environment after disposal of the BDT-M complexes in the environment.<sup>172,174-176,180,182,183,196</sup>

An acid derivative of BDTH<sub>2</sub> (ABDTH<sub>2</sub>) has been designed and synthesized for immobilization on silica-support to use as filtration column packing material. Silica-supported ABDTH<sub>2</sub> (SiABDTH<sub>2</sub>) have shown arsenic capture ability from aqueous media in both batch test and filtration column test. In batch study, SiABDTH<sub>2</sub> captured 100% arsenic from approximately 200 ppb aqueous arsenic solution at pH 5, 7 and 9. SiABDTH<sub>2</sub> also removed 100% arsenic from water at a flow rate of 20 mL/min and 53-69% arsenic at a flow rate of 500 mL/min in filtration column study when SiABDTH<sub>2</sub> was used as column packing material.

Though PyDTH<sub>2</sub>, BDTH<sub>2</sub> and ABDTH<sub>2</sub> had been used as precipitating agent for toxic contaminants, these are insoluble in aqueous media. As a result, ethanolic solution or sodium or potassium salt of ligand is required for the metal removing application which limits its environmental applicability. Introduction of polar functional groups into the molecular framework of these ligands will improve the applicability of ligands directly in aqueous solutions. New materials with a polar functional group incorporated into benzene ring of BDTH<sub>2</sub> and ABDTH<sub>2</sub> molecular framework will have the advantage of having the same toxic metal binding ability of BDTH<sub>2</sub> as well as water solubility. This chapter describes the synthetic methodology of two new dithiol derivatives of BDTH<sub>2</sub>, 5-hydroxy-*N,N'*-bis(2-mercaptoethyl)isophthalamide (abbreviated as HBDTH<sub>2</sub>, Figure 7.1) and 2,2'-((5-hydroxyisophthaloyl)bis(azanediyl))bis(3-mercaptopropanoic acid) (abbreviated as HABDTH<sub>2</sub>, Figure 7.2), and their characterization.

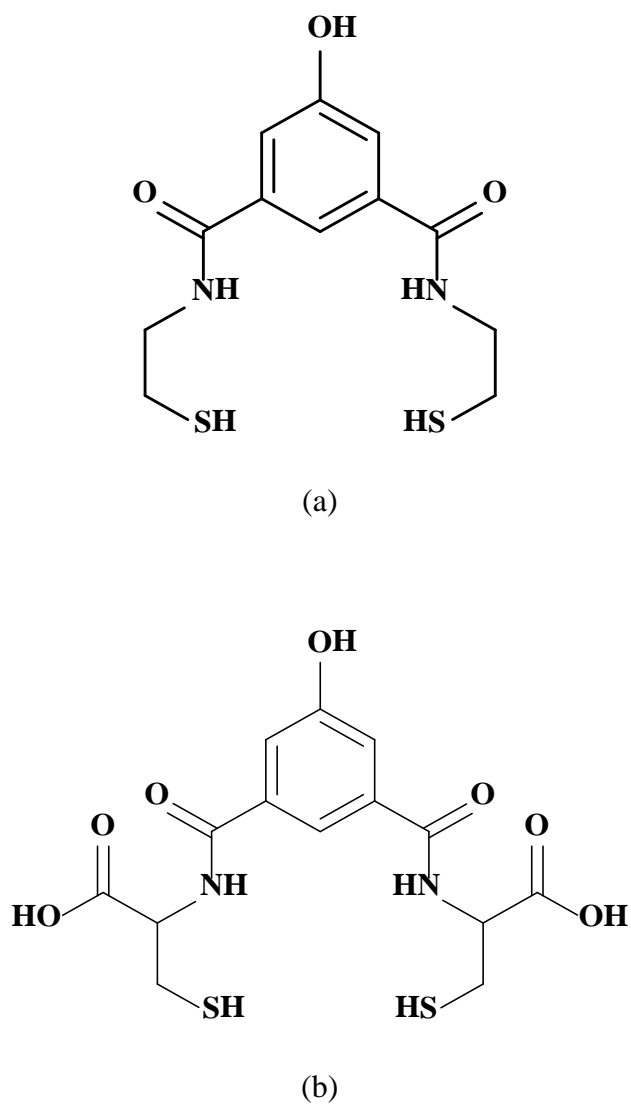


**Figure 7.1.** Molecular structures of (a) 5-hydroxy-*N,N'*-bis(2-mercaptoethyl)isophthalamide and (b) 2,2'-((5-hydroxyisophthaloyl)bis(azanediyl))bis(3-mercaptopropanoic acid)

## 7.2. Results and Discussion

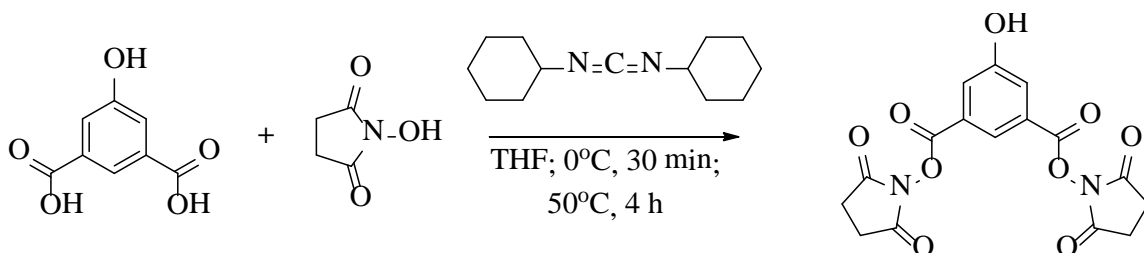
### 7.2.1. HBDTH<sub>2</sub> Synthesis and Characterization

HBDTH<sub>2</sub> was synthesized from 5-hydroxyisophthalic acid in a two-step synthetic pathway (Scheme 7.1). The compound has a similar structural skeleton as BDTH<sub>2</sub> with a hydroxyl group (OH) at meta position on benzene ring. The introduction of a hydroxyl group on the benzene ring increased the solubility of the compound in water which was evident from the synthesis method. In the first step, the carboxylic acid groups of 5-hydroxyisophthalic acid were converted to ester by N-hydroxysuccinimide to obtain N-succinyl ester of 5-hydroxyisophthalic acid (abbreviated as NS5HIPE) in 24% yield as per the reported literature.<sup>288,289</sup> In the second step of synthesis, it was difficult to separate HBDTH<sub>2</sub> from the aqueous media due to its increased solubility. The IR spectra of NS5HIPE showed the presence of characteristic peaks. The bands corresponding to phenolic OH, ester carbonyl and amide carbonyl at 3368, 1774 and 1735 cm<sup>-1</sup>, respectively, were observed by IR. <sup>1</sup>H NMR signals at  $\delta$  8.09 and 7.80 ppm corresponded to aromatic protons, whereas signal at  $\delta$  2.90 ppm corresponded to methylene protons of five membered succinyl rings. In the second step, NS5HIPE was then reacted with cysteamine hydrochloride in dichloromethane to obtain a HBDTH<sub>2</sub> in 12.5% yield. The compound was characterized by proton NMR, IR and mass spectroscopy to confirm the synthesis of product. IR of the compound showed all the prominent peaks. The band at 2550 cm<sup>-1</sup> was observed for S-H stretching which is similar to the thiol peak observed at 2557 cm<sup>-1</sup> for BDTH<sub>2</sub><sup>180,213</sup> and 2568 cm<sup>-1</sup> for ABDTH<sub>2</sub>. The carbonyl (C=O) stretching frequency observed at 1637 cm<sup>-1</sup> indicated the formation of amide linkage in the molecule similar to BDTH<sub>2</sub> and ABDTH<sub>2</sub>. The band at

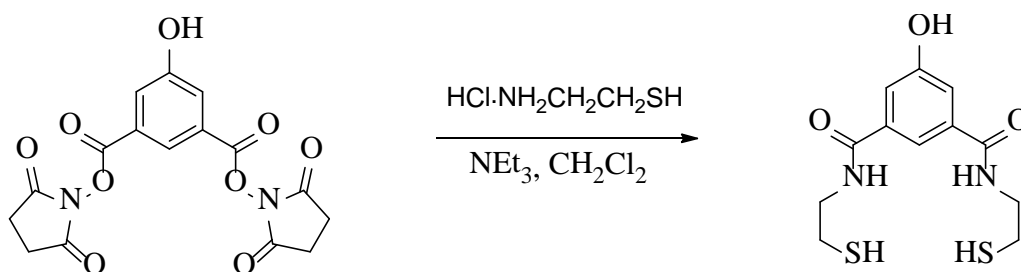


1543  $\text{cm}^{-1}$  corresponded to N-H bending in the molecule.  $^1\text{H}$  NMR of HBDTH<sub>2</sub> in DMSO-*d*<sub>6</sub> also confirmed the presence of thiol proton (S-H) at  $\delta$  2.42 ppm similar to BDTH<sub>2</sub>. The phenolic proton (O-H) and amide proton (N-H) were observed at  $\delta$  9.87 ppm and 8.62 ppm, respectively, whereas aromatic protons were observed at  $\delta$  7.72 ppm and 7.35 ppm. The signals at  $\delta$  3.40 ppm and 2.63 ppm corresponded to  $\alpha$ -methylene C-H and  $\beta$ -methylene C-H, respectively. The MS showed a significant peak at 301 (m/z) confirming the molecular mass of HBDTH<sub>2</sub>. It was also observed that dimer (+m/z = 599) and trimer (+m/z = 897) were also present in mixture of product suggesting the formation of disulfide bond. This was possibly due to the use of excess triethylamine during the reaction process.

Step 1:



Step 2:



**Scheme 7.1.** Two-Step Synthesis of HBDTH<sub>2</sub>

### 7.2.2. HABDTH<sub>2</sub> Synthesis and Characterization

HABDTH<sub>2</sub> was synthesized in a three step synthetic pathway from 5-hydroxyisophthalic acid and S-trityl-L-cysteine (Scheme 7.2). The first step of the synthesis pathway of HABDTH<sub>2</sub> was similar to the initial step of HBDTH<sub>2</sub> synthesis where carboxylic acid of 5-hydroxyisophthalic acid was converted to the ester using N-hydroxysuccinimide to prepare NS5HIPE in 46% yield. The prominent peaks for different functional groups in NS5HIPE were observed in IR spectra. A peak for phenolic

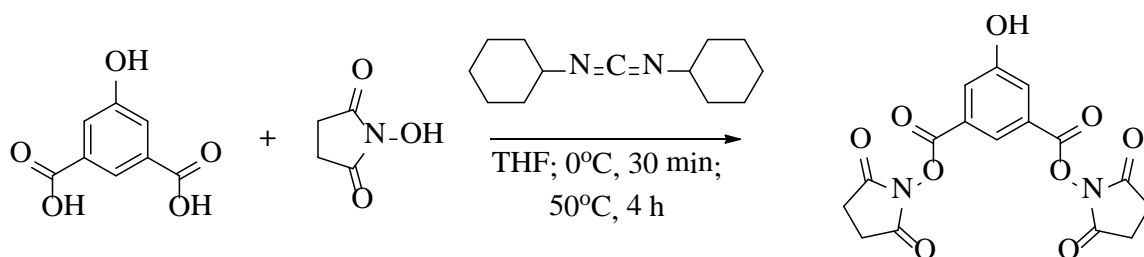
O-H group was observed at  $3326\text{ cm}^{-1}$ . While IR bands at  $3045\text{ cm}^{-1}$ ,  $2932\text{ cm}^{-1}$ ,  $1774\text{ cm}^{-1}$  and  $1735\text{ cm}^{-1}$  were observed for  $\text{sp}^2\text{ CH}$ ,  $\text{sp}^3\text{ CH}$ , ester CO and amide CO, respectively.  $^1\text{H}$  NMR showed aromatic CH at 8.09 ppm and 7.80 ppm, and  $\text{sp}^3\text{ CH}$  at 2.90 ppm. The parent peak for NS5HIPE in mass spectra (-ESI, m/z) was observed at 375. The characterization data indicated the synthesis of NS5HIPE.

NS5HIPE was then reacted with S-trityl-L-cysteine in the presence of triethyl amine ( $\text{NEt}_3$ ) in the following step to prepare S-trityl-HABDT in 65% yield. Trityl group was used to protect the sulfur group in L-cysteine to prevent the nucleophilic reaction of thiol with the activated carbonyl carbon. IR bands were observed at  $3335\text{ cm}^{-1}$ ,  $3048\text{ cm}^{-1}$ ,  $2943\text{ cm}^{-1}$ ,  $1737\text{ cm}^{-1}$ ,  $1659\text{ cm}^{-1}$  and  $1523\text{ cm}^{-1}$  for phenolic OH,  $\text{sp}^2\text{ CH}$ ,  $\text{sp}^3\text{ CH}$ , carboxylic CO, amide CO and N-H bending.  $^1\text{H}$  NMR showed aromatic proton peaks at 7.96 ppm and 7.68 ppm. While aromatic peaks of trityl groups were found at 7.38 ppm, 7.24 ppm and 7.18 ppm. The peak for NH bond was observed at 8.16 ppm. Mass spectra of S-trityl-HABDT showed different fragment of the molecule at m/z 707 ( $\text{C}_{44}\text{H}_{40}\text{N}_2\text{O}_5\text{S}_2$ ), 588 ( $\text{C}_{32}\text{H}_{30}\text{N}_2\text{O}_5\text{S}_2$ ).

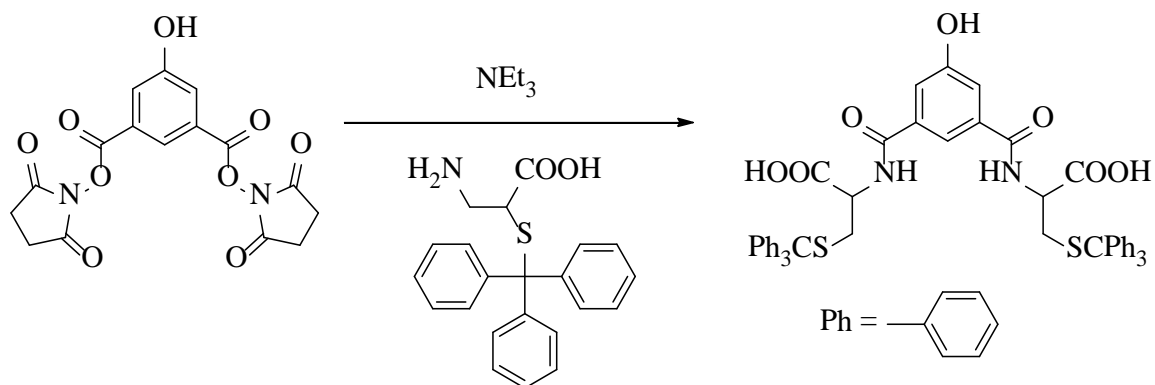
In the final step, protection of thiol in S-trityl-HABDT was removed to obtain HABDTH<sub>2</sub>. S-trityl-HABDT was treated with trifluoroacetic acid in presence of triethylsilane to get the desired product in 61% yield. IR spectra of HABDTH<sub>2</sub> showed characteristic thiol peak at  $2558\text{ cm}^{-1}$ . The IR peak for thiol was consistent with the thiol peak observed for BDTH<sub>2</sub>. Other peaks at  $3347\text{ cm}^{-1}$ ,  $3057\text{ cm}^{-1}$ ,  $2935\text{ cm}^{-1}$ ,  $1728\text{ cm}^{-1}$ ,  $1651\text{ cm}^{-1}$  and  $1537\text{ cm}^{-1}$  were observed for phenolic OH,  $\text{sp}^2\text{ CH}$ ,  $\text{sp}^3\text{ CH}$ , carboxylic CO, amide CO and NH bending, respectively. Proton NMR in  $\text{DMSO}-d_6$  was similar to BDTH<sub>2</sub> and ABDTH<sub>2</sub>. Thiol peak was observed at 2.56 ppm, which was in close

agreement with BDTH<sub>2</sub> and ABDTH<sub>2</sub>. Phenolic OH was found at 10.03 ppm. Proton peaks for NH, sp<sup>2</sup> CH and sp<sup>3</sup> CH were observed at 8.73 ppm, 7.81 ppm and 7.43 ppm, and 4.51 ppm, 3.01 ppm and 2.86 ppm. The parent peak for HABDTH<sub>2</sub> in mass spectra was at m/z 389.

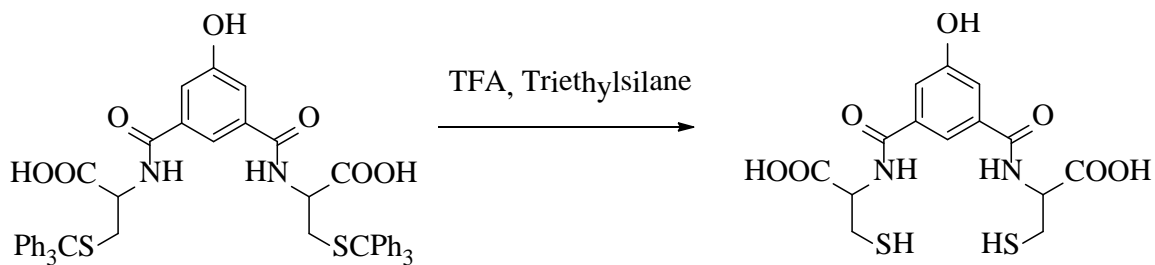
Step 1:



Step 2:



Step 3:



**Scheme 7.2.** Synthetic pathway of HABDTH<sub>2</sub>: Step 1 - NS5HIPE; Step 2 - S-trityl-HABDT; Step 3 - HABDTH<sub>2</sub>

### 7.3. Experimental

#### 7.3.1. Materials and Techniques

All the reactions were carried out at room temperature unless the temperature was mentioned otherwise. The reactions were conducted in the corresponding solvents as mentioned in synthetic procedure. 5-Hydroxyisophthalic acid (99%, Acros Organics), N-hydroxysuccinimide (98+%, Acros Organics), *N,N'*-Dicyclohexylcarbodiimide (99%, Alfa Aesar), 2-mercaptoethylamine hydrochloride (cysteamine hydrochloride, 98+%, Alfa Aesar), S-trityl-L-Cysteine (97%, Acros Organics), triethylamine (99.5%, Mallinckrodt Chemicals), trifluoroacetic acid (99%, Alfa Aesar) and triethylsilane (99%, Aldrich) were used as received. Compounds were characterized by  $^1\text{H}$  nuclear magnetic resonance (NMR), infrared (IR) spectroscopy and mass spectroscopy (MS).  $^1\text{H}$  NMR was obtained with a Varian INOVA instrument at room temperature at an operating frequency of 399.78 MHz with a pulse of 71.2 deg. Mass spectral data was obtained using a Finnigan LTQ at the University of Kentucky Mass Spectrometry Facility. IR data of compounds was produced using KBr pellets with a model Nicolet Avatar 370 DTGS IR spectrophotometer manufactured by Thermo Electron Corporation and reported in  $\text{cm}^{-1}$ .

#### 7.3.2. Synthesis of HBDTH<sub>2</sub>

A two-step synthetic method was attempted including the conversion of an aromatic carboxylic acid to N-succinyl ester of corresponding aromatic acid followed by the reaction of cysteamine hydrochloride to form an amide product similar to BDTH<sub>2</sub> (Scheme 7.1). In the first step, N-hydroxysuccinimide (NHS, 1.01 g, 8.80 mmol) was

added to a stirring solution of 5-hydroxyisophthalic acid (0.80 g, 4.39 mmol) in tetrahydrofuran (THF, 50 mL) at 0°C followed by the addition of N,N'-dicyclohexylcarbodiimide (DCC, 1.91 g, 9.23 mmol) with stirring for 30 mins. Then the reaction mixture was stirred at room temperature for 4 h. At the end of the reaction, THF was removed under vacuum to obtain a white solid followed by redissolution of solid in 30 mL of ethyl acetate. Ethyl acetate layer was filtered to remove any undissolved solid and then washed with saturated NaHCO<sub>3</sub> solution (50 mL x 2) to remove starting materials followed by drying over Na<sub>2</sub>SO<sub>4</sub> and removal under vacuum to obtain a white solid, the N-succinyl ester of 5-hydroxyisophthalic acid (NS5HIPE, 403 mg, 24% yield). IR (KBr, cm<sup>-1</sup>): 3368 (phenolic OH), 2943 (aromatic CH), 2857 (methylene CH), 1774 (acid ester CO), 1735 (N-succinyl CO); <sup>1</sup>H NMR (DMSO-*d*<sub>6</sub>): 8.09 (1H, ts, aromatic CH), 7.80 (2H, ds, aromatic CH), 2.90 (8H, s, succinyl CH); MS (-ESI. m/z): 375 (C<sub>16</sub>H<sub>12</sub>N<sub>2</sub>O<sub>9</sub>).

In the next step, 0.9 mL (6.59 mmol) triethylamine in CH<sub>2</sub>Cl<sub>2</sub> (5 mL) was slowly added to cysteamine hydrochloride (243 mg, 2.14 mmol) in CH<sub>2</sub>Cl<sub>2</sub> (10 mL) with stirring until solid was dissolved in solution. NS5HIPE (400 mg, 1.06 mmol) from the first step was also dissolved in CH<sub>2</sub>Cl<sub>2</sub> (15 mL) before being added drop wise to the stirring solution. The resulting solution was stirred for 24 h. The CH<sub>2</sub>Cl<sub>2</sub> solution was then washed with dilute HCl (5% v/v, 30 mLx2) and dried over Na<sub>2</sub>SO<sub>4</sub> before removal under vacuum to leave behind a white solid that was characterized by <sup>1</sup>H NMR to be the starting material. The combined aqueous layer from CH<sub>2</sub>Cl<sub>2</sub> wash was then extracted with ethyl acetate (25 mL). Ethyl acetate was dried over Na<sub>2</sub>SO<sub>4</sub> and removed under vacuum to obtain 40 mg of solid (12.5% yield). The solid was characterized by <sup>1</sup>H NMR, IR and

mass spectra to be HBDTH<sub>2</sub>. Mp: 120-124°C; IR (KBr, cm<sup>-1</sup>): 3337 (phenolic OH and amide NH), 3061 (aromatic CH), 2933 (methylene CH), 2550 (SH), 1637 (amide CO), 1543 (N-H bending); <sup>1</sup>H NMR (DMSO-*d*<sub>6</sub>, ppm): 9.87 (1H, s, phenolic OH), 8.62 (1H, t, NH), 7.72 (1H, ts, aromatic CH), 7.35 (2H, ds, aromatic CH), 3.40 (4H, q, α-methylene CH), 2.63 (4H, q, β-methylene CH), 2.42 (2H, t, SH); Mass spectra (ESI+, *m/z*): 301 (C<sub>12</sub>H<sub>16</sub>N<sub>2</sub>O<sub>2</sub>S<sub>2</sub>, monomer), 599 (C<sub>24</sub>H<sub>30</sub>N<sub>4</sub>O<sub>4</sub>S<sub>4</sub>, dimer), 897 (C<sub>36</sub>H<sub>44</sub>N<sub>6</sub>O<sub>6</sub>S<sub>6</sub>, trimer).

### 7.3.3. Synthesis of HBDTH<sub>2</sub>

A three step synthetic pathway as shown in Scheme 7.2 was followed for the synthesis of HBDTH<sub>2</sub>. The first step was the conversion of 5-hydroxyisophthalic acid to N-succinyl ester followed by reaction of S-trityl-L-cysteine with an active ester in the second step to give S-trityl-HABDT. In the final step, S-trityl-HABDT was treated with trifluoroacetic acid and triethylsilane to obtain HBDTH<sub>2</sub>.

**Step 1 (NS5HIPE):** NHS (5.26 g, 43.4 mmol) was added to a stirring solution of 5-hydroxyisophthalic acid (3.95 g, 21.7 mmol) in THF (100 mL) at 0°C followed by the addition of N,N'-dicyclohexylcarbodiimide (DCC, 11.0 g, 53.4 mmol) with stirring for 30 mins. Then the reaction mixture was stirred at room temperature for 4 h. At the end of the reaction, solid was removed by filtration before THF was removed under vacuum to obtain a white solid followed by redissolution of solid in 50 mL of ethyl acetate. Ethyl acetate layer was filtered to remove any undissolved solid and washed with saturated NaHCO<sub>3</sub> solution (50 mL x 2) to remove starting materials followed by drying over Na<sub>2</sub>SO<sub>4</sub> and removal under vacuum to obtain white solid as the N-succinyl ester of 5-



hydroxyisophthalic acid (NS5HIPE, 3.75 g, 46% yield). IR (KBr,  $\text{cm}^{-1}$ ): 3326 (phenolic OH), 3045 (aromatic CH), 2932 (methylene CH), 1774 (acid ester CO), 1735 (N-succinyl CO);  $^1\text{H}$  NMR ( $\text{DMSO}-d_6$ ): 8.09 (1H, ts, aromatic CH), 7.80 (2H, ds, aromatic CH), 2.90 (8H, s, succinyl CH); MS (-ESI, m/z): 375 ( $\text{C}_{16}\text{H}_{12}\text{N}_2\text{O}_9$ ).

**Step 2 (S-trityl-HABDT):** NS5HIPE (940.1 mg, 2.5 mmol) was stirred in 50 mL of dimethylformamide (DMF) followed by addition of  $\text{NEt}_3$  (1.5 mL, 11.1 mmol) to the stirring solution drop wise. After complete addition of triethyl amine, solution was stirred for 10 min before addition of S-trityl-L-cysteine (1.9 g, 5.2 mmol) followed by stirring for 20 h under  $\text{N}_2$ . After 20 h, the reaction solution was added drop wise to 25% HCl (300 mL) resulting in immediate formation of precipitate. Solid was then collected through filtration, washed with DI water (200 mL) and dried in vacuum to obtain 1.41 g of apale white powder (65% yield). Mp: 135-138°C; IR: (KBr,  $\text{cm}^{-1}$ ): 3335 (phenolic OH), 3048 (aromatic CH), 2943 (methylene CH), 1737 (carboxylic CO), 1659 (amide CO), 1523 (N-H bending);  $^1\text{H}$  NMR ( $\text{CD}_3\text{OD}$ ): 8.16 (d, 2H, NH), 7.96 (s, 1H, aromatic CH), 7.68 (s, 2H, aromatic CH), 7.38 (d, 6H, trityl CH), 7.24 (t, 6H, trityl CH), 7.18 (t, 3H, trityl CH), 4.50 (m, 2H, methylene CH), 3.15 (m, 2H, methylene CH); MS (+ESI, m/z): 707 ( $\text{C}_{44}\text{H}_{40}\text{N}_2\text{O}_3\text{S}_2$ ), 588 ( $\text{C}_{32}\text{H}_{30}\text{N}_2\text{O}_5\text{S}_2$ ).

**Step 3 (HABDTH<sub>2</sub>):** In the final step, S-trityl-HABDT (1 g, 1.14 mmol) was stirred in 12 mL trifluoroacetic acid for 3 hr followed by addition of triethylsilane (0.8 mL) to the stirring solution with further stirring for another 30 mins. A white precipitate appeared. After 30 mins, solvent and volatilities were removed under vacuum followed by thorough

washing with diethyl ether (20 mL x3). The solid formed was further dried in vacuum to obtain 0.27 g of desired product (61% yield). Mp: 84-86°C; IR (KBr,  $\text{cm}^{-1}$ ): 3347 (phenolic OH), 3057 (aromatic CH), 2935 (methylene CH), 2558 (SH), 1728 (carboxylic CO), 1651 (amide CO), 1537 (N-H bending);  $^1\text{H}$  NMR ( $\text{DMSO-}d_6$ ): 10.03 (s, 1H, OH), 8.73 (d, 2H, NH), 7.81 (s, 1H, aromatic CH), 7.43 (s, 2H, aromatic CH), 4.51 (m, 2H, methylene CH), 3.01 (m, 1H, methylene CH), 2.86 (m, 1H, methylene CH), 2.56 (t, 2H, SH); MS (+ESI, m/z): 389 ( $\text{C}_{14}\text{H}_{16}\text{N}_2\text{O}_7\text{S}_2$ )

#### 7.4. Conclusion

New dithiol ligands, HBDTH<sub>2</sub> and HABDTH<sub>2</sub>, were synthesized and characterized. Both the compounds showed the characteristic thiol peak in IR and  $^1\text{H}$  NMR which is similar to the thiol peak in BDTH<sub>2</sub> and ABDTH<sub>2</sub>. HBDTH<sub>2</sub> was synthesized in two steps with a yield of 12.5%. From the current synthetic pathway of HBDTH<sub>2</sub>, it can be concluded that HBDTH<sub>2</sub> can be synthesized though significant modifications and improvements are required to increase the percent yield of the product. A three step synthetic methodology was carried out to obtain HABDTH<sub>2</sub>, which had a 61% yield at the end of the reaction. Further studies are required to use HBDTH<sub>2</sub> and HABDTH<sub>2</sub> for heavy metal removal from aqueous solutions and various wastewaters. These compounds can also be applied on the surface of s quartz crystal to monitor the concentration of various heavy metals in solution in real time which again requires extensive studies in the future.

## CHAPTER 8

### Conclusions and Future Direction

#### 8.1. Conclusions

The current work has demonstrated the proof of concept of the design and synthesis of an acid derivative of BDTH<sub>2</sub> (ABDTH<sub>2</sub>) followed by immobilization of new dithiol ligands on a solid-support for application as filtration column material for removal of As(III) from water. This thesis work has also demonstrated the synthesis of water soluble dithiol ligands HBDTH<sub>2</sub> and HABDTH<sub>2</sub> for removal of heavy metals and metalloids such as Hg, Cd, Pb and As.

Previous studies have demonstrated that BDTH<sub>2</sub> is an excellent dithiol compound for binding and removal of soft, divalent metals including Pb(II), Cd(II), Cu(II), Mn(II), Zn(II), Fe(II) and Hg(II) from ground water, coal refuse, gold ore, lead battery recycling plant wastewater and contaminated soils. Arsenic is another toxic, environmental contaminant that binds with BDTH<sub>2</sub>. Batch studies at environmental pH showed that arsenate did not bind with BDTH<sub>2</sub>, whereas arsenite did bind with it. This makes BDTH<sub>2</sub> an excellent binding agent for removing As(III) from water. Arsenite is the more toxic form of arsenic present in water than arsenate. However, BDTH<sub>2</sub> is not soluble in water. As a result, in previous studies BDTH<sub>2</sub> has been applied as either a sodium or potassium metallated salt in water or ethanolic solution of BDTH<sub>2</sub> for removal of different metals. This is effective in batch remediation followed by filtration for large scale industrial effluents and environmental waters with a high concentration of dissolved metals. The application of BDTH<sub>2</sub> as a low cost, portable, lightweight column in homes and arsenic

affected areas of developing countries, where large water treatment systems and cost of remediation technologies are issues, is an effective/viable solution only if covalent bond formation between the solid ligand and the species of interest could be achieved quickly enough in a flow scenario. Previous studies using suspension of BDTH<sub>2</sub> with sand and ZVI have shown arsenic capture ability in filtration column scenario. However the leaching of BDTH<sub>2</sub> and iron from filtration column in the effluent remained an issue in the viability of the column.

In the current study, ABDTH<sub>2</sub> was synthesized from isophthaloyl chloride and L-cysteine for immobilization on silica for application/use as filtration column material. ABDTH<sub>2</sub> showed characteristic a thiol peak at 2568 cm<sup>-1</sup> in IR and at 2.60 ppm in <sup>1</sup>H NMR which was similar to thiol compounds. ABDTH<sub>2</sub> was shown to form a covalent bond with As(III) when an ethanolic solution of ABDTH<sub>2</sub> was applied to an aqueous solution of As(III). The absence of a thiol peak in ABDT-As(III) was observed in IR and <sup>1</sup>H NMR. XAFS studies indicated that As(III) was bonded with three sulfur atoms in ABDT-As(III). The average bond length of As-S was 2.26 Å which was consistent with other As-S bonds reported in literature.

Silica-supported ABDTH<sub>2</sub> (SiABDTH<sub>2</sub>) was synthesized by modifying the silica surfaces with  $\gamma$ -aminopropyltriethoxysilane followed by immobilization of ABDTH<sub>2</sub> on the modified silica. Thermogravimetric analysis of SiABDTH<sub>2</sub> showed high decomposition temperature of organic content suggesting the immobilization of ABDTH<sub>2</sub> on silica support. ICP-OES analysis of SiABDTH<sub>2</sub> showed the loading of ABDTH<sub>2</sub> on solid-support in the range of 0.114 – 0.373 mmol/g with various batches of SiABDTH<sub>2</sub> preparation. Batch studies of As(III) removal using SiABDTH<sub>2</sub> indicated 100% capture

of As(III) from approximately 200 ppb aqueous arsenic solutions with application of as low as 0.2 g of SiABDTH<sub>2</sub> at pH 5, 7 and 9. As(III) removal capacity of SiABDTH<sub>2</sub> increased with increase in contact time between SiABDTH<sub>2</sub> and As(III) in solution at different pH's values. A time dependent study showed 92% - 100% As(III) removal within 5 h of application of 0.6 g of SiABDTH<sub>2</sub>. The bonding environment of As(III) on SiABDT-As(III) was determined by XAFS. The K-edge value of As(III) was 11866 eV which was similar to the arsenic K-edge in As<sub>2</sub>S<sub>3</sub>. The As-S bond distance in SiABDT-As(III) was 2.26 Å that was also observed in ABDT-As(III). However, 16% -29% of arsenic leached out of SiABDT-As(III) and leaching percentage remained same over several weeks.

SiABDTH<sub>2</sub> also showed Hg capture ability from aqueous solutions at pH 5, 7 and 9. The percentage of Hg removal increased with increasing amount of SiABDTH<sub>2</sub>. The binding energy of Hg 4f<sub>7/2</sub> and 4f<sub>5/2</sub> was observed at 100.8 (1.5) and 104.8 (1.6) eV by XPS studies of SiABDT-Hg. The binding energy of S changed from 169.8 (3.5) to 163.4 (2.2) eV upon binding with mercury to thiol in SiABDT-Hg. Leaching studies of SiABDT-Hg showed 1.47% -3.67% of Hg leaching over several weeks.

As a proof of concept, SiABDTH<sub>2</sub> has been used as a filtration column material to test the applicability of the material. Filtration columns prepared from SiABDTH<sub>2</sub> were tested at water flow rates of 20 mL/min and 500 mL/min. At a flow rate of 20 mL/min, 100% arsenic removal was observed in effluent from approximately 200 ppb arsenic solution. However at a high flow rate of 500 mL/min, 53.7% of arsenic was captured at the beginning but with time the percentage of arsenic capture increased to 69.1% after 27 L of water had passed through the column. Arsenic leaching studies of SiABDT-As(III)

material from the filtration column indicated insignificant arsenic leaching, which suggested covalent binding of arsenic with thiol.

In the current work, water soluble dithiol ligands, HBDTH<sub>2</sub> and HABDTH<sub>2</sub>, similar to BDTH<sub>2</sub> molecular framework were also designed and synthesized. Polar groups were introduced into the BDTH<sub>2</sub> molecular framework. The new dithiol compounds thus will have the same metal binding capability of BDTH<sub>2</sub> but with an increase in the applicability of ligand in aqueous solutions without the use of metallated salt or ethanolic solutions.

The important outcome of current study is that SiABDTH<sub>2</sub> can be used as an alternative adsorbent for soft heavy metals and metalloids such as Hg, Cd, Pb and As. Adsorption of these metals on SiABDTH<sub>2</sub> occurs through reaction between metals and sulfur of ABDTH<sub>2</sub> units. Solid state NMR, Raman spectroscopy study can further be carried out on SiABDT-As(III) compound to confirm the formation of As(III) bound sulfur on SiABDT-As(III). Laboratory and field study of As(III) removal in presence of various competing ions is required before commercialization of the material.

## **8.2. Future Direction**

The current work demonstrated the “proof of concept” concerning the design and synthesis of ABDTH<sub>2</sub>, immobilization of ABDTH<sub>2</sub> on silica, demonstration of SiABDTH<sub>2</sub> as a filtration column material to remove As(III) and synthesis of new dithiol ligands. Preliminary work had shown that ABDTH<sub>2</sub> bonded with As(III) through the formation of a As-S bond. SiABDTH<sub>2</sub> was shown to capture As(III) both in batch studies and filtration column studies. However study indicated the leaching of certain

percentage of arsenic in water. Extensive study is required to find out the interactions possible between ABDTH<sub>2</sub> and water. Optimization of the synthesis of SiABDTH<sub>2</sub> is also required to improve ABDTH<sub>2</sub> loading on a silica support. Studies are required to optimize As(III) capture ability with optimum water flow rate through the filtration column. The effect of competing ions present in water on the removal of arsenic by SiABDTH<sub>2</sub> also needs to be studied. Field tests of the filtration column are also necessary for successful commercialization of SiABDTH<sub>2</sub> as a filtration column material. Further studies are required on the applicability of HBDTH<sub>2</sub> and HABDTH<sub>2</sub> as soft, heavy metal binding and removal agents. Due to increased solubility in water, these dithiol ligands can be applied directly as metal remediation compounds without having to use ethanolic or metallated salt of ligands.

The proof of concept described in the current work can further be used in the development of a quartz crystal microbalance (QCM) sensor to identify and determine the concentration of contaminants in water in real time. The surface of gold crystal on QCM can be modified with silica, which can be further modified with amionoalkylsilane reagent followed by immobilization of ABDTH<sub>2</sub> on the surface. ABDTH<sub>2</sub> modified QCM can then be connected to the hand-held display unit that will determine the concentration of contaminants in real time. When metal binds with thiol groups on QCM surface, the change in oscillation frequency will be recorded on binding of ABDTH<sub>2</sub> on the QCM surface with metal, due to the change in the mass on the surface of the QCM.

## REFERENCES

- (1) Lide, D. R. In *CRC Handbook of Chemistry and Physics*; 83rd ed.; CRC Press: Boca Raton, FL, 2002, p 4:4.
- (2) Dean, J. A. In *Lange's Handbook of Chemistry*; 11th ed.; McGraw-Hill Book Company: New York, NY, 2002, p 4:8.
- (3) Pearson, R. G. *Journal of Chemical Education* **1968**, *45*, 643.
- (4) Gregus, Z.; Roos, G.; Geerlings, P.; Némethi, B. *Toxicological Sciences* **2009**, *110*, 282.
- (5) Norman, N. C. *Chemistry of Arsenic, Antimony and Bismuth*; Blackie Academic and Professional: London, 1998.
- (6) Baerends, E. J.; Schwarz, W. H. E.; Schwerdtfeger, P.; Snijders, J. G. *Journal of Physics B: Atomic Molecular and Optical Physics* **1990**, *23*, 3225.
- (7) Greenwood, N. N.; Earnshaw, A. *Chemistry of the Elements*; Butterworth-Heinemann: Oxford, 1997.
- (8) Holleman, A. F.; Wiberg, E. *Inorganic Chemistry*; Academic Press: San Diego, 2001.
- (9) *CRC Handbook of Chemistry and Physics*; Lide, D. R., Ed.; CRC Press: Boca Raton, 2008.
- (10) Jones, F. T. *Poult Sci* **2007**, *86*, 2.
- (11) Mohan, D.; Pittman, J. C. U. *Journal of Hazardous Materials* **2007**, *142*, 1.
- (12) Cullen, W. R.; Reimer, K. J. *Chem. Rev.* **1989**, *89*, 713.



- (13) Robinson, B.; Outred, H.; Brooks, R.; Kirkman, J. *Chemical Speciation and Bioavailability* **1995**, 7, 89.
- (14) Bhattacharya, P.; Mukherjee, A. B. *Environmental Reviews* **2001**, 9, 189.
- (15) Vahidnia, A.; Van Der Voet, G. B.; De Wolff, F. A. *Human & experimental toxicology* **2007**, 26, 823.
- (16) *Arsenic: Environmental Chemistry, Health Threats and Waste Treatment*; Henke, K., Ed.; Wiley, 2009.
- (17) Bowell, R. J. *Appl. Geochem.* **1994**, 9, 279.
- (18) Masscheleyn, P. H.; Delaune, R. D.; Patrick, W. H. *Environmental Science & Technology* **1991**, 25, 1414.
- (19) Lasky, T.; Sun, W.; Kadry, A.; Hoffman, M. K. *Environ. Health Perspect.* **2004**, 112, 18.
- (20) Signes-Pastor, A.; Burlo, F.; Mitra, K.; Carbonell-Barrachina, A. A. *Geoderma* **2007**, 137, 504.
- (21) Al-Abed, S. R.; Jegadeesan, G.; Purandare, J.; Allen, D. *Chemosphere* **2007**, 66, 775.
- (22) Fendorf, S.; Eick, M. J.; Grossl, P.; Sparks, D. L. *Environ. Sci. Technol.* **1997**, 31, 315.
- (23) Manning, B. A.; Goldberg, S. *Soil Sci.* **1997**, 162, 886.
- (24) Manning, B. A.; Fendorf, S. E.; Goldberg, S. *Environ. Sci. Technol.* **1998**, 32, 2383.
- (25) Raven, K. P.; Jain, A.; Loeppert, R. H. *Environ. Sci. Technol.* **1998**, 32, 344.

- (26) Smedley, P. L.; Kinniburgh, D. G. *Applied Geochemistry* **2002**, *17*, 517.
- (27) Garelick, H.; Dybowska, A.; Valsami-Jones, E.; Priest, N. *Journal of Soils and Sediments* **2005**, *5*, 182.
- (28) Reith, F.; McPhail, D. C. *Geochim. Cosmochim. Acta* **2007**, *71*, 1183.
- (29) Yudovich, Y. E.; Ketris, M. P. *Int J. Coal Geol* **2005**, *62*, 135.
- (30) Pierce, M. L.; Moore, C. B. *Water Res.* **1982**, *16*, 1247.
- (31) Smith, E.; Naidu, R.; Alston, A. M. *J. Environ. Qual.* **2002**, *31*, 557.
- (32) Livesey, N. T.; Huang, P. M. *Soil Sci.* **1981**, *131*, 88.
- (33) Goldberg, S. *Soil Sci. Soc. Am. J.* **1986**, *50*, 1154.
- (34) Melamed, R.; Jurinak, J. J.; Dudley, L. M. *Soil Sci. Soc. Am. J.* **1995**, *59*, 1289.
- (35) Saxena, V. K.; Kumar, S.; Singh, V. S. *Current Science* **2004**, *86*, 281.
- (36) Le, X. C.; Lu, X.; Li, X. *Anal. Chem.* **2004**, 27A.
- (37) Masscheleyn, P. H.; Delaune, R. D.; Patrick, W. H. *Environ. Sci. Technol.* **1991**, *25*, 1414.
- (38) Mehmood, A.; Hayat, R.; Wasim, M.; Akhtar, M. S. *J. Agric. Biol. Sci.* **2009**, *1*, 59.
- (39) Nagar, R.; Sarkar, D.; Makris, K. C.; Datta, R. *Chemosphere* **2010**, *78*, 1028.
- (40) Gao, S.; Goldberg, S.; Herbel, M. J.; Chalmers, A. T.; Fujii, R.; Tanji, K. *Chemical Geology* **2006**, *228*, 33.
- (41) Fuller, C. C.; Davis, J. A.; Waychunas, G. A. *Geochimica et Cosmochimica Acta* **1993**, *57*, 2271.

- (42) Bissen, M.; Frimmel, F. H. *Acta hydrochimica et hydrobiologica* **2003**, *31*, 9.
- (43) Choong, T. S. Y.; Chuah, T. G.; Robiah, Y.; Gregory Koay, F. L.; Azni, I. *Desalination* **2007**, *217*, 139.
- (44) Greenwood, N. N.; Earnshaw, A. *Chemistry of the elements*; 2 ed.; Reed Educational and Professional Publishing, Ltd.: Oxford, Great Britain, **2001**.
- (45) Nordstrom, D. K.; Archer, D. G. In *Arsenic in Ground Water*; Welch, A. H., Stollenwerk, K. G., Eds.; Kluwer Academic Publishers: Boston, MA, 2003.
- (46) Krause, E.; A., E. V. *The American Mineralogis* **1988**, *73*, 850.
- (47) Islam, F. S.; Gault, A. G.; Boothman, C.; Polya, D. A.; Charnock, J. M.; Chatterjee, D.; Lloyd, J. R. *Nature* **2004**, *430*, 68.
- (48) Matschullat, J. *The Science of The Total Environment* **2000**, *249*, 297.
- (49) Jackson, B. P.; Miller, W. P. *Environ. Sci. Technol.* **1999**, *33*, 270.
- (50) Ruiz-Chanco, M. J.; Lopez-Sanchez, J. F.; Rubio, R. *Anal. Bioanal. Chem.* **2007**, *387*, 627.
- (51) Drahota, P.; Filippi, M. *Environ. Int.* **2009**, *35*, 1243.
- (52) Ballantyne, J. M.; Moore, J. N. *Geochimica et Cosmochimica Acta* **1988**, *52*, 475.
- (53) Webster, J. G.; Nordstrom, D. K. In *Arsenic in Ground Water*; Welch, A. H., Stollenwerk, K. G., Eds.; Kluwer Academic Publishers: Boston, MA, 2003, p 101.
- (54) O'Shea, B.; Jankowski, J.; Sammut, J. *Science of The Total Environment* **2007**, *379*, 151.

- (55) Sullivan, K. A.; Aller, R. C. *Geochimica et Cosmochimica Acta* **1996**, 60, 1465.
- (56) Anawar, H. M.; Akai, J.; Komaki, K.; Terao, H.; Yoshioka, T.; Ishizuka, T.; Safiullah, S.; Kato, K. *Journal of Geochemical Exploration* **2003**, 77, 109.
- (57) Aggett, J.; O'Brien, G. A. *Environmental Science & Technology* **1985**, 19, 231.
- (58) Takamatsu, T.; Kawashima, M.; Koyama, M. *Water Research* **1985**, 19, 1029.
- (59) Peterson, M. L.; Carpenter, R. *Geochimica et Cosmochimica Acta* **1986**, 50, 353.
- (60) Brannon, J. M.; Patrick, W. H. *Environmental Science & Technology* **1987**, 21, 450.
- (61) Belzile, N. *Geochimica et Cosmochimica Acta* **1988**, 52, 2293.
- (62) Benjamin, M. M.; Leckie, J. O. *Journal of Colloid and Interface Science* **1981**, 79, 209.
- (63) Ahmann, D.; Krumholz, L. R.; Hemond, H. F.; Lovley, D. R.; Morel, F. o. M. M. *Environmental Science & Technology* **1997**, 31, 2923.
- (64) McCreadie, H.; Blowes, D. W.; Ptacek, C. J.; Jambor, J. L. *Environmental Science & Technology* **2000**, 34, 3159.
- (65) Muloin, T.; Dudas, M. J. *Journal of Environmental Engineering & Science* **2005**, 4, 461.

- (66) Pott, W. A.; Benjamin, S. A.; Yang, R. S. H. In *Reviews of Environmental Contamination and Toxicology, Vol 169*; Springer-Verlag: New York, 2001; Vol. 169, p 165.
- (67) Schwer, D. R.; McNear, D. H. *Journal of Environmental Quality* **2011**, 40, 1172.
- (68) Schooley, T.; Weaver, M. J.; Mullins, D.; Eick, M. *Journal of Pesticide Safety Education* **2008**, 10, 22.
- (69) Peryea, F. J.; Creger, T. L. *Water, Air, & Soil Pollution* **1994**, 78, 297.
- (70) Peters, S. C.; Blum, J. D.; Klaue, B.; Karagas, M. R. *Environmental Science & Technology* **1999**, 33, 1328.
- (71) Qi, Y.; Donahoe, R. J. *Science of The Total Environment* **2008**, 405, 246.
- (72) O'Connor, R.; O'Connor, M.; Irgolic, K.; Sabrsula, J.; Gurleyuk, H.; Brunette, R.; Howard, C.; Garcia, J.; Brien, J. *Environ. Forensics* **2005**, 6, 83.
- (73) Sadler, R.; Olszowy, H.; Shaw, G.; Bilotto, R.; Connell, D. *Water, Air, & Soil Pollution* **1994**, 78, 189.
- (74) Williams, M. *Environmental Geology* **2001**, 40, 267.
- (75) Roy, J. *Science of The Total Environment* **2008**, 397, 1.
- (76) Tchounwou, P. B.; Patlolla, A. K.; Centeno, J. A. *Toxicol. Path.* **2003**, 31, 575.
- (77) Cantor, K. P.; Lubin, J. H. *Toxicol. Appl. Pharmacol.* **2007**, 222, 252.
- (78) Styblo, M.; Delnomdedieu, M.; Thomas, D. J. *Chemico-Biological Interactions* **1996**, 99, 147.

- (79) Petrick, J. S.; Ayala-Fierro, F.; Cullen, W. R.; Carter, D. E.; Aposhian, H. V. *Toxicology and Applied Pharmacology* **2000**, 163, 203.
- (80) Vega, L.; Styblo, M.; Patterson, R.; Cullen, W.; Wang, C. Q.; Germolec, D. *Toxicology and Applied Pharmacology* **2001**, 172, 225.
- (81) Styblo, M.; Del Razo, L. M.; Vega, L.; Germolec, D. R.; LeCluyse, E. L.; Hamilton, G. A.; Reed, W.; Wang, C.; Cullen, W. R.; Thomas, D. J. *Archives of Toxicology* **2000**, 74, 289.
- (82) Tapio, S.; Grosche, B. *Mutat. Res.* **2006**, 612, 215.
- (83) Basu, A.; Mahata, J.; Gupta, S.; Giri, A. K. *Mutat. Res.* **2001**, 488, 171.
- (84) Patterson, T. J.; Rice, R. H. *Toxicol. Appl. Pharmacol.* **2007**, 221, 119.
- (85) Hoppenhayn-Rich, C.; Biggs, M. L.; Smith, A. E. *Int. J. Epidemiol.* **1998**, 27, 561.
- (86) Mazumder, D. N. G. *Toxicol. Appl. Pharmacol.* **2005**, 206, 169.
- (87) Simeonova, P. P.; Luster, M. I. *Toxicol. Appl. Pharmacol.* **2004**, 198, 444.
- (88) Kwok, R. K. *Toxicol. Appl. Pharmacol.* **2007**, 222, 344.
- (89) Chen, C.-J.; Wang, S.-L.; Chiou, J.-M.; Tseng, C.-H.; Chiou, H.-Y.; Hsueh, Y.-M.; Chen, S.-Y.; Wu, M.-M.; Lai, M.-S. *Toxicol. Appl. Pharmacol.* **2007**, 222, 298.
- (90) Rodriguez, V. M.; Jimenez-Capdeville, M. E.; Giordano, M. *Toxicol. Lett.* **2003**, 145, 1.
- (91) Vahidnia, A.; van der Voet, G. B.; de Wolff, F. A. *Hum. Exper. Toxicol.* **2007**, 26, 823.

- (92) Walton, F. S.; Harmon, A. W.; Paul, D. S.; Drobna, Z.; Patel, Y. M.; Styblo, M. *Toxicol. Appl. Pharmacol.* **2004**, *198*, 424.
- (93) Diaz-Villasenor, A.; Sanchez-Soto, M. C.; Cebrian, M. E.; Ostrosky-Wegman, P.; Hiriart, M. *Toxicol. Appl. Pharmacol.* **2006**, *214*, 30.
- (94) Paul, D. S.; Hernandez-Zavala, A.; Walton, F. S.; Adair, B. M.; Dedina, J.; Matousek, T.; Styblo, M. *Toxicol. Appl. Pharmacol.* **2007**, *222*, 305.
- (95) Diaz-Villasenor, A.; Burns, A. L.; Salazar, A. M.; Sordo, M.; Hiriart, M.; Cebrian, M. E.; Ostrosky-Wegman, P. *Toxicol. Appl. Pharmacol.* **2008**, *231*, 291.
- (96) Lewis, A. S. *Environ Health Perspect* **2007**, *115*.
- (97) Meliker, J.; Wahl, R.; Cameron, L.; Nriagu, J. *Environmental Health* **2007**, *6*, 1.
- (98) Hughes, M. F. *Toxicology Letters* **2002**, *133*, 1.
- (99) Fatoki, O. S. *South African Journal of Science* **1997**, *93*, 366.
- (100) Wu, J.; Shao, Y.; Liu, J.; Chen, G.; Ho, P. C. *Journal of Ethnopharmacology* **2011**, *135*, 595.
- (101) Cohen, S. M.; Arnold, L. L.; Eldan, M.; Lewis, A. S.; Beck, B. D. *Critical Reviews in Toxicology* **2006**, *36*, 99.
- (102) Thomas, D. J.; Styblo, M.; Lin, S. *Toxicology and Applied Pharmacology* **2001**, *176*, 127.
- (103) Delnomdedieu, M.; Basti, M. M.; Otvos, J. D.; Thomas, D. J. *Chemico-Biological Interactions* **1994**, *90*, 139.
- (104) Scott, N.; Hatlelid, K. M.; MacKenzie, N. E.; Carter, D. E. *Chemical Research in Toxicology* **1993**, *6*, 102.

- (105) Radabaugh, T. R.; Aposhian, H. V. *Chemical Research in Toxicology* **1999**, *13*, 26.
- (106) Zakharyan, R. A.; Sampayo-Reyes, A.; Healy, S. M.; Tsapraillis, G.; Board, P. G.; Liebler, D. C.; Aposhian, H. V. *Chemical Research in Toxicology* **2001**, *14*, 1051.
- (107) Suzuki, K. T.; Mandal, B. K.; Ogra, Y. *Talanta* **2002**, *58*, 111.
- (108) Mandal, B. K.; Suzuki, K. T. *Talanta* **2002**, *58*, 201.
- (109) Ferguson, J. F.; Gavis, J. *Water Res.* **1972**, *6*, 1259.
- (110) Oremland, R. S.; Stolz, J. F. *Science* **2003**, *300*, 939.
- (111) Kulp, T. R.; Hoeft, S. E.; Asao, M.; Madigan, M. T.; Hollibaugh, J. T.; Fisher, J. C.; Stolz, J. F.; Culbertson, C. W.; Miller, L. G.; Oremland, R. S. *Science* **2008**, *321*, 967.
- (112) Santini, J. M.; Sly, L. I.; Schnagl, R. D.; Macy, J. M. *Appl. Environ. Microbiol.* **2000**, *66*, 92.
- (113) Oremland, R. S.; Kulp, T. R.; Blum, J. S.; Hoeft, S. E.; Baesman, S.; Miller, L. G.; Stolz, J. F. *Science* **2005**, *308*, 1305.
- (114) Delnomdedieu, M.; Basti, M. M.; Otvos, J. D.; Thomas, D. J. *Chemical Research in Toxicology* **1993**, *6*, 598.
- (115) Dill, K.; Adams, E. R.; O'Connor, R. J.; Chong, S.; McGown, E. L. *Archives of Biochemistry and Biophysics* **1987**, *257*, 293.
- (116) Smith, A. H.; Smith, M. M. H. *Toxicology* **2004**, *198*, 39.
- (117) Frey, M. M.; Edwards, M. A. *Journal of the American Water Works Association Other Information* **1997**, *89*, 105.



- (118) Welch, A. H.; Lico, M. S.; Hughes, J. L. *Ground Water* **1988**, 26, 333.
- (119) Harper, T. R.; Kingham, N. W. *Water Environment Research* **1992**, 64, 200.
- (120) Ficklin, W. H. *Talanta* **1983**, 30, 371.
- (121) Sullivan, C.; Tyrer, M.; Cheeseman, C. R.; Graham, N. J. D. *Science of The Total Environment* **2010**, 408, 1770.
- (122) Leist, M.; Casey, R. J.; Caridi, D. J. *Hazard. Mater.* **2000**, 76, 125.
- (123) Selvin, N.; Upton, J.; Simms, J.; Barnes, J. *Water. Sci. Technol.* **2002**, 2, 11.
- (124) Chen, A. S. C.; Snoeyink, V. L.; Fiessinger, F. *Environmental Science & Technology* **1987**, 21, 83.
- (125) Bang, S.; Pena, M.; Patel, M.; Lippincott, L.; Meng, X.; Kim, K.-W. *Environmental Geochemistry and Health* **2011**, 33, 133.
- (126) Maliyekkal, S. M.; Philip, L.; Pradeep, T. *Chemical Engineering Journal* **2009**, 153, 101.
- (127) Jiang, J. Q. *Water Science and Technology* **2001**, 44, 89.
- (128) Clifford, D. A.; Subramonian, S.; Sorg, T. J. *Environmental Science & Technology* **1986**, 20, 1072.
- (129) Clifford, D. A.; Ghurye, G. L. In *Environmental Chemistry of Arsenic*; Frankenberger Jr., W. T., Ed.; Marcel Dekker: New York, 2002.
- (130) Kabengi, N. J.; Daroub, S. H.; Rhue, R. D. *Journal of Colloid and Interface Science* **2006**, 297, 86.

- (131) Chuang, C. L.; Fan, M.; Xu, M.; Brown, R. C.; Sung, S.; Saha, B.; Huang, C. P. *Chemosphere* **2005**, *61*, 478.
- (132) Choong, T. S. Y.; Chuah, T. G.; Robiah, Y.; Koay, F. L. G.; Azni, I. *Desalination* **2007**, *217*, 139.
- (133) Mahimairaja, S.; Bolan, N. S.; Adriano, D. C.; Robinson, B. *Adv. Agron.* **2005**, *86*, 1.
- (134) Hering, J. G.; Chen, P. Y.; Wilkie, J. A.; Elimelech, M.; Liang, S. *J. Am. Water Work Assoc.* **1996**, *88*, 155.
- (135) Lee, Y.; Um, I.-h.; Yoon, J. *Environmental Science & Technology* **2003**, *37*, 5750.
- (136) Masih, D.; Seida, Y.; Izumi, Y. *Water, Air, & Soil Pollution: Focus* **2009**, *9*, 203.
- (137) Zhu, H.; Jia, Y.; Wu, X.; Wang, H. *Journal of Hazardous Materials* **2009**, *172*, 1591.
- (138) Younggran, J.; Fan, M.; Van Leeuwen, J.; Belczyk, J. F. *Journal of Environmental Sciences* **2007**, *19*, 910.
- (139) Bang, S.; Korfiatis, G. P.; Meng, X. *Journal of Hazardous Materials* **2005**, *121*, 61.
- (140) Lien, H.-L.; Wilkin, R. T. *Chemosphere* **2005**, *59*, 377.
- (141) Lackovic, J. A.; Nikolaidis, N. P.; Dobbs, G. M. *Environmental Engineering Science* **2000**, *17*, 29.
- (142) Su, C.; Puls, R. W. *Environmental Science & Technology* **2001**, *35*, 1487.

- (143) Nikolaidis, N. P.; Dobbs, G. M.; Lackovic, J. A. *Water Research* **2003**, *37*, 1417.
- (144) Banerjee, K.; Amy, G. L.; Prevost, M.; Nour, S.; Jekel, M.; Gallagher, P. M.; Blumenschein, C. D. *Water Research* **2008**, *42*, 3371.
- (145) Raven, K. P.; Jain, A.; Loeppert, R. H. *Environmental Science & Technology* **1998**, *32*, 344.
- (146) Shafiquzzaman, M.; Azam, M. S.; Nakajima, J.; Bari, Q. H. *Desalination* **2010**, *261*, 41.
- (147) Sabbatini, P.; Rossi, F.; Thern, G.; Marajofsky, A.; de Cortalezzi, M. M. *Desalination* **2009**, *248*, 184.
- (148) Ning, R. Y. *Desalination* **2002**, *143*, 237.
- (149) Schneiter, R. W.; Middlebrooks, E. J. *Environ. Int.* **1983**, *9*, 289.
- (150) Sato, Y.; Kang, M.; Kamei, T.; Magara, Y. *Water Research* **2002**, *36*, 3371.
- (151) Xia, S.; Dong, B.; Zhang, Q.; Xu, B.; Gao, N.; Causseranda, C. *Desalination* **2007**, *204*, 374.
- (152) Weng, Y.-H.; Chaung-Hsieh, L. H.; Lee, H.-H.; Li, K.-C.; Huang, C. P. *Journal of Hazardous Materials* **2005**, *122*, 171.
- (153) Hsieh, L.-H. C.; Weng, Y.-H.; Huang, C.-P.; Li, K.-C. *Desalination* **2008**, *234*, 402.
- (154) Issa, N. B.; Rajaković-Ognjanović, V. N.; Jovanović, B. M.; Rajaković, L. *V. Analytica Chimica Acta* **2010**, *673*, 185.

- (155) Visoottiviseth, P.; Ahmed, F. In *Reviews of Environmental Contamination Volume 197*; Springer New York: 2009; Vol. 197, p 77.
- (156) Teixeira, M. C.; Ciminelli, V. S. T. *Environmental Science & Technology* **2004**, 39, 895.
- (157) Teixeira, M. C.; Ciminelli, V. S. T.; Dantas, M. S. S.; Diniz, S. F.; Duarte, H. A. *Journal of Colloid and Interface Science* **2007**, 315, 128.
- (158) Murugesan, G. S.; Sathishkumar, M.; Swaminathan, K. *Bioresource Technology* **2006**, 97, 483.
- (159) Mercier, L.; Pinnavaia, T. J. *Microporous and Mesoporous Materials* **1998**, 20, 101.
- (160) Feng, X.; Fryxell, G. E.; Wang, L.-Q.; Kim, A. Y.; Liu, J.; Kemner, K. M. *Science* **1997**, 276, 923.
- (161) Makkuni, A.; Bachas, L. G.; Varma, R. S.; Sikdar, S. K.; Bhattacharyya, D. *Clean Technologies and Environmental Policy* **2005**, 7, 87.
- (162) White, B. R.; Stackhouse, B. T.; Holcombe, J. A. *Journal of Hazardous Materials* **2009**, 161, 848.
- (163) Merrifield, J. D.; Davids, W. G.; MacRae, J. D.; Amirbahman, A. *Water Research* **2004**, 38, 3132.
- (164) Guo, X.; Du, Y.; Chen, F.; Park, H.-S.; Xie, Y. *Journal of Colloid and Interface Science* **2007**, 314, 427.
- (165) DeMarco, M. J.; SenGupta, A. K.; Greenleaf, J. E. *Water Research* **2003**, 37, 164.

- (166) Xiao, L.; Wildgoose, G. G.; Crossley, A.; Knight, R.; Jones, J. H.; Compton, R. G. *Chemistry – An Asian Journal* **2006**, *1*, 614.
- (167) Hao, J.; Han, M.-J.; Wang, C.; Meng, X. *Microporous and Mesoporous Materials* **2009**, *124*, 1.
- (168) Tripathy, S. S.; Raichur, A. M. *Chemical Engineering Journal* **2008**, *138*, 179.
- (169) Hao, J.; Han, M.-J.; Meng, X. *Journal of Hazardous Materials* **2009**, *167*, 1215.
- (170) Gupta, V. K.; Saini, V. K.; Jain, N. *Journal of Colloid and Interface Science* **2005**, *288*, 55.
- (171) Joshi, A.; Chaudhuri, M. *Journal of Environmental Engineering* **1996**, 769.
- (172) Blue, L. Y.; Jana, P.; Atwood, D. A. *Fuel* **2010**, *89*, 1326.
- (173) Kadokura, H.; Katzen, F.; Beckwith, J. *Annual Review of Biochemistry* **2003**, *72*, 111.
- (174) Matlock, M. M.; Howerton, B. S.; Van Aelstyn, M. A.; Nordstrom, F. L.; Atwood, D. A. *Environ. Sci. Technol.* **2002**, *36*, 1636.
- (175) Matlock, M. M.; Howerton, B. S.; Van Aelstyn, M.; Henke, K. R.; Atwood, D. A. *Water Res.* **2003**, *37*, 579.
- (176) Matlock, M. M.; Howerton, B. S.; Atwood, D. A. *J. Hazard Mater.* **2001**, *B84*, 73.
- (177) Blue, L. Y.; Van Aelstyn, M. A.; Matlock, M.; Atwood, D. A. *Water Research* **2008**, *42*, 2025.

- (178) Kostal, J.; Mulchandani, A.; Gropp, K. E.; Chen, W. *Environmental Science & Technology* **2003**, *37*, 4457.
- (179) Zaman, K. M.; Blue, L. Y.; Huggins, F. E.; Atwood, D. A. *Inorganic Chemistry* **2007**, *46*, 1975.
- (180) Matlock, M. M.; Howerton, B. S.; Atwood, D. A. *Ind. Eng. Chem. Res.* **2002**, *41*, 1579.
- (181) Matlock, M. M.; Howerton, B. S.; Atwood, D. A. *Advances in Environmental Research* **2003**, *7*, 347.
- (182) Matlock, M. M.; Howerton, B. S.; Atwood, D. A. *Water Res.* **2002**, *36*, 4757.
- (183) Matlock, M. M.; Howerton, B. S.; Atwood, D. A. *Adv. Environ. Res.* **2003**, *7*, 495.
- (184) Chusuei, C. C.; Zaman, K. M.; Atwood, D. A. *Colloid Surf. A-Physicochem. Eng. Asp.* **2008**, *331*, 155.
- (185) Benesch, R. E.; Benesch, R. *Journal of the American Chemical Society* **1955**, *77*, 5877.
- (186) Li, H.; Hanson, C.; Fuchs, J. A.; Woodward, C.; Thomas, G. J. *Biochemistry* **1993**, *32*, 5800.
- (187) Podhradský, D.; Drobnica, L.; Kristian, P. *Cellular and Molecular Life Sciences* **1979**, *35*, 154.
- (188) Ferguson, J. F.; Gavis, J. *Water Research* **1972**, *6*, 1259.
- (189) Blue, L. Y., University of Kentucky, 2009.

- (190) Shaikh, T. A.; Bakus, R. C.; Parkin, S.; Atwood, D. A. *J. Organomet. Chem.* **2006**, *691*, 1825.
- (191) Beak, D. G.; Wilkin, R. T.; Ford, R. G.; Kelly, S. D. *Environ. Sci. Technol.* **2008**, *42*, 1643.
- (192) Matlock, M. M.; Henke, K. R.; Atwood, D. A. *J. Hazard Mater.* **2002**, *B92*, 129.
- (193) Matlock, M. M.; Henke, K. R.; Atwood, D. A.; Robertson, D. *Water Res.* **2001**, *35*, 3649.
- (194) Matlock, M. M.; Howerton, B. S.; Atwood, D. A. *Adv. Environ. Res.* **2003**, *7*, 347.
- (195) Matlock, M. M.; Howerton, B. S.; Henke, K. R.; Atwood, D. A. *J. Hazard Mater.* **2001**, *B82*, 55.
- (196) Matlock, M. M.; Howerton, B. S.; Robertson, J. D.; Atwood, D. A. *Ind. Eng. Chem. Res.* **2002**, *41*, 5278.
- (197) Edsall, J. T.; Wyman; Jeffries *Biophysical Chemistry*; Academic Press, Inc.: New York, 1958.
- (198) Dawson, R. M. C. e. a. *Data for Biochemical Research*; Clarendon Press: Oxford, 1959.
- (199) Luo, D.; Smith, S. W.; Anderson, B. D. *Journal of Pharmaceutical Sciences* **2005**, *94*, 304.
- (200) Nelson, K. J.; Parsonage, D.; Hall, A.; Karplus, P. A.; Poole, L. B. *Biochemistry* **2008**, *47*, 12860.

- (201) Naor, M. M.; Jensen, J. H. *Proteins: Structure, Function, and Bioinformatics* **2004**, 57, 799.
- (202) Jalilehvand, F.; Leung, B. O.; Mah, V. *Inorganic Chemistry* **2009**, 48, 5758.
- (203) Jalilehvand, F.; Leung, B. O.; Izadifard, M.; Damian, E. *Inorganic Chemistry* **2005**, 45, 66.
- (204) Ni Dhubhghaill, O.; Sadler, P. In *Bioinorganic Chemistry*; Springer Berlin / Heidelberg: 1991; Vol. 78, p 129.
- (205) Alonzo, G.; Bertazzi, N.; Consiglio, M. *Inorganica Chimica Acta* **1984**, 85, L35.
- (206) Farrer, B. T.; McClure, C. P.; Penner-Hahn, J. E.; Pecoraro, V. L. *Inorganic Chemistry* **2000**, 39, 5422.
- (207) Teixeira, M. C.; Ciminelli, V. S. T. *Environmental Science & Technology* **2004**, 39, 895.
- (208) Bardwell, J. C.; Lee, J. O.; Jander, G.; Martin, N.; Belin, D.; Beckwith, J. *Proceedings of the National Academy of Sciences* **1993**, 90, 1038.
- (209) Annis, I.; Hargittai, B.; Barany, G. In *Methods in Enzymology*; Gregg, B. F., Ed.; Academic Press: 1997; Vol. Volume 289, p 198.
- (210) Bulaj, G. *Biotechnology Advances* **2005**, 23, 87.
- (211) Alan Aitken, R.; P. Armstrong, D.; H. B. Galt, R.; T. E. Mesher, S. *Journal of the Chemical Society, Perkin Transactions I* **1997**, 935.
- (212) West, K. R.; Bake, K. D.; Otto, S. *Organic Letters* **2005**, 7, 2615.



- (213) Atwood, D. A.; Delcamp, J.; Zaman, M. K. *Main Group Chemistry* **2006**, 5, 137.
- (214) Yablonskii, O. P.; Rodionova, N. M.; Lapuka, L. F. *Journal of Applied Spectroscopy* **1973**, 19, 1303.
- (215) Threeprom, J.; Som-Aum, W.; Lin, J. M. *Journal of Analytical Chemistry* **2007**, 62, 1126.
- (216) Garrett, R. H.; Grisham, C. M. *Biochemistry*; 3<sup>rd</sup> ed.; Thomson Brooks/Cole: Belmont, CA, 2007.
- (217) Rey, N. A.; Howarth, O. W.; Pereira-Maia, E. C. *Journal of Inorganic Biochemistry* **2004**, 98, 1151.
- (218) Arpadjan, S.; Çelik, G.; Taskesen, S.; Güçer, S. *Food and Chemical Toxicology* **2008**, 46, 2871.
- (219) Emadi, A.; Gore, S. D. *Blood Reviews*, 24, 191.
- (220) Zhang, W.-b.; Gan, W.-e.; Lin, X.-q. *Analytica Chimica Acta* **2005**, 539, 335.
- (221) Ng, J. C.; Wang, J.; Shraim, A. *Chemosphere* **2003**, 52, 1353.
- (222) Kapp, R. In *Encyclopedia of Toxicology*; Philip, W., Ed.; Elsevier: New York, 2005, p 168.
- (223) C. Ng, J.; Johnson, D.; R. Moore, M.; Imray, P.; Chiswell, B. *Analyst* **1998**, 123, 929.
- (224) Sharma, V. K.; Sohn, M. *Environ. Int.* **2009**, 35, 743.
- (225) Jain, C. K.; Ali, I. *Water Research* **2000**, 34, 4304.
- (226) Kumaresan, M.; Riyazuddin, P. *Current Science* **2001**, 80, 837.

- (227) Banks, C. H.; Daniel, J. R.; Zingaro, R. A. *Journal of Medicinal Chemistry* **1979**, 22, 572.
- (228) Shaikh, T. A.; Bakus Ii, R. C.; Parkin, S.; Atwood, D. A. *Journal of Organometallic Chemistry* **2006**, 691, 1825.
- (229) Sommer, K.; Becke-Goehring, M. *Zeitschrift für anorganische und allgemeine Chemie* **1967**, 355, 182.
- (230) Sommer, K.; Becke-Goehring, M. *Zeitschrift für anorganische und allgemeine Chemie* **1967**, 355, 192.
- (231) Gailer, J.; Lindner, W. *Journal of Chromatography B: Biomedical Sciences and Applications* **1998**, 716, 83.
- (232) Mizumura, A.; Watanabe, T.; Kobayashi, Y.; Hirano, S. *Toxicology and Applied Pharmacology* **2010**, 242, 119.
- (233) Percy, A. J.; Gailer, J. *Bioinorg. Chem. Appl.* **2008**.
- (234) Ona-Nguema, G.; Morin, G.; Wang, Y.; Foster, A. L.; Juillot, F.; Calas, G.; Brown, G. E. *Environmental Science & Technology* **2010**, 44, 5416.
- (235) Smith, P. G.; Koch, I.; Gordon, R. A.; Mandoli, D. F.; Chapman, B. D.; Reimer, K. J. *Environmental Science & Technology* **2004**, 39, 248.
- (236) Ravel, B. *J. Synchrot. Radiat.* **2001**, 8, 314.
- (237) Ravel, B.; Newville, M. *J. Synchrot. Radiat.* **2005**, 12, 537.
- (238) Mullen, D. J. E.; Nowacki, W. Z. *Kristall.* **1972**, 136, 48.
- (239) Pappalardo, G. C.; Chakravorty, R.; Irgolic, K. J.; Meyers, E. A. *Acta Crystallographica Section C* **1983**, 39, 1618.
- (240) Bostick, B. C.; Fendorf, S.; Brown, G. E., Jr. *Mineral Mag* **2005**, 69, 781.

- (241) Ghosh, A.; Mukiibi, M.; Sáez, A. E.; Ela, W. P. *Environmental Science & Technology* **2006**, *40*, 6070.
- (242) Liu, C.-Y.; Sun, P.-J. *Analytica Chimica Acta* **1981**, *132*, 187.
- (243) Maquieira, A.; Elmahadi, H. A. M.; Puchades, R. *Anal. Chem.* **1994**, *66*, 1462.
- (244) Autry, H. A.; Holcombe, J. A. *Analyst* **1995**, *120*, 2643.
- (245) Abu-Daibes, M. A.; Pinto, N. G. *Chemical Engineering Science* **2005**, *60*, 1901.
- (246) Ritchie, S. M. C.; Kissick, K. E.; Bachas, L. G.; Sikdar, S. K.; Parikh, C.; Bhattacharyya, D. *Environmental Science & Technology* **2001**, *35*, 3252.
- (247) Arakaki, L. N. H.; da Fonseca, M. G.; da Silva Filho, E. C.; de M. Alves, A. P.; de Sousa, K. S.; Silva, A. L. P. *Thermochimica Acta* **2006**, *450*, 12.
- (248) Arakaki, L. N. H.; Filha, V. L. S. A.; de Sousa, K. S.; Aguiar, F. P.; da Fonseca, M. G.; Espínola, J. G. P. *Thermochimica Acta* **2006**, *440*, 176.
- (249) Julius, S. *Journal of Catalysis* **1978**, *54*, 285.
- (250) Rayaner-Canham, G.; Overton, T. In *Descriptive Inorganic Chemistry*; 5th Edition ed.; W. H. Freeman and Company: New York, NY, 2010, p 315.
- (251) Zhuravlev, L. T. *Langmuir* **1987**, *3*, 316.
- (252) Yoshinaga, K.; Yoshida, H.; Yamamoto, Y.; Takakura, K.; Komatsu, M. *Journal of Colloid and Interface Science* **1992**, *153*, 207.
- (253) An, Y.; Chen, M.; Xue, Q.; Liu, W. *Journal of Colloid and Interface Science* **2007**, *311*, 507.
- (254) Ishida, H.; Chiang, C.-h.; Koenig, J. L. *Polymer* **1982**, *23*, 251.

- (255) Chiang, C.-H.; Ishida, H.; Koenig, J. L. *Journal of Colloid and Interface Science* **1980**, 74, 396.
- (256) Hasegawa, I.; Imamura, W.; Takayama, T. *Inorganic Chemistry Communications* **2004**, 7, 513.
- (257) Yamana, T.; Tsuji, A.; Yasuda, Y.; Masuda, K.; Mizukami, Y. *Chem. Pharm. Bull.* **1972**, 20, 881.
- (258) Cai, M.; Sha, J.; Xu, Q. *Journal of Molecular Catalysis A: Chemical* **2007**, 268, 82.
- (259) Airoidi, C.; Arakaki, L. N. H. *Polyhedron* **2001**, 20, 929.
- (260) Grigoropoulou, G.; Stathi, P.; Karakassides, M. A.; Louloudi, M.; Deligiannakis, Y. *Colloids and Surfaces A: Physicochemical and Engineering Aspects* **2008**, 320, 25.
- (261) Vidic, R. D.; Siler, D. P. *Carbon* **2001**, 39, 3.
- (262) Boccelli, D. L.; Small, M. J.; Dzombak, D. A. *Environmental Science & Technology* **2005**, 39, 6501.
- (263) Webb, S. M. *Phys. Scr.* **2005**, T115, 1011.
- (264) Atwood, D.; Zaman, M.; Atwood, D., Ed.; Springer Berlin / Heidelberg: 2006; Vol. 120, p 163.
- (265) Hutson, N. D.; Attwood, B. C.; Scheckel, K. G. *Environmental Science & Technology* **2007**, 41, 1747.
- (266) Wang, J.; Deng, B. L.; Wang, X. R.; Zheng, J. Z. *Environmental Engineering Science* **2009**, 26, 1693.
- (267) Zhu, J.; Deng, B.; Yang, J.; Gang, D. *Carbon* **2009**, 47, 2014.

- (268) Yan, Y. L.; Helfand, M. A.; Clayton, C. R. *Applied Surface Science* **1989**, 37, 395.
- (269) Finster, J.; Klinkenberg, E. D.; Heeg, J.; Braun, W. *Vacuum* **1990**, 41, 1586.
- (270) Nefedov, V. I.; Salyn, Y. V.; Solozhenkin, P. M.; Pulatov, G. Y. *Surface and Interface Analysis* **1980**, 2, 170.
- (271) Humbert, P. *Solid State Commun.* **1986**, 60, 21.
- (272) Sodhi, R. N. S.; Cavell, R. G. *Journal of Electron Spectroscopy and Related Phenomena* **1986**, 41, 1.
- (273) Carroll, T. X.; Ji, D.; Maclaren, D. C.; Thomas, T. D.; Saethre, L. J. *Journal of Electron Spectroscopy and Related Phenomena* **1987**, 42, 281.
- (274) Calareso, C.; Curro, G. M.; Grasso, V.; Silipigni, L. *Journal of Vacuum Science & Technology A: Vacuum, Surfaces, and Films* **2000**, 18, 306.
- (275) Barr, T. L.; Seal, S. *Journal of Vacuum Science & Technology A: Vacuum, Surfaces, and Films* **1995**, 13, 1239.
- (276) Shirley, D. A. *Physical Review B* **1972**, 5, 4709.
- (277) Barr, T. L. *Modern ESCA*; CRC Press: Boca Raton, 1994.
- (278) Scott, K. N.; Green, J. F.; Do, H. D.; McLean, S. J. *J. Am. Water Works Assoc.* **1995**, 87, 114.
- (279) Jekel, M.; Removal of arsenic in drinking water treatment, In: Nriagu JO, editor. *Arsenic in the environment: part 1: cycling and characterization*: New York, 1994, p 119.
- (280) Katsoyiannis, I. A.; Zouboulis, A. I. *Water Research* **2002**, 36, 5141.

- (281) Ren, Z.; Zhang, G.; Paul Chen, J. *Journal of Colloid and Interface Science* **2011**, 358, 230.
- (282) Leupin, O. X.; Hug, S. J. *Water Research* **2005**, 39, 1729.
- (283) Lukens, W. W.; Bucher, J. J.; Shuh, D. K.; Edelstein, N. M. *Environmental Science & Technology* **2005**, 39, 8064.
- (284) Berg, M.; Luzi, S.; Trang, P. T. K.; Viet, P. H.; Giger, W.; Stüben, D. *Environmental Science & Technology* **2006**, 40, 5567.
- (285) Steele, R. A.; Opella, S. J. *Biochemistry* **1997**, 36, 6885.
- (286) Qian, H.; Sahlman, L.; Eriksson, P.-O.; Hambræus, C.; Edlund, U.; Sethson, I. *Biochemistry* **1998**, 37, 9316.
- (287) Veglia, G.; Porcelli, F.; DeSilva, T.; Prantner, A.; Opella, S. J. *Journal of the American Chemical Society* **2000**, 122, 2389.
- (288) Megens, R. P.; van den Berg, T. A.; de Bruijn, A. D.; Feringa, B. L.; Roelfes, G. *Chemistry – A European Journal* **2009**, 15, 1723.
- (289) Alliger, G. E.; Müller, P.; Cummins, C. C.; Nocera, D. G. *Inorganic Chemistry* **2010**, 49, 3697.

## **VITA**

### **Personal Details**

Place of Birth: Midnapore, WB, India

### **Education**

- Master of Technology (M.Tech.) in Rubber Technology, Indian Institute of Technology, Kharagpur, India, 2001  
Thesis title: Introducing New Composition of Rubber and Chemicals in off the Road Truck Tires  
Advisor: Dr. Tapan K. Chaki
- Master of Science (M.Sc.) in Chemistry, Vidyasagar University, WB, India, 1999
- Bachelor of Science with Honors (B.Sc.) in Chemistry, Vidyasagar University, WB, India, 1997

### **Research Experience**

- Removal of trivalent arsenic from water with silica supported thiol ligand (for ongoing Ph.D.)
- Development of conductive rubber composition for chips used in electronics and cell phones (2002-2003)
- Development of new composition of rubber and chemicals for the off the road truck tires (for M.Tech., 2000-2001)

### **Honors/Grants**

- International Student Scholarship at University of Kentucky, 2012
- Graduate Student Travel Grant, University of Kentucky, 2010 and 2011
- Graduate Student Research Grant, United States Geological Survey (USGS) Student Research Enhancement Program, 2010
- Council of Scientific and Industrial Research (CSIR) scholarship, Government of India, 2000
- Graduate Aptitude Test for Engineering (GATE) scholarship, Government of India, 2000

### **Professional Affiliations**

American Chemical Society

### List of Publications

- Bhowmik, S., Jana, P., Chaki, T. K. and Ray, S., “Surface modification of Polypropylene Under Different Electrodes of DC Glow Discharge and Its Physicochemical Characteristics”, *Surface and Coatings Technology*, **2004**, *185(1)*, 81-91
- Blue, L., Jana, P. and Atwood, D. A., “Aqueous Mercury Precipitation with the Synthetic Dithiolate, BDTH<sub>2</sub>”, *Fuel*, **2010**, *89*, 1326-1330
- Jana, P.; Athalye, R., Parkin, S., Kabengi, N., Chikwana, E., Grunwald, C. and Atwood, D. A., “Fundamental Properties of the Heavy Metal Precipitation Agent, BDTH<sub>2</sub>” (in preparation) to be submitted to *Environmental Science & Technology*
- Jana, P.; Atwood, D. A., “Silica-Supported Dithiol Filtration Column for Aqueous Arsenic Removal from Water” (in preparation)
- Jana, P.; Chusuei, C. C.; Sells, J. A. and Atwood, D. A., “Aqueous Hg(II) Removal with Silica (SiO<sub>2</sub>)-Supported Thiol Chelating Ligand” (in preparation)
- Jana, P.; Chusuei, C. C.; Sells, J. A. and Atwood, D. A., “Polystyrene Pendant Thiol Ligand for Hg(II) Removal from Aqueous Solution” (in preparation)

### Conference Presentation

- Poster Presentation, 239<sup>th</sup> American Chemical Society Conference (San Francisco, CA), “Solid-supported thiols for aqueous mercury removal”, March 21-25, 2010
- Poster Presentation, The Tracy Farmer Institute for Sustainability & the Environment (Lexington, KY), “Aqueous arsenic and mercury capture with new solid-supported reagents”, September 22, 2010
- Lecture Presentation, Kentucky Water Resource Annual Symposium (Lexington, KY), “Aqueous Arsenic(III) Removal with a Thiol-Containing Filtration Column”, March 21, 2011
- Lecture Presentation, 5<sup>th</sup> Annual Graduate Student Interdisciplinary Conference (UK, Lexington, KY), “Design and Synthesis of Thiol-containing Filtration Column Packing Material for Aqueous Arsenic(III) Removal”, April 1, 2011

### Extracurricular Activities

Student officer, Graduate Student Association (GSA), Department of Chemistry, University of Kentucky, 2010-2011